Progress in Retinal and Eye Research 69 (2019) 80–115

Contents lists available at ScienceDirect

Progress in Retinal and Eye Research

journal homepage: www.elsevier.com/locate/preteyeres

# Myopic maculopathy: Current status and proposal for a new classification and grading system (ATN)

Jorge Ruiz-Medrano[a,1], Javier A. Montero[b,c,d,1], Ignacio Flores-Moreno[e,1], Luis Arias[a,1], Alfredo García-Layana[c,f,1], José M. Ruiz-Moreno[c,e,g,h,1,*]

[a] Department of Ophthalmology, Bellvitge University Hospital, Barcelona, Spain
[b] Department of Ophthalmology, Rio Hortega University Hospital, Valladolid, Spain
[c] Red Temática de Investigación Cooperativa en Salud: ""Prevención, detección precoz, y tratamiento de la patología ocular prevalente, degenerativa y crónica" (RD16/0008/0021), Spanish Ministry of Health, Instituto de Salud Carlos III, Spain
[d] Retina Unit, Oftalvist, Madrid, Spain
[e] Puerta de Hierro-Majadahonda University Hospital, Madrid, Spain
[f] Department of Ophthalmology, Clínica Universidad de Navarra, Pamplona, Spain
[g] Department of Ophthalmology, Castilla La Mancha University, Albacete, Spain
[h] Vissum Corporation, Spain

ARTICLE INFO

*Keywords:*
Pathologic myopia
Staphyloma
Myopic maculopathy
Myopic traction maculopathy
Myopic choroidal neovascularization
High myopia
Myopic maculopathy classification
ATN classification system

ABSTRACT

Myopia is a highly frequent ocular disorder worldwide and pathologic myopia is the 4th most common cause of irreversible blindness in developed countries. Pathologic myopia is especially common in East Asian countries. Ocular alterations associated with pathologic myopia, especially those involving the macular area—defined as myopic maculopathy—are the leading causes of vision loss in patients with pathologic myopia.

High myopia is defined as the presence of a highly negative refractive error (> −6 to −8 diopters) in the context of eye elongation (26–26.5 mm). Although the terms high myopia and pathologic myopia are often used interchangeably, they do not refer to the same eye disease. The two key factors driving the development of pathologic myopia are: 1) elongation of the axial length and 2) posterior staphyloma.

The presence of posterior staphyloma, which is the most common finding in patients with pathologic myopia, is the key differentiating factor between high and pathologic myopia. The occurrence of staphyloma will, in most cases, eventually lead to other conditions such as atrophic, traction, or neovascular maculopathy. Posterior staphyloma is for instance, responsible for the differences between a myopic macular hole (MH)—with and without retinal detachment—and idiopathic MH. Posterior staphyloma typically induces retinal layer splitting, leading to foveoschisis in myopic MH, an important differentiating factor between myopic and emmetropic MH.

Myopic maculopathy is a highly complex disease and current classification systems do not fully account for the numerous changes that occur in the macula of these patients. Therefore, a more comprehensive classification system is needed, for several important reasons. First, to more precisely define the disease stage to improve follow-up by enabling clinicians to more accurately monitor changes over time, which is essential given the progressive nature of this condition. Second, unification of the currently-available classification systems would establish standardized classification criteria that could be used to compare the findings from international multicentric studies. Finally, a more comprehensive classification system could help to improve our understanding of the genetic origins of this disease, which is clearly relevant given the interchangeable—but erroneous—use of the terms high and pathologic myopia in genetic research.

## 1. Introduction

Myopia is a common disorder estimated to affect approximately 1.6 billion people worldwide. This disorder is becoming increasingly prevalent and by the year 2020, it is estimated that up to 2.5 billion people will be affected, with 27%–33% of these presenting high myopia.

* Corresponding author. Department of Ophthalmology, Castilla La Mancha University, Albacete, Spain.
*E-mail address:* josemaria.ruiz@uclm.es (J.M. Ruiz-Moreno).

[1] Percentage of work contributed by each author in the production of the manuscript is as follows: Jorge Ruiz-Medrano 25%, Javier A Montero 15%, Ignacio Flores-Moreno 15%, Luis Arias 10%, Alfredo Gracía-Layana 10%, Jose M Ruiz-Moreno 25%.

https://doi.org/10.1016/j.preteyeres.2018.10.005
Received 31 July 2018; Received in revised form 18 October 2018; Accepted 22 October 2018
Available online 01 November 2018

Prevalence rates for both myopia and high myopia are expected to continue rising in the coming decades, which implies that ocular complications and vision loss associated with this disorder will also increase (Holden et al., 2016).

Globally, the prevalence of simple myopia is considered to be as high as 81.6%–96.5% according to different series (Koh et al., 2016a, 2014, Lee et al., 2013, 2011). The prevalence of high myopia is difficult to determine with certainty due to the lack of a standardized definition, ranging from 1% to 4%, reaching its highest rates in East Asia with a prevalence of 6.8–21.6%. High myopia is usually defined as a spherical equivalent of $> -6.0$ diopters or an ocular axial length $\geq 26.0$ or 26.5 mm (Ohno-Matsui, 2017; Silva, 2012; Wolf et al., 2014). Nonetheless, there is some controversy surrounding these cut-off points, with some authors contending that the spherical equivalent to define high myopia should be $> -8.0$ diopters (Shimada et al., 2013).

The precise definition of pathologic myopia is also controversial. Originally, pathologic myopia was described as the presence of structural changes causing vision loss in the context of high myopia (Morgan et al., 2012; Tokoro, 1988). Although axial elongation is generally believed to play a key role in these degenerative changes (Moriyama et al., 2011), axial elongation is not, by itself, the only marker of pathologic myopia given that posterior staphyloma has been occasionally reported in eyes without high myopia (Wang et al., 2016).

Changes to the shape of the globe induced by pathologic myopia are responsible for the macular, peripheral, and optic disc alterations described in these patients. These structural changes—particularly the macular alterations—may, over time, cause severe vision loss in patients with severe myopia (Morgan et al., 2012; Ohno-Matsui et al., 2016c). Indeed, pathologic myopia is one of the leading causes of blindness worldwide, accounting for 5.8%–7.8% of cases of blindness in Europe (Cedrone et al., 2006). In China, it is estimated that pathologic myopia may be responsible for complete vision loss in up to 6.7 million people, with a further 7.1 million presenting low visual acuity (Cheng et al., 2013).

Myopic macular degeneration is one of the main causes of irreversible blindness in certain regions of the world, becoming an important problem particularly in East Asia (Iwase et al., 2006). In Japan, this degenerative disease accounts for 12.2% of severe vision loss (Yamada et al., 2010). The leading cause of blindness in East Asia are complications related to pathologic myopia (Chan et al., 2016; Foster and Jiang, 2014; Morgan et al., 2012). In Spain, pathologic myopia is the 4th leading cause of legal blindness, only exceeded by age-related macular degeneration, glaucoma, and diabetic retinopathy (Gomez-Ulla and Ondategui-Parra, 2012). It is estimated that approximately 900,000 people in Spain (2%–3% of the population) have pathologic myopia. In consistency with the rising prevalence rates worldwide, pathologic myopia has also become more common in Spain in recent years (Gomez-Ulla and Gil-Martinez, 2015).

## 2. Posterior staphyloma

### 2.1. Concept

The presence of a posterior staphyloma is the most characteristic finding, and the main marker, of pathologic myopia (Ohno-Matsui et al., 2016c). Spaide defined posterior staphyloma as “an outpouching of the wall of the eye that has a radius of curvature that is less than the surrounding curvature of the wall of the eye” (Spaide, 2013). This was the first widely-accepted definition of posterior staphyloma; however, Ohno-Matsui et al. observed that peripapillary and nasal staphylomas do not always induce a drastic curvature compared to surrounding tissues, but rather a nasal distortion of the eye shape (Ohno-Matsui et al., 2012), leading those authors to add “a nasally-distorted type of globe” to the definition of staphyloma. In a later study, that same group (Ohno-Matsui et al., 2016c) suggested that posterior staphyloma should not be considered a characteristic lesion of myopic maculopathy, contradicting earlier studies (Avila et al., 1984; Chang et al., 2013; Chen et al., 2012; Gao et al., 2011; Vongphanit et al., 2002a), but rather the main cause of myopic maculopathy.

Nevertheless, while most ophthalmologists would agree that posterior staphyloma is likely one of the main causes of myopic maculopathy, it cannot be considered its only cause given that axial elongation without posterior staphyloma can also lead to myopic maculopathy, although this is much less common (Ohno-Matsui et al., 2016c). It is likely that excessive axial elongation may trigger stress in the posterior pole that may lead to the appearance of local or diffuse degeneration of the sclera and/or retina and/or choroid, and that any of these degenerative changes can induce pathological changes in the other tissues.

Even though posterior staphyloma may not be the primary defect, its appearance does determine more severe alterations and a higher prevalence of myopic maculopathy. Myopic traction maculopathy (Baba et al., 2003; Benhamou et al., 2002; Hirakata and Hida, 2006; Oie et al., 2005; Rahimy et al., 2013; Wu et al., 2009) and diffuse chorioretinal atrophy (Ohno-Matsui, 2014) are significantly more common, while best corrected visual acuity (BCVA) has been reported to be lower in eyes with staphyloma than in eyes that do not show it (Ohno-Matsui, 2014; Steidl and Pruett, 1997).

Increasing age and axial length are relevant risk factors related to the appearance of pathologic alterations in highly myopic patients (Chen et al., 2012; Shih et al., 2006; Verkicharla et al., 2015) as well as in eyes with staphyloma progression (Gözüm et al., 1997), Even though young highly myopic patients do not tend to show posterior staphylomas (Kobayashi et al., 2005), they can be found in 13.2% of young highly myopic patients aged 3–19 years old. Logically and in line with these authors’ results, the prevalence of posterior staphyloma rises to 53.5% in patients aged 60–86 years old (Curtin, 1977).

Optical coherence tomography (OCT) is a non-invasive imaging tool that has vastly improved our ability to study and detect changes at different levels of the posterior pole. Longer wavelength (1.050–1.060 nm), deep penetrance swept-source (SS)-OCT offers clear visualization of the sclera and orbital fat tissue, thus facilitating morphological analysis of the posterior pole in eyes with high myopia. However, it is often difficult to obtain good quality images in patients with high myopia due to the characteristic lengthening of the posterior part of the globe.

Horizontal SS-OCT b-scans of the macula in highly myopic patients reveal a progressively increasing concavity as the axial length increases and different slopes depending on the size and location of the staphyloma. At first, the concavity is minimal (Fig 1a), but over time it increases, eventually involving the optic disc (Fig 1b). In some cases, the optic disc can be seen at the bottom of the concavity (Fig 1c). The profile may be regular (Fig 1d, e) or, less commonly, presents a clear irregularity (Fig 1f). In most cases, vertical b-scans produce regular, concave-profile images (Fig 1g), with the exception of dome-shaped macula (DSM) (Fig 1h).

It has been postulated that several different mechanisms—involving the process of emmetropization and structural defects in collagen fibres—can cause posterior staphyloma. In highly myopic eyes, posterior staphyloma appears to be related to a defective scleral structure. Grossniklaus and Green evaluated the histological characteristics of 308 highly myopic eyes (Grossniklaus and Green, 1992), finding that the two most common histological findings were a myopic configuration of the optic nerve (a tilted disk in almost 40% of the eyes) and staphyloma (35% of eyes), which was primarily located in the posterior pole.

Scleral changes in highly myopic eyes involve diffuse of local thinning, with thinned collagen bundles, greater interfibrillary separation, decreased collagen striations, and a lamellar structure similar to that of corneal stroma, seemingly permitting sliding of the scleral lamellae (Curtin and Teng, 1985). Posterior staphyloma is characterized by the presence of an abrupt margin. Compared to the normal retina, the ectatic area has a relative pallor associated with an increased visibility of choroidal vessels (Fig 2). The height of the staphyloma

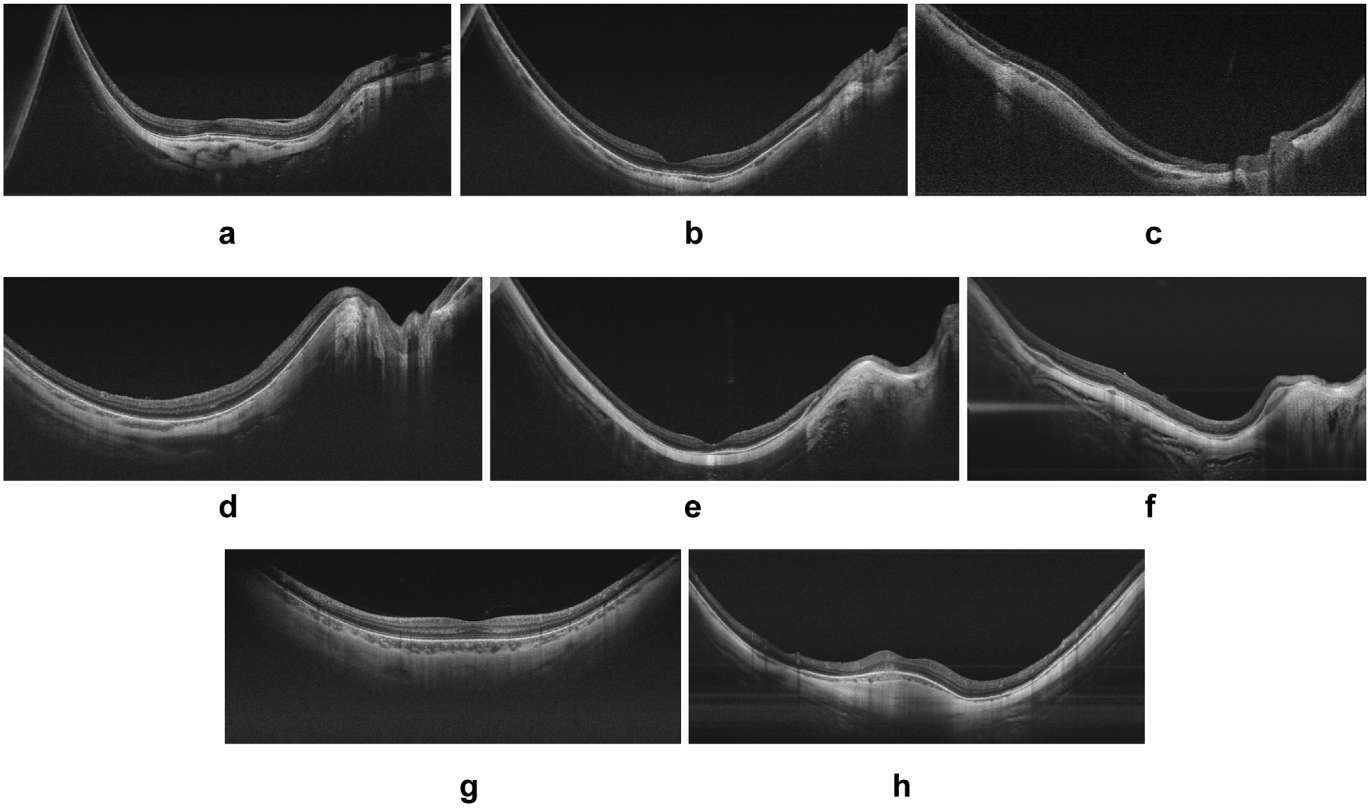


**Fig. 1.** Horizontal swept-source optical coherence tomography b-scans of the macula of highly myopic eyes. A progressively increasing concavity is observed as axial length grows, growing from a small concavity (a) to larger concavity (b). In other cases, the optic disc is seen at the bottom of the concavity (c). The profile may be regular (d, e) or, in some cases, clearly irregular (f). In most cases, vertical b-scans show regular, concave-profile images (g) with the exception of dome-shaped macula (h).

correlates with the extent of scleral thinning. Ohno-Matsui et al. described the presence of multiple conus pits in highly myopic eyes (Curtin, 1977; Ohno-Matsui, 2016). Those authors also reported a condition resembling peripapillary scleral schisis in the neighbouring areas. Posterior staphyloma is frequently associated with chorioretinal atrophy. In fact, these two signs are the most common myopia-related macular findings, occurring in around 20–23% of highly myopic eyes in adults (Chang et al., 2013).

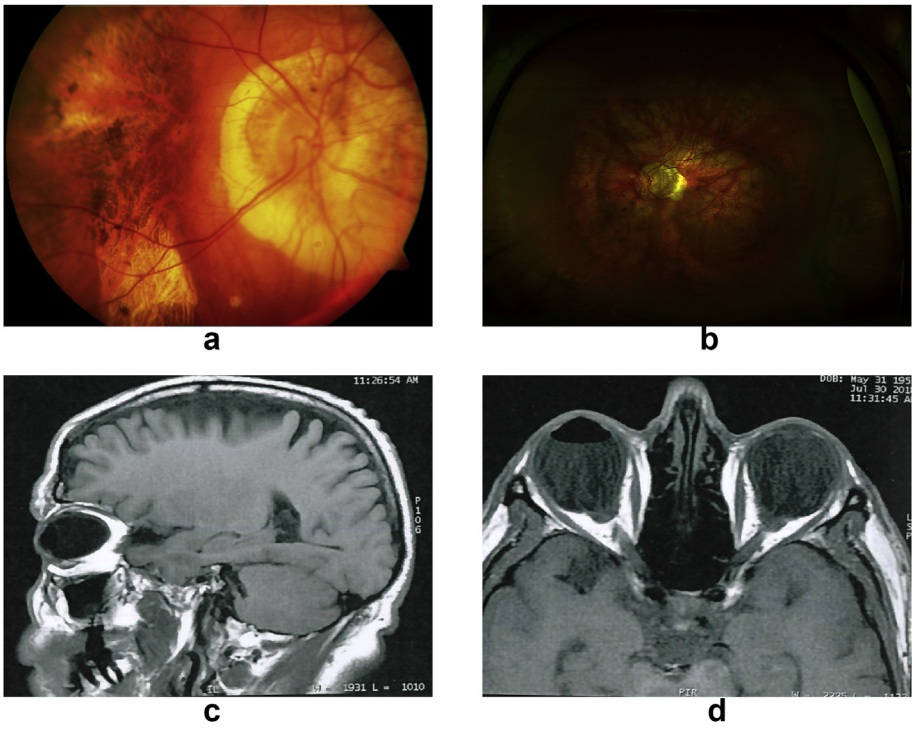


**Fig. 2.** Vertical posterior staphyloma in a highly myopic eye with marked RPE and chorioretinal atrophy (a). 34-year-old highly myopic patient with a posterior staphyloma, after scleral buckling surgery (b). Magnetic resonance imaging of an aphakic highly myopic patient after left eye retinal detachment surgery, showing intraocular gas in the anterior chamber and posterior staphyloma (c, d).

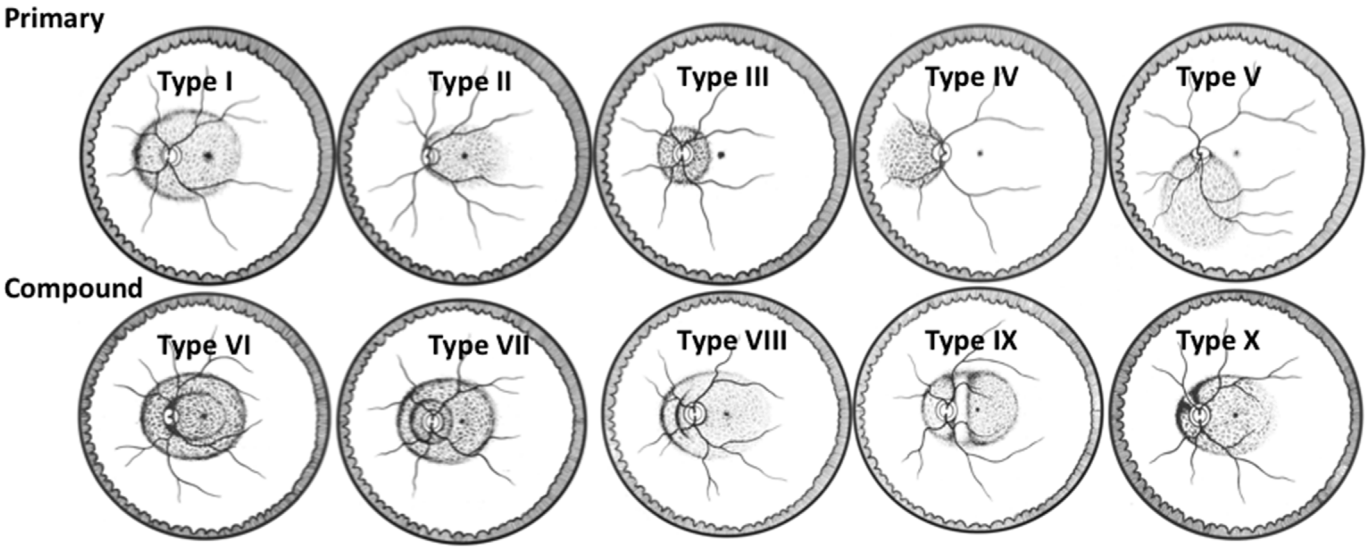


**Fig. 3.** Curtin classification of staphylomas. Primary staphylomas involve the posterior pole of the eye (Type I – Type V). Types VI and VII are compound staphylomas combining Type I with other forms. Type VIII is formed by a Type I with multiple steps across its walls. Type IX and X are formed by a Type I staphyloma divided into compartments. From (Curtin 1977).

### 2.2. Classification

Curtin classified posterior staphyloma into 10 types—five primary and five compound forms—based on their funduscopic appearance (Fig 3). In his system, primary staphylomas are classified according to the area they involve, as follows: posterior pole of the eye (Type I), macular area (Type II), peripapillary area (Type III), the area nasal to the disk (Type IV) and the area below the disk (Type V). Compound staphylomas are primarily type I staphylomas combined with other forms (Types VI and VII) or that involve multiple steps across the wall of a primary Type I staphyloma (Type VIII). By contrast, Types IX and X are formed by a Type I staphyloma divided into compartments (Curtin, 1977).

Posterior pole staphyloma (Type I) is by far the most common type of staphyloma. By contrast, the least common types are peripapillary and inferior staphylomas, both of which are rare. Staphylomas tend to expand and deepen with age, eventually becoming symmetric. Legal blindness is more prevalent in eyes with staphyloma types VII, VI and III and blindness is most commonly associated with diffuse chorioretinal atrophy affecting the peripapillary area. In Curtin's series of 403 eyes with staphyloma, the mean overall prevalence of staphyloma-related blindness was 34.5%, ranging from 13% to 53.5%, respectively, in the youngest and oldest age groups.

Ohno-Matsui expanded on Curtin's classical classification by adding nasal and peripapillary staphylomas with nasal distortion (Ohno-Matsui, 2014). Those authors found that, in two-thirds of cases, both eyes in highly myopic patients have a similar shape, and the part of the fundus that most protrudes is usually located along or slightly below the central sagittal axis. In that study, almost half of the eyes had multiple protrusions and thus were more likely to present myopic chorioretinal atrophy.

Recently-developed imaging technologies have improved the quantification and classification of staphylomas. Ikuno et al. used spectral-domain (SD)-OCT to measure posterior staphylomas in highly myopic eyes, finding that the size of the staphyloma closely correlated with refractive errors, choroidal thickness, and axial length (Ikuno et al., 2009). Other authors have used SS-OCT to determine the contour of the outer surface of the eyes and thus to establish the relationship between the shape of this area and myopic chorioretinal lesions.

Recently, a new system was proposed to classify the curvatures of the inner sclera according to data obtained through SS-OCT and magnetic resonance imaging (MRI) (Ohno-Matsui, 2016). The authors of that study suggested that the inner scleral surface in highly myopic eyes has four different curvature patterns, as follows: 1) Curvatures that slope toward the optic nerve, in which the scleral curvature is almost flat, with the optic nerve located in the lower part of the fundus and the fovea on the slope towards the optic disc. This pattern can be observed mostly on horizontal OCT scans; 2) Symmetrical curvatures centred on the fovea in which the sclera appears at the bottom of the fundus, protruding towards the orbital apex. Both of these first two patterns are similar to those found in emmetropic eyes; 3) Asymmetrical curvatures in which the sclera protrudes strongly towards the orbital apex while the most inferior part of the fundus is away from the fovea. All of the eyes in that study that were classified as asymmetrical curvatures presented a staphyloma; and 4) Irregular curvatures in which the scleral curve is irregular. Our group previously described the use of SS-OCT to characterize highly myopic eyes; in that study, we observed patterns similar to those described above (Ruiz-Moreno and Ruiz-Medrano, 2015).

Due to the extreme thinness of the choroid in highly myopic eyes, the curvature of both the retina and Bruch's membrane closely follow that of the sclera. In emmetropic eyes, however, this pattern is not followed because the choroid is much thicker; moreover, although there are two different scleral curvature patterns (types 1 and 2, described above, i.e., either sloping towards the optic disk [type 1] or symmetrical [type 2]), the curvature of the retinal pigment epithelium (RPE) is not necessarily identical to the curvature of the sclera. In the series by Ohno-Matsui et al. (Ohno-Matsui, 2014), the staphyloma was present along the anteroposterior axis in almost 80% of eyes and in the inferior sclera in the remaining 20%, a finding that suggests that the inferior sclera was thinner and more likely to present staphyloma. Patients with irregular curvatures were older, more myopic, and had thinner central thickness compared to younger patients. Those authors hypothesized that the greater weakness in this area might be attributable to its location at the closure of the embryonic ocular fissure.

The mean scleral thickness (228 μm) in highly myopic eyes described by Ohno-Matsui and colleagues was similar to that reported by Curtin and Teng (233 μm) and by Imamura et al. (281 μm) (Curtin and Teng, 1985; Imamura et al., 2011; Ohno-Matsui et al., 2012). The prevalence of posterior staphyloma in those studies was highest (100% of the cases in both studies) in eyes with asymmetrical, irregular chorioretinal and patchy atrophy. Myopic choroidal neovascularization

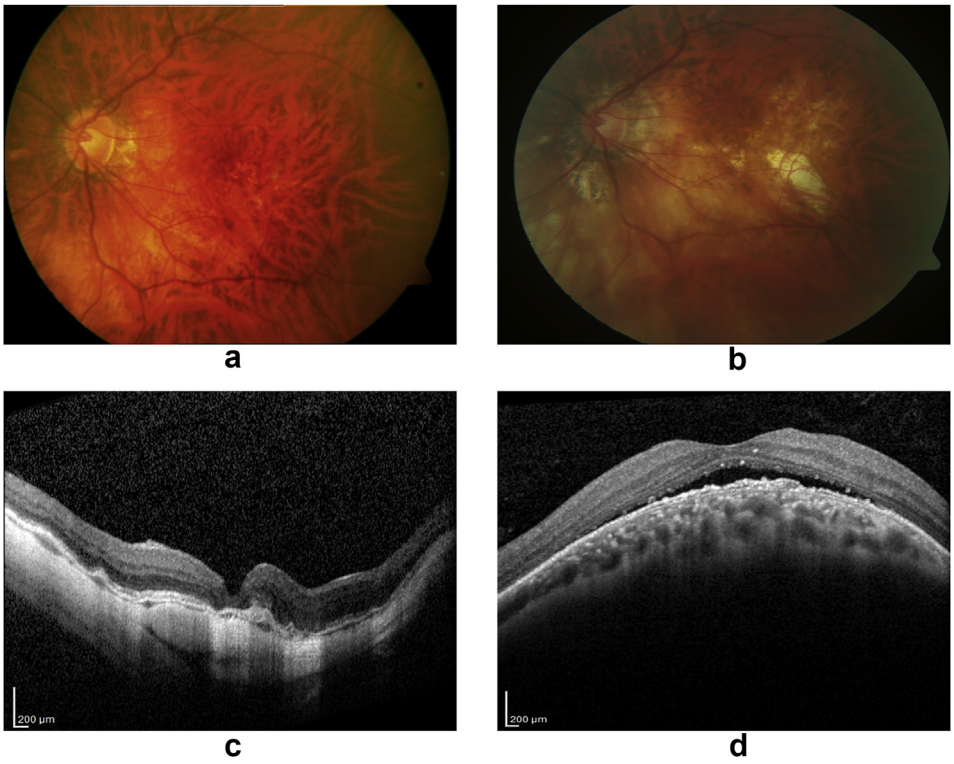


**Fig. 4.** Progressive retinal, choroidal and RPE thinning and atrophy starting from a lacquer crack (a) permitting visualization of choroidal vessels and sclera (b). Spectral domain OCT shows retinochoroidal thinning with myopic choroidal neovascularization (c) and dome-shaped macula (d), with concave sclera and localized submacular serous retinal detachment.

(mCNV) was more prevalent in eyes with irregular staphyloma. The presence of myopic traction maculopathy (MTM) was more frequent among eyes with irregular, asymmetric staphylomas. Ohno-Matsui et al. found that irregular curvatures were more common among elderly patients and in eyes with longer axial lengths and that those eyes were more likely to present lesions characteristic of high myopia (Ohno-Matsui et al., 2012). Miyake et al. used colour maps created through OCT, finding that eyes with chorioretinal atrophy show a steep, curved shape with an undulated surface in the posterior pole (Miyake et al., 2014b).

Numerous authors have assessed the role of staphylomas in the development of chorioretinal atrophy. A clinical quantification of posterior staphyloma showed that a shallower staphyloma depth was associated with worse BCVA and a higher prevalence of mCNVs; by contrast, larger staphylomas were associated with a higher prevalence of conus formation, RPE defects, lacquer cracks, and chorioretinal atrophy (Steidl and Pruett, 1997). Studies using ultrasound and MRI to obtain three-dimensional (3D) images of myopic eyes have detected an association between chorioretinal atrophy and the presence of two or more protruding areas in the back of the eye (Moriyama et al., 2011). Miyake et al. (Miyake et al., 2014a) used OCT imaging to response to anti- vascular endothelial growth factor (VEGF) treatment for mCNV, finding an association between chorioretinal atrophy and larger posterior pole curvatures and undulations. In that same study, chorioretinal atrophy in eyes with mCNV was associated with lower to moderate curvature; no association between retinal detachment and retinoschisis was found. Enhanced-depth imaging OCT (EDI-OCT) has also been used to evaluate the sclera and to determine the mean submacular scleral thickness. Hyashi et al. and Imamura et al. used EDI-OCT to measure subfoveal scleral thickness in highly myopic eyes, finding a mean, respectively, of 284 µm and 291 µm (range, 132–434 µm) (Hayashi et al., 2013; Imamura et al., 2011).

Several groups have used high-resolution MRI with 3D volume rendering to analyse the topography of the myopic fundus (Moriyama et al., 2011; Ohno-Matsui et al., 2012). Based on the findings from those studies, the authors classified highly myopic eyes according to their shape into different types based on the degree of symmetry between the temporal and nasal halves of the posterior eye segment. Laterally-symmetric eyes were subdivided into barrel and cylinder types. Eyes showing asymmetry in the temporal and nasal halves were further subdivided into nasal and temporal distortion. Nearly 80% of patients presented a symmetric shape in both eyes.

Posterior staphyloma deepens and changes its shape with age. Type I or II staphylomas may evolve into a type IX staphyloma due to the development of a ridge-like protrusion temporal to the optic disk resulting in stretching of the peripapillary sclera (Hsiang et al., 2008).

Ohno-Matsui and colleagues (Ohno-Matsui, 2014) evaluated the role of staphyloma in the development of myopic maculopathy. In that study, the authors concluded that diffuse chorioretinal atrophy and mCNV were more common in staphylomatous eyes than in eyes without staphyloma. They also found that MTM was more common in highly myopic eyes without staphyloma or in eyes with irregular, asymmetric staphyloma.

Fernandez-Vega et al. found that the following conditions were all more common in staphylomatous vs. non-staphylomatous eyes: RPE alterations, neurosensory retinal detachment, retinal cysts, retinoschisis, edge-related mCNV, polypoidal vasculopathy, and optic disk and visual field damage. This location of mCNV is less common than mCNV in the staphyloma fundus. Also, the protrusion appears to have a greater height in eyes without mCNV. Eyes with relative scleral thickening may have a lower risk of neovascular complications (Ellabban et al., 2014; Ohsugi et al., 2013).The aforementioned conditions are more common in inferior and inferonasal staphylomas (Curtin's Type V), although they may arise in other types of staphyloma; moreover, any convexity or edge protruding towards the vitreous cavity might be associated with these conditions (Coco et al., 2012). Hayashi et al. found that subfoveal scleral thickness was associated with staphyloma height but not with the extent of chorioretinal atrophy (Hayashi et al., 2013). Those findings are somewhat controversial considering that other authors have found scleral thickness to be associated with lacquer cracks, mCNV, chorioretinal atrophy, and myopic conus (Steidl and Pruett, 1997).

## 3. Myopic maculopathy

Among the many clinical features of high myopia, probably the most characteristic are those conditions that affect the posterior part of the eye due to axial length elongation, stretching of the posterior eye wall, and staphyloma. These changes may also threaten vision since they often lead to irreversible retinal photoreceptor damage and central visual loss. Scleral ectasia involving the posterior pole of the eye is relatively common, usually leading to poor visual prognosis in adults. Most of the complications related to myopic maculopathy may lead to irreversible macular photoreceptor damage and central visual loss.

The following are considered the most characteristic findings of myopic maculopathy (Fig 4):

- Retinal, choroidal, and scleral thinning (Ikuno et al., 2013; Ohno-Matsui et al., 2018), which often present as variably-shaped posterior staphylomas (Curtin and Karlin, 1971).
- Chorioretinal atrophy, which may appear in different patterns, such as tessellated fundus, diffuse atrophy, patchy atrophy, and lacquer cracks.
- Choroidal neovascularization (Ruiz-Moreno et al., 2009a, 2010, 2011, 2013b, 2015; Silva et al., 2010).
- Maculopathy associated with tractional changes in myopic eyes has varying consequences, including myopic macular hole (MH), and myopic foveoschisis, among others.
- Dome-shaped macula, characterized by the concave shape of the sclera and often associated with serous, non-progressive retinal detachment (Gaucher et al., 2008).
- Macular Bruch membrane holes, as a distinct form of chorioretinal atrophy (CRA) characterized by the absence of the choriocapillaris, Bruch's membrane, RPE, and photoreceptors. Bruch's membrane holes can be a hallmark of patchy atrophy and can be associated to lacquer cracks, staphyloma or diffuse atrophy (Ohno-Matsui et al., 2016a).

In 1970, Curtin and Karlin were the first to propose a definition for myopic maculopathy, which included the presence of all of the following: chorioretinal atrophy; central pigment spots; lacquer cracks; posterior staphyloma; and optic disc changes (Curtin and Karlin, 1971). Tokoro would later classify myopic maculopathy into four categories: 1) tessellated fundus, 2) diffuse chorioretinal atrophy, 3) patchy chorioretinal atrophy, and 4) macular haemorrhage (Tokoro, 1998). Avila proposed a new classification system in 1984 (Avila et al., 1984). Despite the numerous proposed classification systems, most published studies on pathologic myopia have not used any of these (Avisar et al., 2006; Buch et al., 2004; Cedrone et al., 2003; Cotter et al., 2006; Iwase et al., 2006; Klaver et al., 1998).

Liu et al. defined "degenerative myopia" as follows: ≥ 6 negative diopters in the presence of atrophic changes and stretching of the macula (Liu et al., 2010). Asakuna defined myopic maculopathy as the presence of ≥ one of the following: diffuse chorioretinal atrophy at the posterior pole, patchy chorioretinal atrophy, lacquer cracks, or macular atrophy (Asakuma et al., 2012). The definition of this entity proposed by Vongphanit et al. was as follows: the presence of staphyloma, lacquer cracks, Fuch's spot, and myopic chorioretinal thinning or atrophy (Vongphanit et al., 2002b). Given these heterogenous definitions and terminology, an international group of experts in high myopia met in order to develop a simplified, systematic classification based on a meta-analysis of pathologic myopia (META-PM) (Ohno-Matsui et al., 2015). This group classified myopic maculopathy into five different categories based on atrophic changes, as follows: no myopic retinal lesions (category 0), tessellated fundus only (category 1), diffuse chorioretinal atrophy (category 2), patchy chorioretinal atrophy (category 3), and macular atrophy (category 4). Up to three "plus" signs could be added to any of these categories to indicate the presence of lacquer cracks, mCNV, and Fuch's spot. The developers of that classification system emphasized their hope that future epidemiological studies and clinical trials would adopt this classification system in order to standardize findings. That system was an important step forward, as it greatly simplified the identification of atrophic changes into defined categories, while also allowing for a neovascular component to be added. However, many patients with macular alterations due to high myopia are not sufficiently represented by that atrophy-centred classification system.

Patients with vitreomacular interface alterations caused by longer axial length, as occurs in patients with myopic foveoschisis, should also be included in pathologic myopia classification systems. At present, however, the classification proposed by Ohno-Matsui et al. does not include macular conditions of tractional origin or neovascular maculopathy, which, even if they are present, are only considered as an extra factor in other categories. Given these drawbacks, one of the aims of the present review is to propose a new, more comprehensive classification system, which is described in detail at the end of this document.

Given that some eyes present axial elongation in the context of high myopia but show no alterations in the curvature of the posterior pole—that is, axial myopia without staphyloma - it is clear that axial elongation alone is insufficient for a diagnosis of posterior staphyloma. In fact, posterior staphyloma has been described in eyes without high myopia (Wang et al., 2016). Nevertheless, it must be acknowledged that the vast majority of patients with posterior staphyloma present axial elongation. The development of a posterior staphyloma induces a large increase in axial length, while the surface of the posterior pole—-including the macular area and the optic disc—widens substantially, up to twice the size of regular eyes (Ohno-Matsui et al., 2016c). Another working hypothesis is that excessive axial elongation triggers stresses in the posterior pole of the eye, which can lead—almost stochastically—to degeneration in the retina and/or choroid, rupture of Bruch's membrane, and staphyloma. In the presence of any of these alternations, other pathological changes are accelerated due to an increase in stresses and strains.

One of the aims of the present review is to provide a straightforward definition of "myopic maculopathy". The proposed definition is as follows: macular alterations induced by high myopia, in which an excessive axial length and/or posterior staphyloma is the main common factor but not the only factor (as we discuss later in this paper). These macular alterations include not only atrophic changes, which are the basis of the majority of current classifications, but also neovascular alterations, traction-induced changes to the macula, and specific modifications of the posterior pole profile that may cause myopia-related conditions, such as DSM. For these reasons, myopic maculopathy can be classified into one of three categories: 1) atrophic myopic maculopathy, 2) neovascular myopic maculopathy, and 3) tractional myopic maculopathy. However, none of these should exclude the others, as different types of myopic maculopathy may coexist in the same eye, as we have observed in our clinical practice.

The main factor that is common to all three of these categories is the presence of increased axial length, posterior staphyloma, or both, leading to a decrease in BCVA. One study found a linear correlation between the degree of staphyloma and the presence of atrophy or lacquer cracks (Steidl and Pruett, 1997). Ohno-Matsui found that BCVA was lower in eyes with staphyloma (regardless of type) compared to eyes without any staphyloma (Ohno-Matsui, 2014). Diffuse chorioretinal atrophy and myopic traction maculopathy are significantly more common in eyes with a wide staphyloma (Ohno-Matsui, 2014).

Paradoxically, a preserved choriocapillaris is theoretically required for mCNV to develop, which is why mCNV seems more common in eyes with less advanced staphylomas. However, Ishida et al. used SS-OCT to evaluate 124 eyes from 112 patients with mCNV, finding a possible direct communication between short posterior ciliary arteries and CNV through a defect in Bruch's membrane (Ishida et al., 2018); on the other hand, OCT-based studies of staphylomas describe a high prevalence of MTM (Baba et al., 2003; Benhamou et al., 2002; Forte et al., 2007; Henaine-Berra et al., 2013; Hirakata and Hida, 2006; Oie et al., 2005;

Panozzo and Mercanti, 2004; Rahimy et al., 2013; Takano and Kishi, 1999; Wu et al., 2009). Vitreoretinal interface alterations are more common in larger staphylomas (Ripandelli et al., 2008).

Myopic MH is more common among eyes with posterior staphyloma. Oie et al. compared highly myopic eyes with full-thickness MH, with and without retinal detachment, concluding that posterior staphylomas are significantly more common in eyes with MH-related retinal detachment (Oie et al., 2005).

Both Ohno-Matsui et al. and Verkicharla et al. (Ohno-Matsui, 2014; Verkicharla et al., 2015) suggest that pathologic myopia should be defined as category 2 myopic maculopathy, with the presence of plus signs or posterior staphyloma. However, we disagree with those authors. In our opinion pathologic myopia should be defined as the presence of axial elongation or a posterior staphyloma that induces myopic maculopathy. However, it is crucial to keep in mind the progressive nature of pathologic myopia. In this regard, newer, more complete classification systems are needed to include and better describe all of these options. Moreover, the availability of a more comprehensive system would facilitate follow-up of these patients.

## 4. Atrophic myopic maculopathy

Atrophic myopic maculopathy (AMM) could be considered the myopic equivalent of atrophic AMD, either as the primary consequence of myopic choroidopathy or as an outcome of neovascularization. AMM is associated with a progressive decrease in BCVA.

Chorioretinal degeneration of the posterior pole is considered the most common change in the fundus (Curtin, 1979). This condition has been described as circumscribed areas of choroidal degeneration initially involving the crescent and consisting of focal patches of tissue deprived from the RPE and choriocapillaris, with pigment clumping inside or at the edge of the lesion. These areas subsequently become confluent, forming large geographic areas of atrophy that merge with an enlarged peripapillary degenerative zone (Fig 5).

Although the pathogenesis of AMM is not well-understood, it is believed to be associated with the staphyloma, which may cause local changes to the choroid and retina that progressively damage the neighbouring tissues; in addition, excessive axial elongation is associated with stretching of the ocular coats, as evidenced by retinal vessel straightening and chorioretinal thinning (Blach et al., 1965; Curtin, 1988, 1977; Curtin and Karlin, 1971). It is uncertain whether these changes are part of a genetically-predetermined abiotrophic process that is independent from scleral thinning, or whether these alterations are caused by biomechanical changes induced by scleral expansion with normal intraocular pressure, which is the more widely-accepted mechanism (Mcmonnies, 2016). These changes are probably induced by a structural weakness that reduces the scleral mechanical resistance to normal intraocular pressure or by the action of extraocular muscles. It has also been suggested that the axis of astigmatism may play a role in early myopic chorioretinal degenerative changes (Ahmad et al., 2010).

Light microscopy shows the effects of scleral elongation on the posterior pole; these effects include scleral distension and thinning with choroidal attenuation and loss, RPE pigment loss, and loss of the outer retinal layers (Grossniklaus and Green, 1992). These degenerative changes first affect the external retinal layers, only later affecting the inner layers. These alterations are more evident in eyes with DSM, in which Bruch's membrane is often defective, and this defect may be associated with the loss of the RPE as well as the outer and central retinal layers and choriocapillaris (Fang et al., 2017). In this process, the choroid degenerates and atrophies, larger choroidal vessels and melanocytes disappear, and the choriocapillaris becomes thinner (Grossniklaus and Green, 1992; Okabe et al., 1979). RPE cells become enlarged and eventually degenerate and disappear and are replaced by Müller cells. Bruch's membrane becomes thinner, divided, and fragmented and the neurosensory retina becomes thinner.

As in AMD, aging affects the RPE and thus damage to the RPE is more severe among elderly highly myopic patients. The RPE becomes attenuated with pigment deposits. The spatial distribution of lipofuscin generally matches that of rods and reflects the pattern of age-related loss of rod photoreceptors. Lipofuscin fluorescence increases linearly until the 8th decade and then declines; in such cases, the decrease in autofluorescence may indicate removal of atrophic RPE cells (Delori

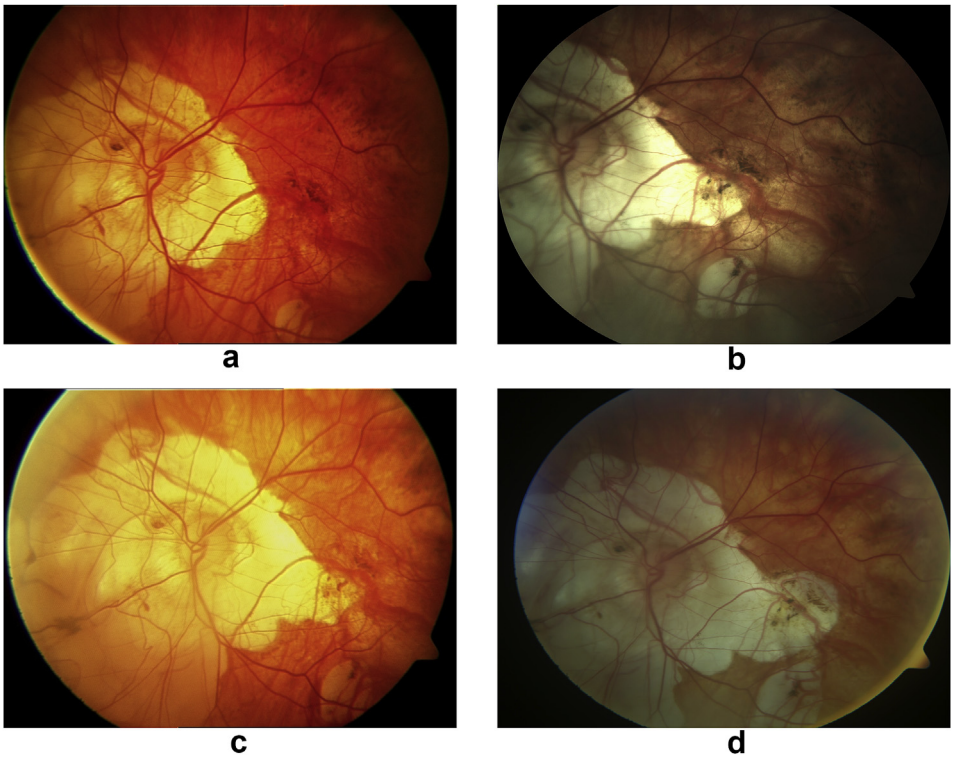


**Fig. 5.** Progressive enlargement of the area of chorioretinal atrophy surrounding the optic disk, which eventually involves the fovea.

et al., 2001). Multifocal electroretinography reveals early functional changes in the outer retina, which may precede chorioretinal atrophy (Ishikawa et al., 1990).

Anteroposterior elongation induces progressive thinning and stretching of the ocular layers, with retinal vessel rectification, retinal and choroidal thinning, and the development of a tractional crescent. Stretching of ocular tissues induces changes in choroidal haemodynamics, causing loss of choroidal stroma and vessel obliteration, leading to choroidal thinning (Stafford, 1982). Choroidal thinning, which has been observed on EDI-OCT, is typically associated with age and the degree of myopia (Fujiwara et al., 2009). Focal areas of atrophy may be present; these areas typically appear as rounded or irregular forms and they can be small or large, isolated or multiple; these foci tend to grow and merge over time. Choroidal and RPE thinning facilitates visualization of larger choroidal vessels.

Even though atrophic changes are not always directly related to ocular elongation, they often occur when elongation is present. Occlusion of the large and small choroidal vessels leads to the development of fibrotic tissue (Okabe et al., 1982) and photoreceptor loss (due to reduced oxygenation), which reduces retinal thickness, thus leading to central vision loss.

The choroidal volume on EDI-OCT is smaller in highly myopic eyes than in emmetropic eyes, even without AMM (Barteselli et al., 2014). To satisfy the metabolic demands of the normal retina, blood flow in the choroid is high; however, a thinned choroid may be unable to provide the required amount of oxygen and nutrients, which in turns negatively affects retinal function. Some reports suggest that choroidal thinning may predict the formation of lacquer cracks. AMM progression is preceded by choroidal thinning, which can be seen one both EDI-OCT and SS-OCT, as reported by Zaben et al. (Zaben et al., 2015). AMM becomes more severe over time (Ikuno et al., 2013) (Fig 6). In such cases, patients retain a relatively good BCVA until choriocapillaris atrophy induces RPE atrophy (Gupta et al., 2016; Pang et al., 2015). As choroidal thinning increases, the RPE becomes affected and blue autofluorescence decreases (Fig 7). On SD-OCT, highly myopic eyes with AMM present thinning of the retinal nerve fibre layer (Koh et al., 2016b). However, the most striking findings are thinning of the choroid and choriocapillaris followed by retinal destructuring.

Choroidal thinning is associated with age, axial length, sex, and staphyloma. It is more intense in eyes with previous MTM or mCNV (Barteselli et al., 2014). Studies have shown that extreme choroidal thinning can be compatible with good BCVA as well as preserved fundus autofluorescence (FAF), suggesting that choroidal thickness alone is not a reliable indicator of visual function (Pang et al., 2015). However, the complete disappearance of the choroid implies a definite decline in BCVA.

On microperimetry, choroidal thinning is associated with diffuse choroidal atrophy, lacquer cracks, and decreased macular sensitivity in the external macular rings. Macular sensitivity decreases with age and with the increasing severity of the myopia. Changes in the mean macular sensitivity correlate closely with choroidal thickness, age, spherical equivalent, and BCVA but not with retinal thickness (Zaben et al., 2015).

Macular thinning causes dispersion of the luteal pigment and hinders foveal localization. However, in the early stages of myopic elongation, increased axial length has been associated with increased macular thickness (Lam et al., 2007), probably due to a mechanical effect of vitreomacular traction, even in the absence of macular retinoschisis.

Systemic conditions may play a role in the development and enlargement of macular atrophy. Chen et al. (Chen et al., 2012) identified increased systemic blood pressure (BP) as a risk factor for developing myopic maculopathy: an increase of 10 mm Hg in systemic BP increases the odds of developing maculopathy by a factor of 1.5 in highly myopic patients after adjusting for confounding factors. Patients with more severe forms of macular atrophy and mCNV have higher systemic BP than patients with less severe macular changes. A similar association has been found for exudative AMD (Klein et al., 2007). It has also been reported that systemic BP influences choroidal thickness, with higher BP associated with a thinner choroid, which may further compromise choroidal thickness in hypertensive myopic patients, thereby affecting choroidal circulation and aggravating myopic maculopathy (Usui et al., 2012).

Aging has an impact on the anatomical and functional outcomes of patients with myopic maculopathy. Shih et al. (Shih et al., 2006) evaluated the effect of myopic maculopathy on BCVA, finding a significant correlation between lower BCVA and age in myopic eyes. Those authors also observed that aging was associated with more advanced forms of AMM and worse BCVA, and with the development and coalescence of atrophic areas, extension of lacquer cracks, increased areas of atrophic choriocapillaris, and a higher likelihood of presenting mCNV ingrowths from ruptured Bruch's membrane (Ohno-Matsui and Tokoro, 1996; Shih et al., 2006).

Lacquer cracks are ruptures in the RPE-Bruch's membrane-choriocapillaris complex and are usually associated with posterior staphyloma. The presence of mCNV may indicate an anomalous response of a wound-healing mechanism. These lesions appear as multiple yellowish-white irregular lines, usually horizontally-oriented, and can be linear or stellate, occasionally branching or crisscrossing. They are more common in males and decrease with age. Fluorescein angiography (FA) shows a window defect appearing as hyper-fluorescent tracks without any leakage. On FAF, there is a hypoautofluorescent pattern.

Avila and colleagues were the first to propose a classification system to describe the natural course of AMM based on FA and stereoscopic fundus photographs. The proposed classification system consists of six different grades ranging from M0 to M5, as follows: M0, normal-appearing posterior pole; M1, choroidal pallor and tessellation; M2, choroidal pallor and tessellation with posterior pole staphyloma and lacquer cracks; M3, Bruch's membrane rupture with superficial chorioretinal atrophy; M4, the same changes as M3 but with focal areas of deep choroidal atrophy; and M5, the same as M4 plus large geographic areas of deep choroidal atrophy (Avila et al., 1984). However, due to the study design—a cross-sectional survey rather than a longitudinal study—that classification system had some errors, such as including staphyloma and lacquer cracks as part of the process of progression. That classification system was later modified to include rounded atrophic lesions and lesions surrounding lacquer cracks in stage M3 (Tokoro, 1998).

A few longitudinal studies have been performed to assess myopic maculopathy progression caused by increasing atrophy (Vongphanit et al., 2002b), which is associated with progressive vision decrease (Shih et al., 2006). Of those studies, perhaps the most comprehensive was performed by Hayashi et al., who observed that the early presence of lacquer cracks and staphyloma subsequently affected the progression of atrophy (Hayashi et al., 2010). Those authors retrospectively evaluated 429 highly myopic patients (spherical equivalent $> -8.00$ diopters or axial length $\geq 26.5$ mm) who had more than 5 years follow-up. Myopic maculopathy was classified according to a modified version of Tokoro's definition as follows: tessellated fundus, diffuse chorioretinal atrophy, patchy chorioretinal atrophy, and macular haemorrhage (Tokoro, 1998). Patchy chorioretinal atrophy was further subdivided into atrophy associated with lacquer cracks, atrophy associated with posterior staphyloma, and circular lesions in areas with advanced diffuse chorioretinal atrophy (Fig 8). The authors described a tentative progression pattern for myopic maculopathy in which the first sign is a tessellated fundus, which may progress to diffuse atrophy or lacquer cracks or—less commonly—to mCNV. Lacquer cracks and patchy atrophy are the most common predisposing factors for the development of mCNV. Patchy atrophy represents a complete atrophy of the RPE-choriocapillaris. Tissue damage at the edge of these lesions may induce the development of mCNV (Ohno-Matsui et al., 2003). More recently, Fang et al. reported on a large series of highly myopic eyes with a mean follow-up of $18.7 \pm 7.1$ years (Fang et al., 2018). Progression to

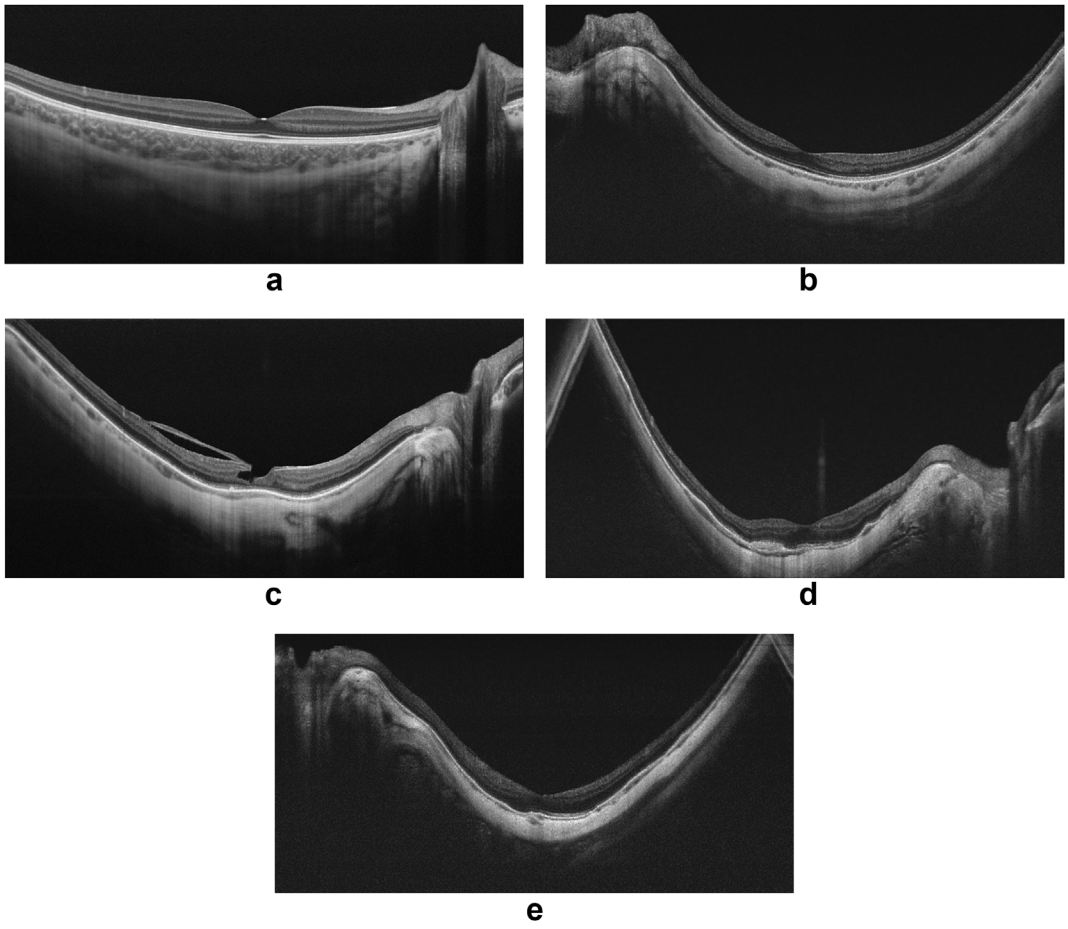


**Fig. 6.** Macular choroidal thickness in an emmetropic eye (a) and in highly myopic eyes presenting a thin choroid in all four cases: (b) highly myopic eye with normal retinal layers; (c) highly myopic patient showing myopic traction maculopathy, lamellar macular hole, and normal outer retinal layers; (d) highly myopic eye with Fuch's spot and loss of outer retinal layers; (e) highly myopic eye with normal inner retinal layers and focal disruptions of outer layers.

myopic maculopathy was detected in 74.3% of the eyes with pathologic myopia and was more common in eyes with more severe forms of atrophy, especially those that presented macular atrophy and patchy atrophy at baseline. The risk of progression was higher among older patients and those with parapapillary atrophy, longer initial axial length, and axial elongation. Rates of progression were also higher among elderly patients and women, mainly among those with pathologic myopia at baseline. The authors hypothesized that the holes in Bruch's membrane that appear in patchy atrophy might play a role in this higher progression rate versus eyes with diffuse atrophy due to choroidal thinning. This faster progression was observed even in the absence of lacquer cracks or CNV and was attributed to the enlargement of Bruch's membrane defects following axial elongation. The authors propose a progression scheme of myopic atrophy based on changes related to choroidal thinning, from normal to tessellated fundus and extension from peripapillary diffuse chorioretinal atrophy to macular diffuse atrophy.

In the more severe forms of myopic atrophy, the atrophic changes may be mostly related to the presence and enlargement of Bruch's membrane holes, such as the progression from lacquer cracks to patchy atrophy and finally patchy-related macular atrophy, and the progression from myopic CNV towards CNV-related macular atrophy (Fang et al., 2018) (Scheme 1 bottom). However, in that study the authors did not evaluate the role of the staphyloma, an acknowledged limitation of the study.

Diffuse atrophy can lead to circular areas of atrophy or to lacquer cracks and to the formation of mCNV. Myopic CNV can progress to macular atrophy in the surrounding areas (Fig 9). Lacquer cracks may induce further localized atrophic areas, which grow from the border of the cracks, or it may lead to the development of mCNV. Atrophic patches may coalesce to form larger atrophic areas leading to macular atrophy. However, these atrophic changes do not progress in a uniform manner. Increasing age and the presence of a staphyloma both promote the development of atrophy.

In their series, Hayashi et al. observed that 40% of highly myopic eyes—particularly eyes with posterior staphyloma—showed progressive chorioretinal atrophy. These findings suggest that posterior staphyloma should not be considered a single stage in the classification system, but rather a key component of the progression of atrophy. Hayashi and colleagues further subdivided diffuse atrophy into lacquer cracks and genuinely diffuse atrophy. Macular haemorrhages were classified according to their association with mCNV, and areas of focal atrophy were subdivided into three types: 1) atrophy originating from lacquer cracks (more common in the perifoveal area), 2) atrophy that develops within an area of diffuse atrophy, and 3) atrophy derived from the staphyloma.

Hayashi et al. described the progression of myopic maculopathy (Hayashi et al., 2010), as follows: tessellated fundi evolve into diffuse atrophy with lacquer cracks, which is followed by progression and an increasing area of patchy atrophy in eyes with lacquer cracks. Next, there is enlargement of the diffuse atrophic areas followed by the emergence of atrophic patches in eyes with diffuse atrophy. Finally, the atrophic areas become enlarged and coalesce. These changes were less evident in eyes with tessellated fundi. Those authors found that lacquer cracks appeared at a relatively early stage of maculopathy and were unrelated to other changes, such as diffuse atrophy or staphyloma,

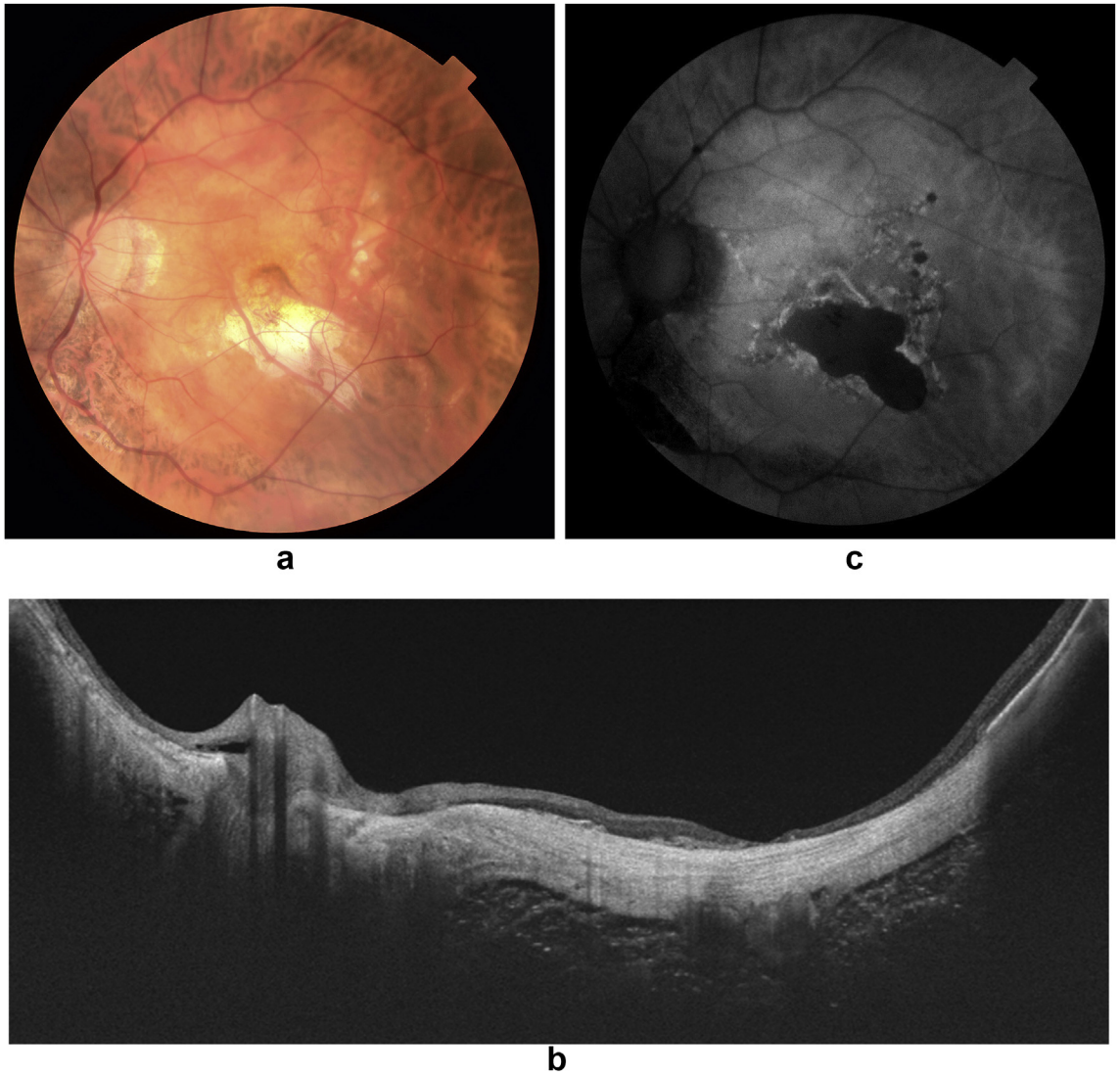


**Fig. 7.** Fundus photography (a), swept-source optical coherence tomography (b) and blue autofluorescence (c) in a highly myopic patient. Loss of the choriocapillaris is associated with decreased blue autofluorescecnce and disappearance of the RPE and outer nuclear layer.

which theoretically, appear earlier than lacquer cracks.

Myopic CNV is more common in eyes with tessellated fundi, lacquer cracks, and diffuse and patchy atrophy. Myopic CNV is followed by an enlargement and coalescence of the atrophic areas, which further reduces visual function. Eyes with posterior staphylomas are more prone to progressive tessellation towards diffuse and patchy atrophy. Progression of these atrophic changes tends to occur more quickly in more advanced stages beyond the tessellated fundus, and especially in eyes that already present some degree of atrophy or mCNV.

Although intravitreal administration of anti- VEGF induces regression of the mCNV, chorioretinal atrophy still can appear around the regressed mCNV. Moreover, this atrophic area may become enlarged, thus reducing BCVA. Uemoto et al. (Uemoto et al., 2012) identified three main factors associated with enlargement of the atrophic area after intravitreal injection: 1) size of the mCNV at baseline; 2) number of injections required to inactivate the lesion; and 3) duration of follow-up. Those authors also observed that the extent of the decrease in mCNV after treatment and the presence of subretinal blood might play a role in determining the final outcome. Finally, the rate at which the mCNV shrinks has been associated with the development of chorioretinal atrophy, which might be related to RPE damage induced by centripetal contraction of the RPE surrounding the mCNV (Hayashi et al., 2009; Uemoto et al., 2012).

Based on our clinical experience, several other factors may play a role in this process: age; the time elapsed between mCNV development and treatment; and the type of treatment used—photodynamic therapy (PDT) induces more atrophy than intravitreal anti-VEGF drugs (Montero and Ruiz-Moreno, 2003; Ruiz-Moreno et al., 2008, 2009a, 2010, 2011, 2013b, 2015; Silva et al., 2010).

The most common patterns of progression are from tessellated atrophy to diffuse atrophy with lacquer cracks, followed by growth of the atrophic areas surrounding the lacquer cracks and the diffuse atrophy into atrophic patches and then by atrophy in the mCNV after neovascularization, followed by coalescence of the atrophic areas. Diffuse atrophy may evolve into atrophic patches or lacquer cracks with or without mCNV, and lacquer cracks may lead to focal atrophy or mCNV. Atrophic areas can merge to form geographic areas of atrophy while mCNV may evolve into areas of diffuse atrophy. Age, axial length, and staphyloma all seem to play a role in the progression of myopic maculopathy (Hayashi et al., 2010) (Scheme 1).

Due to the wide clinical variation, the evaluation and classification of highly myopic eyes is challenging. Yoshihara et al. developed a classification system to quantify tessellation based on three tessellated fundus indices. That system demonstrated good repeatability with regard to the subjective and objective classification of the degree of tessellation. In that system the mean red, green, and blue intensity are

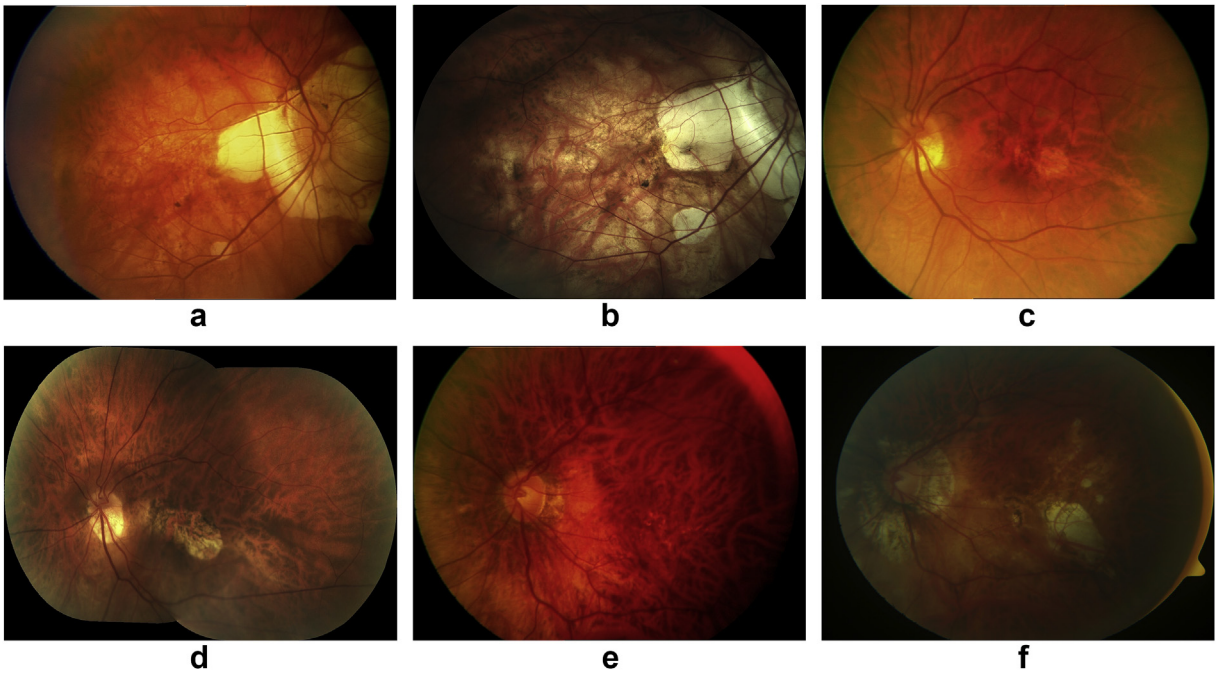


**Fig. 8.** Chorioretinal atrophy progression patterns associated with diffuse chorioretinal atrophy (a,b), border of the staphyloma (c,d) and lacquer cracks (e,f) according to Tokoro's classification (Tokoro 1998).

assessed in the area located between the fovea and the optic disk (Yoshihara et al., 2014). More recently Ohno-Matsui et al. proposed a new classification and grading system for myopic atrophy (Ohno-Matsui et al., 2015). Those authors found that early atrophic changes—that is, tessellated and diffuse atrophy—were more common among younger patients and those with milder myopia and shorter axial lengths. However, Hayashi et al. found that, compared to diffuse atrophy, patchy atrophy was associated with longer axial lengths, lacquer cracks, and mCNV (Hayashi et al., 2010).

Patients with patchy atrophy have a worse visual prognosis than those with lacquer cracks, especially when the atrophic areas merge. Aging further aggravates this atrophy by inducing enlargement and coalescence of lacquer cracks, thus increasing the atrophic areas and the risk of neovascularization. Perimetric defects are common in highly myopic eyes. Myopic fundus lesions can explain some defects. Ohno-Matsui et al. observed a decrease of nearly 15% in the outermost macular isopter in highly myopic eyes (Ohno-Matsui et al., 2011).

Electrophysiological findings usually show substantial alterations. Electroretinogram (ERG) studies usually show that a and b waves are equally affected, with deep a waves and reduced b waves. Dark adaptation is affected in eyes with more extensive atrophic changes (Blach et al., 1966). The ERG wave amplitude pattern is inversely related to axial length (Hidajat et al., 2003). Electrooculogram values are usually low, but not necessarily below the lower limit of normal values. However, the extent of this reduction seems to be related to the degree of chorioretinal atrophy (Blach et al., 1966).

Fluorescein angiography shows very low contrast in highly myopic eyes due to the low choroidal blood flow and the decreased light absorption caused by choroidal and RPE thinning, which leads to an increased reflection of light in the sclera. FAF studies show four well-defined patterns: 1) an area of reduced FAF around lacquer cracks and mCNV surrounded by an area of augmented FAF; 2) well-defined small or multi-lobular areas with reduced FAF within an area of increased FAF; 3) larger, well-defined lobular or multilobular areas of reduced FAF within an area of increased FAF; and 4) wide areas of reduced FAF in the regions of chorioretinal atrophy (Parodi et al., 2015; Sawa et al., 2008). These areas of decreased FAF are associated with decreased vision and emerge relatively late in the process despite the progressive thinning of the choriocapillaris.

### 4.1. Management

At present, the available options to manage myopic chorioretinal atrophy are limited, especially the most advanced forms of this condition. However, since patients maintain peripheral vision, low vision aids—such as high-addition monofocal, bifocal, or trifocal lenses, and hand-held or self-standing magnification systems—may be useful in some cases. However, published data on the value of such aids is limited (Bray et al., 2017; Kollbaum et al., 2013; Vincent, 2017).

Early and aggressive management of myopic mCNV by intravitreal anti-VEGF therapies may help to reduce the progression of atrophic areas surrounding lacquer cracks and mCNV. An alternate approach might be to limit the extent and progression of the posterior staphyloma, which reportedly plays a role in the progression of macular atrophy (Steidl and Pruett, 1997). Some authors (Mateo et al., 2012) have attempted to encircle the sclera behind the macula—as is done in macular buckling to manage myopic foveoschisis with both hard silicone implant and macular plombe—successfully reducing retinal thickness with this technique. However, a drawback of this approach is localized areas of RPE atrophy, which was the most common complication observed by Mateo and colleagues.

Presently there are no pharmacological treatments for chorioretinal atrophy. However, human RPE transplantation may be useful to treat degenerative retinal conditions. Transplantation of RPE sheets and suspensions of individual RPE cells have been used to treat AMD and this approach could also be used for myopic chorioretinal atrophy. We recently searched www.clinicaltrials.gov (access date, May 29, 2018), finding 62 entries for *dry AMD*, 278 for *wet AMD*, 23 for *myopic CNV* and only 10 (3 of which were for stem cell therapy) for *myopic macular degeneration*. One of the phase 1–2 trials (NCT02122159) identified by this search involved subretinal injection of fully-differentiated human RPE cells derived from embryonic stem cells (MA09-hRPE) in patients with myopic macular degeneration. However, that trial had been withdrawn from the database (as of May 29, 2018) for unknown reasons. Two other trials (NCT01920867 and NCT03011541) are currently underway. Those studies—which use a combination of retrobulbar,

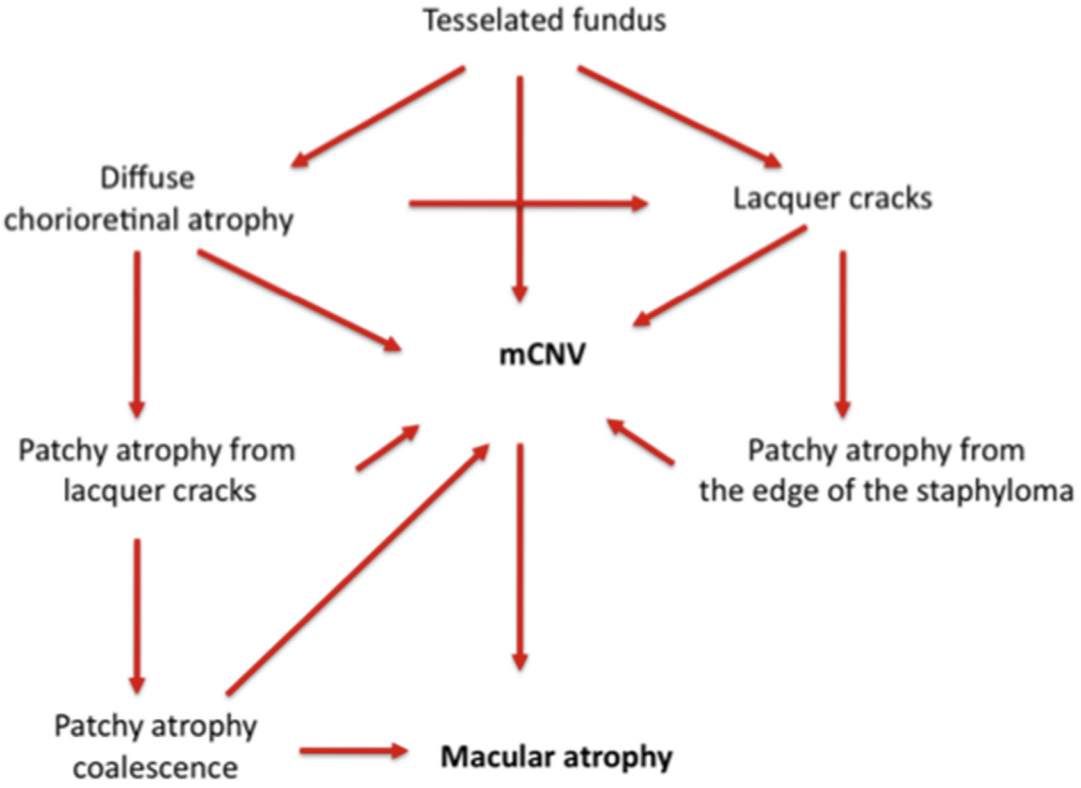


**Changes related to progressive choroidal thinning**

Normal fundus → Tesselated fundus

Peripapillary diffuse chorioretinal atrophy → Macular diffuse atrophy

**Changes related to formation and enlargement of Bruch's membrane holes**

Lacquer cracks → Patchy atrophy → Patchy-related macular atrophy

Myopic CNV → CNV-related macular atrophy

**Scheme 1.** Top: Progression patterns towards chorioretinal atrophy from a range of different initial lesions combined with the development of mCNV. Modified from (Hayashi et al.2010). Bottom: Progression patterns related to changes in choroidal thinning and Bruch's membrane holes. Modified from (Fang et al. 2018).

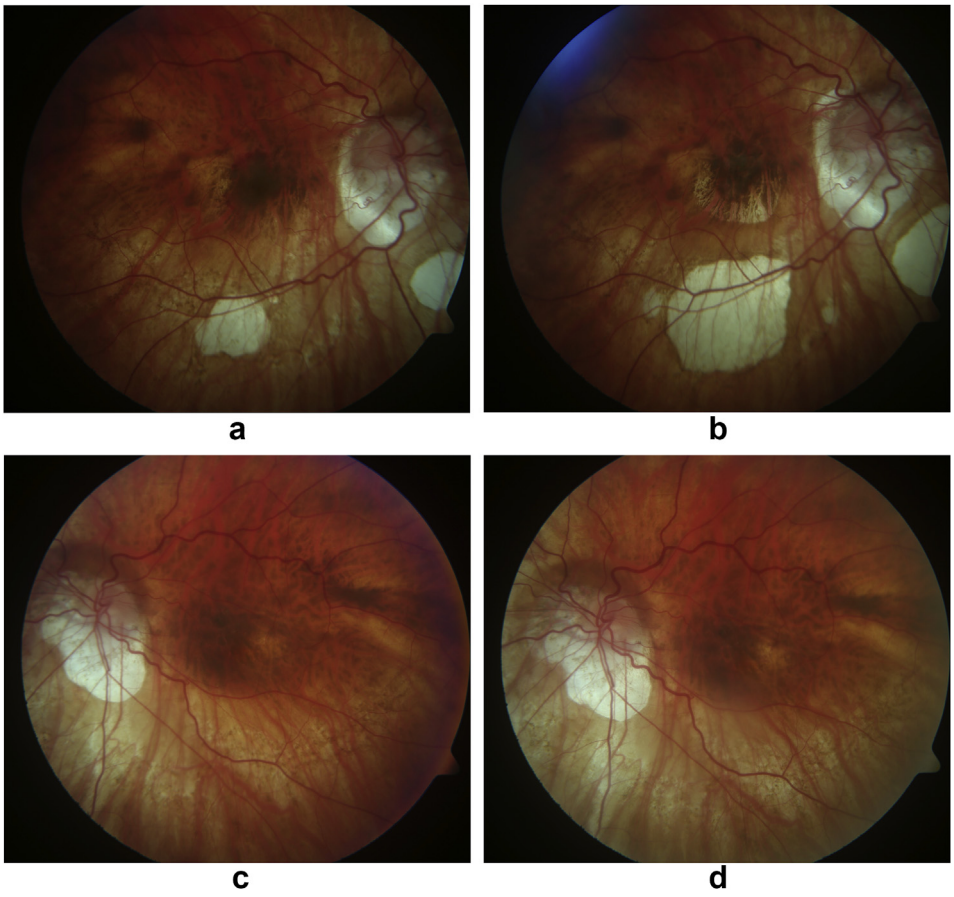


**Fig. 9.** Right (a,b) and left (c,d) eyes from the same myopic patient. Note the progression of the atrophic area in the left eye (c–d) surrounding the central, healed myopic choroidal neovascularization.

subtenon, intravitreal, intraocular, subretinal, and intravenous injections of autologous bone marrow-derived stem cells—are currently recruiting patients with various retinal or optic nerve conditions such as macular degeneration, retinitis pigmentosa, Stargardt, glaucoma, ischemic optic neuropathy, and optic atrophy. Given previous experience with mCNV associated with AMD and high myopia, it seems likely that these promising new therapies for atrophic AMD may eventually play a role in the management of chorioretinal atrophy.

## 5. Neovascular myopic maculopathy

### 5.1. Concept

Neovascular myopic maculopathy is attributed to a disease originating in the choroid, which distorts retinal anatomy due to neovascularization in pathologic myopia. Fuch's spot is defined as any dark spot in the macula in high myopic patients, the presence of which is indicative of late stage mCNV. Secondary to CNV, hyperplasia and migration of RPE cells to the subretinal or intraretinal tissue lead to the development of this spot. Chorioretinal atrophy will typically develop around this lesion, over time leading to atrophic myopic maculopathy (Soubrane, 2008).

### 5.2. Pathogenesis

Several hypotheses have been proposed to explain the pathogenesis of mCNV. The presence of lacquer cracks has been associated with a higher incidence of mCNV, although the development of CNV in patients with previously-existing lacquer cracks has not been available to demonstrate this (Ohno-Matsui et al., 2018). Lacquer cracks are also common in the fellow eyes of patients with mCNV.

Compared to healthy controls, higher VEGF levels have been found in the aqueous humour of patients with mCNV (Tong et al., 2006). One study reported a decrease in VEGF and an increase in pigment epithelium-derived factor (PEDF) in the aqueous humour after three injections of bevacizumab in patients with mCNV (Chan et al., 2008). This suggests that an imbalance between pro- and anti-angiogenic factors leads to the development of mCNV, as occurs in other CNV retinal pathologies, such as neovascular AMD.

There is some evidence to suggest that exposure of RPE cells to certain extracellular matrix components increases VEGF production, while disruption of Bruch's membrane facilitates the emigration of VEGF to the choroidal space, which can then stimulate CNV development (Kwak et al., 2000). Elongation of the myopic eye is usually due to posterior staphyloma, which may facilitate the development of holes or a rupture in Bruch's membrane, as described in patchy chorioretinal macular atrophy (Ohno-Matsui et al., 2016a) and in myopic macular atrophy secondary to CNV (Ohno-Matsui et al., 2016b). Exposure of RPE cells leads to an increase in VEGF, which diffuses through defects (caused by posterior staphyloma) in Bruch's membrane, thus promoting choroidal CNV (Soubrane, 2008). Thinner choroids, characteristic of high myopic patients (Flores-Moreno et al., 2013), could explain the low exudation observed in mCNV, observed as subtle leakage on fluorescein angiography.

### 5.3. Demographics

In a general population-based study involving 4319 participants, Fuch's spot—considered a consequence of mCNV—was present in 3 eyes from 3 patients (prevalence rate, 0.1%). Of the participants in that

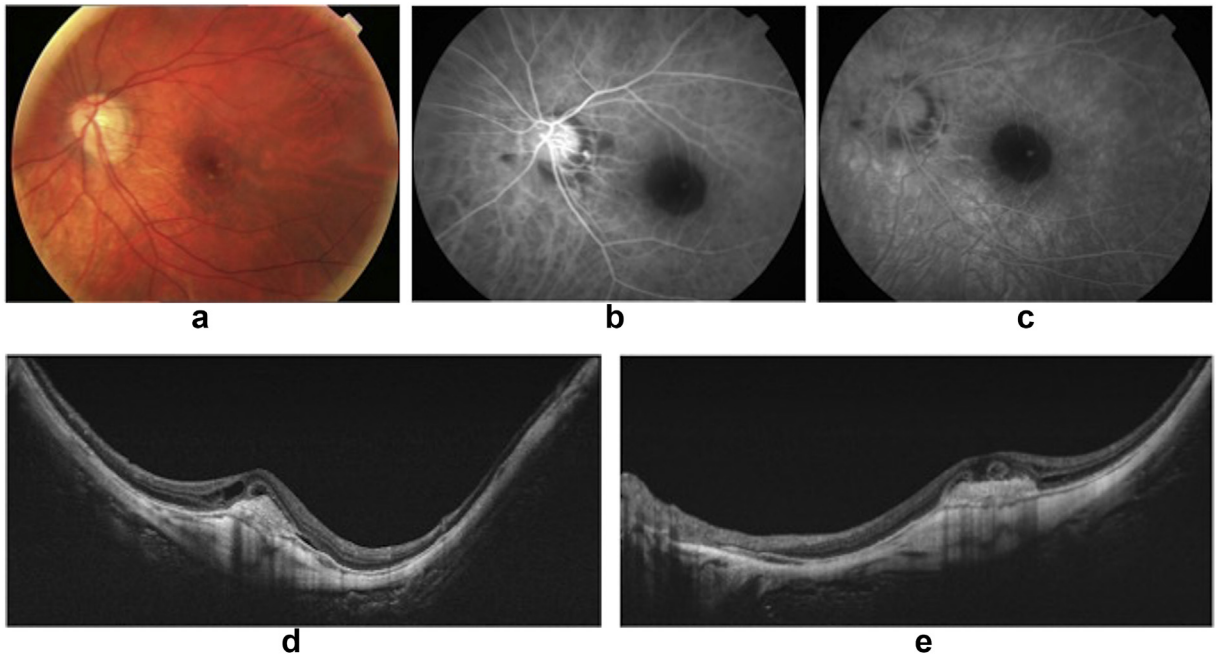


**Fig. 10.** Retinography (a), fluorescein angiography (b,c) and spectral-domain optical coherence tomography (d,e) of a highly myopic patient with myopic choroidal neovascularization (mCNV). These two techniques have a combined sensitivity for the diagnosis of mCNV of up to 97% (García-Layana et al., 2006).

study with myopic retinopathy, the 3 patients with Fuch's spot accounted for 1.5% of that subgroup (Liu et al., 2010). In an older (2002) population-based study performed in Australia, the prevalence of Fuch's spot was also 0.1%; interestingly, the mean spherical equivalent (−11.7 diopters) was higher in these patients (Vongphanit et al., 2002b). In both of those population studies, high myopic patients with retinopathy were re-examined 5 years after the initial examination without any new Fuch's spots being identified in either study.

The reported prevalence of CNV in eyes with pathologic myopia ranges from 5.2% (United States) to 11.3% (Japan) (Cheung et al., 2017). According to one study, 14% of patients have bilateral CNV (Cohen et al. 1996): in that same study, CNV in patients under age 50 was secondary to high myopia in 62% of cases. In the study by Ohno-Matsui et al. (Ohno-Matsui et al., 2003), patients with pathologic myopia were followed for ≥ 3 years (mean, 10.8), during which 10.2% of eyes (n = 32) developed CNV; notably, half of those eyes were the fellow eyes of pre-existing mCNV. In addition, 3.7% of the eyes in the diffuse CRA group developed CNV during follow-up: 20% in the patchy CRA group and 29.4% in eyes with previous lacquer cracks. Epidemiologic studies suggest that mCNV is more common in females (Cohen et al., 1996; Wong et al., 2014).

### 5.4. Clinical characteristics and natural history

The most common symptoms of neovascular myopic maculopathy are sudden, painless vision loss, and central scotoma, usually associated with metamorphopsia. These symptoms are secondary to the build-up of fluid and distortion of the retinal anatomy. The fundus in mCNV presents as a greyish area with hyperpigmented borders, and it is common to observe small amounts of retinal haemorrhage. Myopic CNVs are typically classic neovascular membranes or type 2 neovascularization (Freund et al., 2010), mainly located close to the fovea, although juxtafoveal and extrafoveal localizations are not uncommon. Peripapillary CNV—which develops around the peripapillary chorioretinal atrophy (called periconus CNV)—may also occur.

Characteristically, mCNV has a primary phase during which neovascularization develops slowly, probably due to a thin choroid, which becomes progressively thinner as the axial length increases (Flores-Moreno et al., 2013). At this primary stage, CNV activity itself will not cause long-term vision loss. However, CRA developing around the regressed neovascular lesion—probably secondary to RPE damage—will likely play a key role, leading to poor BCVA in the future (Neelam et al., 2012).

### 5.5. Diagnosis

#### 5.5.1. Fluorescein angiography

FA is the most widely-accepted test to study retinal and choroidal circulation in myopic patients. The diagnosis of mCNV is confirmed by FA, which is performed when there is clinical suspicion of mCNV. FA typically reveals a hyperfluorescent area in early frames indicative of filling of the neovascular complex, with late leakage into the CNV area, usually in a classic pattern, which is a sign of neovascular tissue activity. Compared to other causes of CNV, leakage in mCNV is sometimes seen as a subtle change between early and late frames, probably due to a thinner choroid in mCNV (Flores-Moreno et al., 2013). FA is useful to identify the presence, type, extension, and activity of the membrane. FA also helps to differentiate mCNV from other causes of CNV. The differential diagnosis in the presence of macular haemorrhage secondary to lacquer cracks is sometimes challenging, and in this regard FA can be helpful because in cases with mCNV, there is no leakage on the various frames of the angiogram.

Leveziel and colleagues have shown that FA is more sensitive than SD-OCT in new-onset mCNV (Leveziel et al., 2013). In that study, dye leakage was observed on the FA in 82% of eyes whereas exudation signs were present on SD-OCT in only 48.6% of eyes. By combining these two imaging modalities, the sensitivity for the diagnosis of mCNV increases to 97% (García-Layana et al., 2006) (Fig 10).

#### 5.5.2. Indocyanine green angiography

Indocyanine green angiography (ICGA) is sometimes used as a complementary test in the diagnosis of myopic CNV, although it is not very sensitive, as myopic CNV does not show hypercyanescent images in the angiogram. ICGA provides good visualization of the choroidal vessels and lacquer cracks and penetrates through blood, pigment and exudates, which is why it is a valuable complement to other tests in

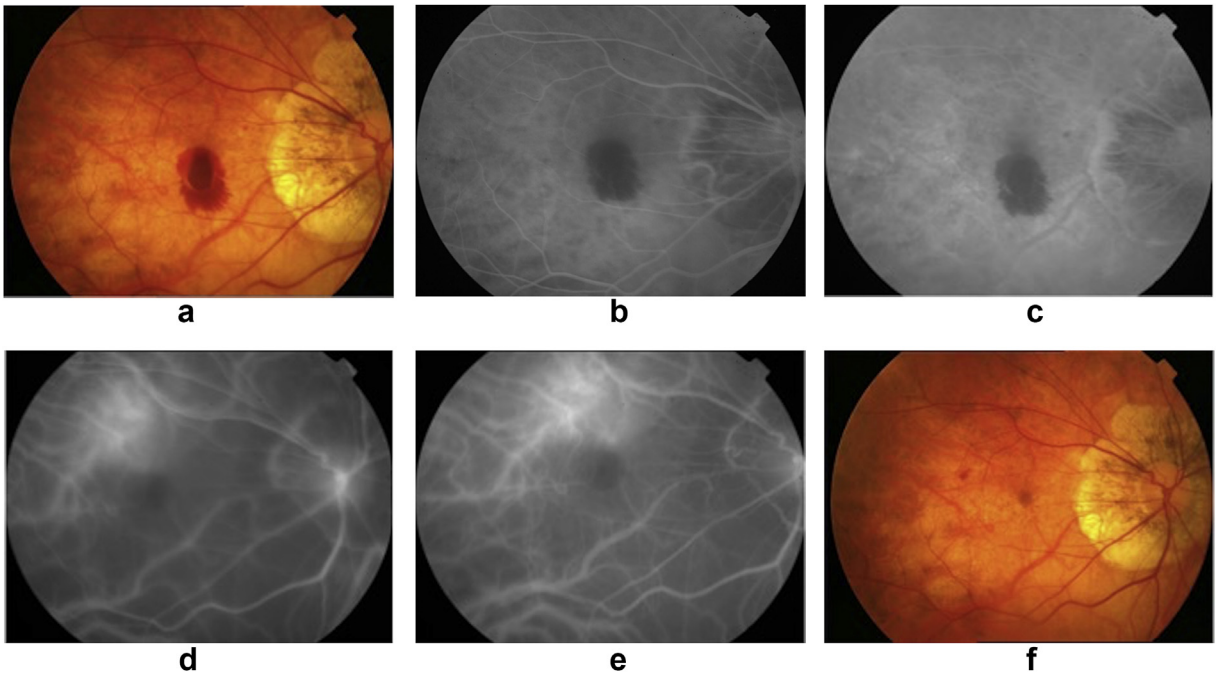


**Fig. 11.** Fundus photography of a highly myopic patient with macular haemorrhage (a). Fluorescein angiography cannot rule out the presence of an active neovascular membrane (b, c). On indocyanine green angiography, no choroidal neovascularization is visible (d, e) and therefore the patient was not treated. Clear improvement is evident one month later(f).

diagnosing difficult cases of mCNV. It is particularly useful as a complementary test in myopic patients with dense macular haemorrhages, helping to confirm mCNV located below the haemorrhage (Fig 11).

### 5.5.3. Fundus autofluorescence

FAF provides good visualization of lipofuscin contained in the RPE. This imaging technique also provides a very good delimitation of CRA, mostly patchy atrophy. However, FAF cannot be used to diagnose new-onset mCNV. On FAF, two different patterns—a hyperautofluorescent pattern and a patchy pattern—have been identified in eyes with mCNV. After treatment with intravitreal ranibizumab, the course of the disease and prognosis differ depending on which pattern is observed. The hyperautofluorescent pattern is associated with a better BCVA gain and fewer atrophic changes while the patchy pattern implies a worse post-treatment prognosis. The hyperautofluorescent pattern is more common, as evidenced in the study by Parodi et al., who observed this pattern in two of the three cases (Parodi et al., 2015) (Fig 7).

### 5.5.4. Optical coherence tomography

OCT is a non-invasive technique that has been successfully used to diagnose and monitor treatment response in mCNV. SD- and SS-OCT both provide a good resolution of the anatomy in high myopic eyes, including the retina, choroid, sclera and, even the retrobulbar elements, such as orbital fat.

Three different stages of CNV have been identified based on the characteristics observed on OCT: active lesion, scar, and atrophic stage (Fig. 12). Active mCNV appears as a dome-shaped elevation with a hyperreflective component above the RPE; given that most cases of mCNV are type 2 CNV, this elevation is associated with retinal thickening and intraretinal fluid, which appears as retinal cysts and subretinal fluid on OCT imaging (Leveziel et al., 2013; Ohno-Matsui et al., 2016c). Interruption of the external limiting membrane (ELM) or lack of ELM visibility correlate with the leakage area observed on FA, and for this reason a missing or interrupted ELM is a good indicator of CNV activity, which is useful for both diagnosis and follow-up (Battaglia Parodi et al., 2016). On OCT imaging, the scar stage is characterized by hyperreflectivity in the inner surface of the CNV, with attenuation of the tissue below. In this stage, there is usually a migration of pigment from the RPE, resulting in a Fuch's spot. During the atrophic stage, the neovascular lesion flattens and CRA develops in the CNV area, resulting in a decrease in BCVA. Reflectivity increases below the atrophic area due to a decrease in RPE pigmentation (Baba et al., 2002) (Fig 12).

### 5.5.5. Optical coherence tomography angiography (OCTA)

OCTA is a novel, dye-less, non-invasive technique based on OCT technology that can detect movement—attributed to the flow of erythrocytes inside the vessels—between scans. OCTA provides high-quality layered images of the retina and choriocapillaris. Simultaneous b-scans show the exact area of flow and the segmentation, which helps to reduce interpretation errors.

Myopic CNV images on the OCTA scan are represented as two different subtypes: 1) a well-organized, interlacing pattern, suggesting a mature membrane, and 2) a small, disorganized vascular loop subtype, indicative of an immature lesion (Bruyere et al., 2017). However, not all authors agree about these patterns. Several authors have failed to identify any clear pattern, describing the lesions as irregular, with poor margin definition, central capillaries, and without any well-defined centre (Cheng et al., 2017; Querques et al., 2016). The neovascular complex appears in the avascular outer retinal slabs of OCTA. This pattern is clearly attenuated after anti-VEGF therapy, showing a decreased flow signal or even a complete regression of the neovascular vessels (Cheng et al., 2017).

The sensitivity of OCTA to diagnosis mCNV is high (90%–94.1%) as is the specificity (93.75%) (Bruyere et al., 2017; Miyata et al., 2016; Querques et al., 2016). However, identifying the neovascular complex in patients with large CRA areas, bad fixation, and very long axial length remains challenging. Despite the advantages of OCTA, this imaging technique has several limitations, mostly in eyes with a long axial length or a deep posterior staphyloma. Layer segmentation is often difficult in these cases, but is crucial to image interpretation. Unfortunately, the images are difficult to interpret in many cases due to motion, projection, and masking artefacts, in addition to a low fixation in many high myopic patients. Consequently, at present, OCTA should be performed in combination with SD-OCT or SS-OCT, using B-scan or

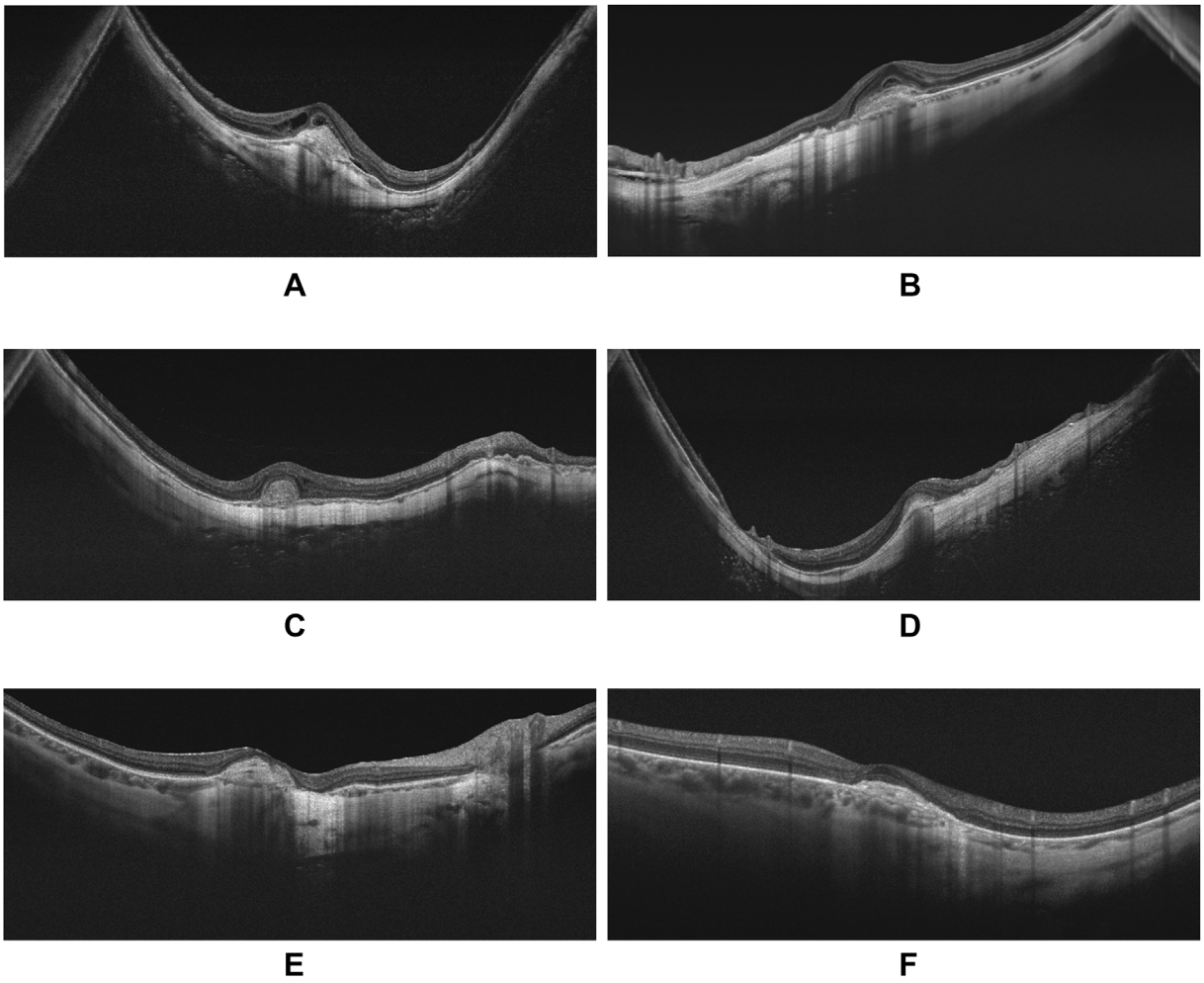


**Fig. 12.** Dome-shaped elevation with hyperreflective component above the retinal pigment epithelium suggesting active choroidal neovascularization (CNV) (a,b); The scar stage is seen on optical coherence tomography, indicated by hyperreflectivity of the inner surface of the CNV with attenuation of the tissue below (c,d). Reflectivity increases below the developing atrophic areas, with a flattening of the lesion (e,f).

*en face* mode, plus FA to check for the presence of CNV activity. In cases where FA or ICGA is absolutely or relatively contraindicated OCTA is preferred to FA or ICGA (Kashani et al., 2017).

OCTA is a promising imaging technique in retinal vascular diseases, and it will undoubtedly help physicians better understand the physiopathology of these diseases. However, the technology requires more development to improve the overall quality of the image, to reduce artefacts, and to obtain better field-of-view and segmentation, especially in high myopic eyes with thin choroids, thin sclera, and posterior staphyloma. Although OCTA will not replace FA or ICGA, it has already decreased the routine use of those techniques (Fig. 13 and 14).

OCTA may be of value in several conditions in which it is difficult to make an accurate differential diagnosis. One example is the multifocal choroiditis (MFC)-punctate inner choroidopathy (PIC) spectrum, which usually affects young myopic women who develop focal deep retinal and choroidal inflammation and have a tendency to develop CNV lesions. In contrast to mCNV, MFC-PIC lesions tend to be multiple, bilateral, with a yellow-white colouring initially, and they may induce an anterior chamber reaction. FAF can accurately detect active lesions. On FA, these lesions usually show optic disc staining, which is not found in highly myopic patients. It is sometimes difficult to distinguish between active inflammatory lesions and CNV because the clinical signs and multimodal imaging findings are similar(Astroz et al., 2018). In this regard, OCTA is highly valuable due to its capacity to detect CNV lesions, which can be seen as an organized high-flow network located in the outer retinal and choriocapillaris images, and to differentiate between CNV and active inflammatory lesions, which show no flow on OCTA (Astroz et al., 2018).

### 5.6. Treatment

#### 5.6.1. Historical treatments

In patients with mCNV, final BCVA tends to be poor due to the development of CRA around the regressed membrane (Hayashi et al., 2010). Indeed, this poor outcome explains the strong interest in finding an effective treatment.

In the past, the mCNV was surgically resected based on the notion that removal of the neovascular complex would help to maintain vision without damaging the RPE since most mCNVs are located above the RPE (type 2 CNV). For many reasons—scar formation, central scotoma, recurrences, and the long learning curve and invasive nature of the surgical procedure—this complex surgical technique was abandoned (Neelam et al., 2012).

In subfoveal mCNV, the classic treatment approach was macular translocation, whose objective was the transfer of the foveal neurosensory retina to another location with a (theoretically) better RPE-Bruch membrane-choriocapillaris complex. In this complex and difficult surgical technique, the retina was rotated around the optic nerve and the fovea replaced (Soubrane, 2008). However, nowadays, this approach is rarely used.

Laser photocoagulation has been used to treat mCNV, but this treatment approach has important limitations. For example, in

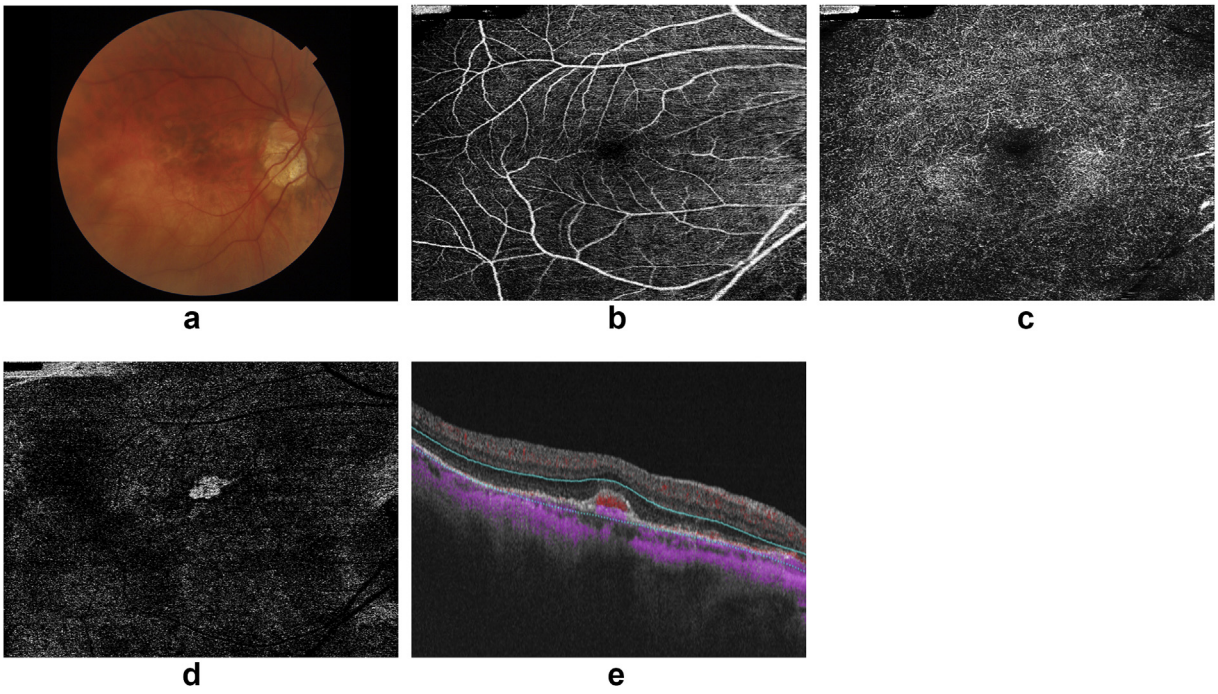


**Fig. 13.** Fundus photography of the right eye of a highly myopic patient (a). Optical coherence tomography (OCT) angiography shows normal superficial and deep plexi (b, c). A deeper section just above the retinal pigment epithelium shows myopic choroidal neovascularization (d). Flow is confirmed by OCT b-scans inside the hyperreflective lesion (e).

subfoveal CNV, the treatment caused central scotoma and visual loss (Soubrane, 2008). Due to the expansion of the CRA and a high recurrence rate, laser photocoagulation has largely been abandoned (Neelam et al., 2012), except in certain well-defined cases such as extrafoveal or juxtafoveal lesions (Fig 15).

### 5.6.2. Photodynamic therapy (PDT)

In the VIP clinical trial (Verteporfin in PhotodynamicTherapy (VIP) Group Study, 2001), PDT was compared to sham treatment in patients with mCNV, resulting in a greater improvement in BCVA. In that trial, BCVA had stabilized at the 12-month follow up in 72% of patients treated with PDT versus only 44% of the placebo group, with the PDT group twice as likely to present a 5-letter improvement in BCVA. However, at the 24-month follow-up, there were no inter-group differences in BCVA stabilization, although the distribution of changes in BCVA indicate that the PDT group had better outcomes at month 24 (Blinder et al., 2003). Theoretically, PDT dissipates less laser energy to the RPE and neurosensory retina, and thus there is less tissue destruction and scar expansion than occurs with laser photocoagulation (Blinder et al., 2003; Verteporfin in Photodynamic Therapy (VIP) Group Study, 2001).

Visual prognosis after PDT in mCNV patients depends on the age at diagnosis, with worse results in older patients (Coutinho et al., 2011; Ergun et al., 2004; Montero and Ruiz-Moreno, 2003). A prospective study of patients diagnosed with mCNV treated by PDT found that BCVA was significantly better in younger patients during the first two years of follow-up, although this difference did not remain significant after longer follow-up (Ruiz-Moreno et al. 2008). The health of the chorioretinal tissue may have a large effect on BCVA after PDT treatment, which explains why younger patients with better initial BCVA may develop less CRA and scarring. Age may also play a role in inducing choriocapillaris sclerosis and RPE defects, as has been reported for CRA (Curcio et al., 2000). In a previous study conducted by our group, most of the patients who underwent PDT achieved stabilization or improvement in BCVA, with a (non-significant) trend towards improvement during the four-year follow-up. In that study, the number of lines gained was positively correlated with the initial size of the neovascular lesion (Ruiz-Moreno et al. 2008). Coutinho et al. evaluated long-term safety and efficacy of PDT, finding that, at 5-year follow-up, two-thirds of patients improved or stabilized BCVA (Coutinho et al., 2011).

The location of the mCNV has a large influence on final BCVA after PDT. Juxtafoveal lesions have a relatively smaller chorioretinal atrophy area and better BCVA compared to subfoveal lesions (Hayashi et al., 2011). Several authors support the use of PDT to treat juxtafoveal lesions, but PDT carries a substantial risk of increasing the size of the CNV, as studies have shown that a juxtafoveal CNV can become a subfoveal CNV after PDT (Bandello et al., 2003). Another prognostic factor is the pretreatment degree of myopia. Kwak et al. found that eyes with longer axial lengths and greater chorioretinal degeneration may express less VEGF and consecutively experience less CNV growth (Kwak et al., 2000). Several studies have corroborated this finding, showing that more myopic eyes obtain better final BCVA (Pece et al., 2006); nevertheless, several other studies have failed to confirm those findings (Ergun et al., 2004; Montero and Ruiz-Moreno, 2003).

PDT induces overexpression of VEGF and other hypoxia-induced factors, leading to a recurrence in the neovascular lesion and thus the need for retreatment. Combining PDT with intravitreal corticosteroids may reduce the number of retreatments needed. Unfortunately, evidence to support this approach is not strong due to the small sample sizes in the studies performed to date. Marticorena et al. reported better outcomes in 12 eyes from 12 patients treated with PDT plus intravitreal triamcinolone (Marticorena et al., 2006). By contrast, Chan et al. found no differences between patients treated with PDT alone and those who received PDT combined with intravitreal triamcinolone (Chan et al. 2007), although those authors did find that a subgroup of patients—those with a larger CNV and lower initial BCVA—may benefit from the combination therapy. Side effects from intravitreal triamcinolone, such as cataract formation and an increase in intraocular pressure, limit the use of this combined approach to elderly patients, who usually have worse BCVA and a poorer response to PDT, or to patients with frequent recurrences, or those with large mCNV lesions (Chan et al., 2007).

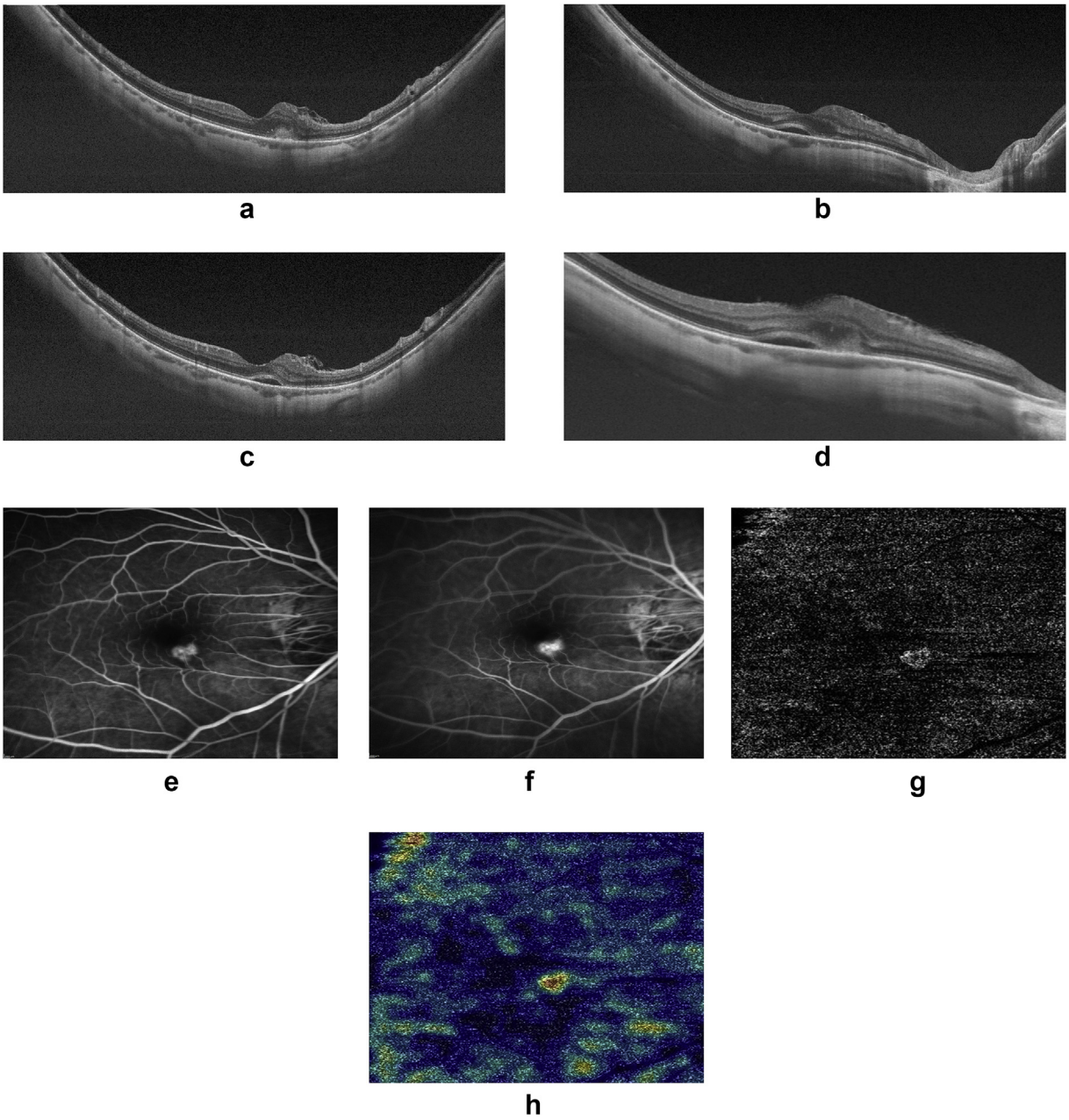


**Fig. 14.** Optical coherence tomography (OCT) b-scans of a highly myopic patient suffering from choroidal neovascularization (CNV). A hyperreflective lesion is accompanied by subretinal fluid (a–d). Fluorescein angiography (FA) confirm the presence of a classic CNV (e, f). OCT angiography shows a neovascular lesion with the exact same shape as seen on FA (g), with flow represented by warm colours (h).

When PDT was first developed, it was considered an important advance because it was substantially more effective than other treatments available at the time. However, the emergence of anti-VEGF therapy, which obtains better visual outcomes than PDT, has relegated PDT to use as a second-line treatment for mCNV (Silva, 2012).

### 5.6.3. Anti-VEGF treatment

*5.6.3.1. Bevacizumab*. Several studies have reported excellent results with intravitreal anti-VEGF agents for the treatment of CNV secondary to AMD (Brown et al., 2006; Rosenfeld et al., 2006). Based on the results of those studies and considering the high VEGF levels in eyes with mCNV, together with the known role of VEGF in mCNV pathogenesis (Tong et al., 2006), researchers and clinicians began to investigate the use of anti-VEGF drugs in mCNV. Nguyen et al. were the first to report good results in patients previously-treated with PDT for mCNV (Nguyen et al., 2005). In that study, the researchers administered intravenous bevacizumab (5 mg/kg), which resulted in an improved BCVA in both patients. In a small, prospective study, Arias et al. administered intravenous bevacizumab in 17 eyes with mCNV, obtaining good results at six months of follow-up: 41% of patients increased at least one line, and 17% increased more than six lines. The patients received a mean of one intravitreal injection during follow-up- (Arias et al., 2008).

Other studies with longer follow-up (≥12 months) of follow up, using a similar initial protocol (3 monthly intravitreal injections of 1.25 mg of bevacizumab) have successfully improved BCVA without any systemic or ocular side effects (Gharbiya et al. 2009; Ruiz-Moreno et al. 2009b; Chan et al. 2009). Due to the intrinsic characteristics of mCNV, the loading dose used in those studies (three monthly injections) is somewhat controversial. As a result, other authors have preferred to

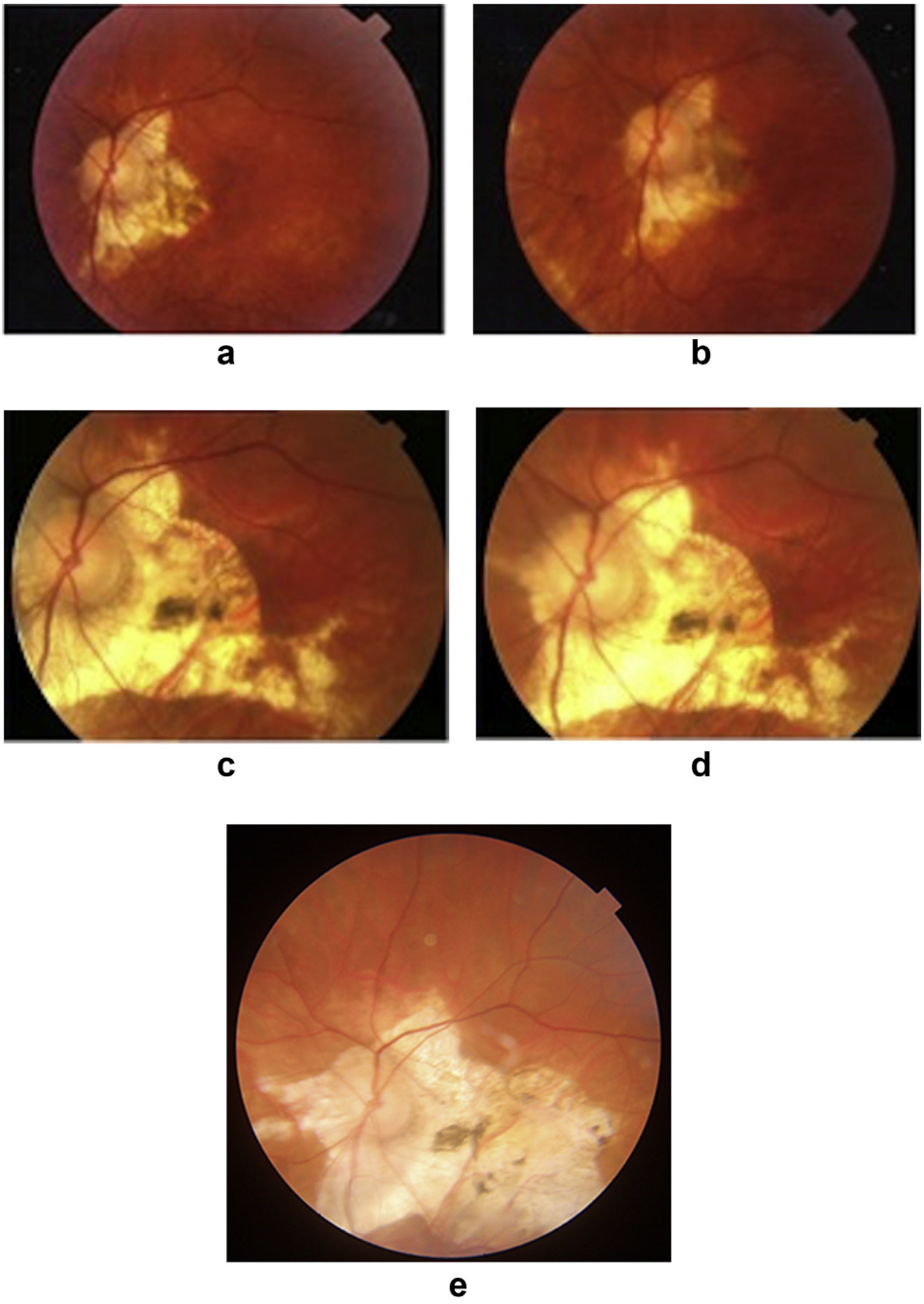


**Fig. 15.** Highly myopic patient who underwent laser photocoagulation to treat myopic choroidal neovascularization. The area of chorioretinal atrophy grew considerably throughout the follow-up.

use only a single initial injection, with retreatment as needed, with good outcomes at one-year (Ikuno et al. 2009; Wu and Chen 2009). Ruiz-Moreno et al. retrospectively evaluated 107 eyes with subfoveal or juxtafoveal CNV treated with one initial intravitreal dose of bevacizumab (1.25 mg) followed by a *pro re nata* regimen (PRN), finding that BCVA increased from 0.72 to 0.53 (logMAR, p = 0.001) after one year of follow-up. In addition, 45% of eyes achieved a BCVA better than 20/65, and 30% gained 3 or more lines (15 ETDRS letters). However, 40% of the eyes required retreatment, with a mean of 0.8 ± 1.3 re-injections. Outcomes were better in younger patients (< 50 years). The gain in BCVA occurred mainly during the first 3 months, after which vision stabilized. There were no differences between patients with or without previous PDT treatment, and the pattern of visual gain was comparable in both groups (Ruiz-Moreno et al. 2010). The results of the aforementioned studies suggest that a single intravitreal injection of bevacizumab with a PRN follow-up may be the treatment of choice for mCNV.

Studies that have performed long-term follow-up of patients treated with bevacizumab have reported good outcomes. One retrospective, non-randomized, multicenter study followed 92 eyes for 4 years. The initial anti-VEGF protocol (either 1 or 3 intravitreal injections) was left to the clinical judgment of the investigators, with PRN as the follow-up protocol. The main outcome measure was change in BCVA. BCVA (ETDRS letters) was 46.1 at baseline (standard deviation [SD], 16.8); at months 12, 24, 36, and 48, the BCVA results were, respectively, 55.5 (18.6), 50.1 (20.1), 54.2 (21.9), and 53.1 (22.5), all of which were statistically significant. The mean number of injections was 4.9 (5.4). Neither the spherical equivalent nor the number of injections affected

the final outcome (Ruiz-Moreno et al. 2013a,b). Another study with a longer follow-up retrospectively evaluated patients who received a mean of 3.3 (2.3) injections. During the first 3 years of follow-up, BCVA improved and stabilized; however, this improvement was no longer statistically significant at years 4, 5, and 6 of follow-up (Ruiz-Moreno et al. 2015).

Most of the patients in the studies conducted to date to evaluate anti-VEGF in mCNV were previously treated with PDT. As a result, it is difficult to extrapolate the findings from those studies to treatment-naïve mCNV patients. However, some studies have performed a subanalysis to compare eyes with and without previous PDT, showing better outcomes in eyes without previous PDT (Ruiz-Moreno et al. 2009a; Arias et al. 2008; Chan et al. 2009).

#### 5.6.3.2. Ranibizumab

*5.6.3.2.1. Clinical trials.* The REPAIR trial was a prospective, phase II, multicentric study of 65 treatment-naïve mCNV patients diagnosed by SD-OCT and FA. Patients received a median of 3 injections during the 12-month follow-up period. Median time to retreatment was 2 months. The mean improvement in ETDRS letters was 13.8 at the 12-month follow up, with the largest improvement observed after the first month (gain of 8.7 letters). BCVA improved in most (86%) of the patients, with a mean increase of ≥15 letters in 36.9% of eyes. Central retinal thickness (CRT) decreased significantly—by a mean of −135 μm; similar to the BCVA outcomes, the largest decrease in CRT occurred during the first month (mean, −109 μm) (Tufail et al., 2013).

RADIANCE was a phase III, double-masked, randomized controlled trial (RCT) of 277 patients with mCNV. Patients were allocated one of three different treatment arms, as follows: 1) ranibizumab guided by BCVA stabilization criteria, 2) ranibizumab guided by disease activity criteria, or 3) verteporfin PDT, with ranibizumab allowed from month 3 onwards. The primary objective was to demonstrate the superiority of ranibizumab to PDT at month 3. The aims of the trial were successfully met as all three groups showed significant improvement, with the greatest gains in the ranibizumab groups: +10.5 ( ± 8.2) ETDRS letters (group 1), +10.6 ( ± 7.3) (group 2), and +2.2 ( ± 9.5) (group 3) (both $p < 0.00001$). The secondary objective of that study was to demonstrate the noninferiority of ranibizumab guided by disease activity criteria versus BCVA stabilization criteria at month 6. The results showed no differences between those groups in mean change in BCVA: group 2, +11.7 ( ± 8.2) vs. group 1, +11.9 ( ± 8.8); $p < 0.00001$). At 12 months' follow-up, the percentage of eyes in each group gaining ≥15 letters was as follows: 53.3% (group 1), 51.7% (group 2), and 32.7% (group 3). The decrease in CRT observed in groups 1 and 2 was maintained from month 3 (−61 μm and −77.6 μm, respectively) to month 12 (−66.6 μm and −71.3 μm, respectively). In the PDT treatment group, the mean thickness decreased progressively, from −12 μm at month 3 to −60.8 μm at month 12. The mean number of ranibizumab injections was 4.6 in group 1, 3.5 in group 2, and 2.4 in group 3. The authors concluded that intravitreal ranibizumab provides better outcomes in mCNV compared to initial PDT treatment followed by intravitreal ranibizumab (Wolf et al., 2014).

The RADIANCE trial showed that patients treated with intravitreal ranibizumab obtained significantly greater improvements on many quality of life (QoL) parameters than PDT-treated patients (Wong et al., 2015). DSM (diagnosed by OCT) was present in 18% of the patients in the RADIANCE trial, and ranibizumab was equally effective in eyes with or without DSM (Ceklic et al., 2014). Those findings underscore the importance of diagnosing DSM in eyes with suspected mCNV, as such eyes are more likely to respond to anti-VEGF therapy, although subretinal fluid may remain secondary to this inward bulge.

*5.6.3.2.2. Clinical studies.* Numerous uncontrolled, non-randomized studies have also demonstrated good response to ranibizumab in patients with mCNV (Table 1). One study reported short-term improvement in BCVA from the first month after a single dose of ranibizumab, with 31% of patients achieving an increase of 3 or more lines and with most patients maintaining significant gains in BCVA at 3 and 6 months (Silva et al., 2008). Clinical studies with ≥12 months of follow-up confirm the safety and efficacy of ranibizumab, which requires only a limited number of injections (Lorenzo et al., 2011; Monés et al., 2009; Silva et al., 2010; Wong et al., 2015). Although ranibizumab improves functionality in patients previously treated with PDT, the available data suggests that PDT-naïve patients have better outcomes (Lorenzo et al., 2011; Silva et al., 2010).

Kung et al. (Kung et al., 2014) retrospectively compared initial dosing regimens of ranibizumab. In one group (25 eyes), patients received a single initial injection while a second group (21 eyes) received three consecutive monthly injections. Both groups were re-treated if active disease remained. Overall, the second group required more injections (mean, 3.57 vs. 2.32; $p < 0.001$). However, the retreatment rate was lower in the group that received a loading dose of 3 monthly injections ($p < 0.037$). At the 12-month follow-up, there were no differences in BCVA or CMT between the groups, leading the authors to conclude that three initial injections are not necessary but that close follow-up is crucial (Kung et al., 2014). Similar results were reported in other studies that performed the same comparison (i.e., single initial ranibizumab injection vs. three consecutive monthly injections) (Lorenzo et al., 2011; Monés et al., 2009; Silva et al., 2010; Wong et al., 2015). Based on the current evidence, it appears that a single initial injection should be the initial treatment protocol, similar to the protocol for bevacizumab.

Calvo-González et al. prospectively evaluated patients who received a loading dose of three ranibizumab injections (mean follow-up, 15.9 months), finding that the BCVA improved by 7.8 ETDRS letters after the first injection and by 12.6 ETDRS letters after the third monthly injection. This improvement was maintained throughout the follow-up period. Those findings led the authors to recommend a loading dose of three monthly injections (Calvo-Gonzalez et al., 2011).

Lalloum et al. prospectively evaluated 32 eyes from 32 patients treated with intravitreal ranibizumab (mean follow-up, 17 months), finding an increase of ≥3 lines in 46.8% of patients and a mean decrease of 103 μm in CRT (on SD-OCT) (Lalloum et al., 2010).

Long-term studies have reported heterogenous results after the second year, with some studies reporting that BCVA is stable or may even improve during the third year (Franqueira et al., 2011) while other studies have reported a decrease in BCVA over the course of follow-up (39 months) (Cohen et al. 2015). These contrasting findings may be due to the close follow-up performed by Cohen et al. and to differences in the number of injections over time.

Several studies have compared ranibizumab to bevacizumab in patients with mCNV. Gharbiya et al. performed a RCT to compare outcomes (visual acuity, CRT, and number of intravitreal injections) (Gharbiya et al., 2010). At 6 months of follow-up, the ranibizumab group had obtained an increase of 17.31 letters versus 15.87 letters in the bevacizumab group, a non-significant difference ($p = 0.68$). In both groups CRT decreased significantly (206 μm and 185 μm, respectively) without any statistically significant differences between the groups ($p = 0.72$). Similarly, no between-group differences were observed in the mean number of injections (2.81 vs. 2.44, respectively). These findings led the authors to conclude that, overall, there appear to be no significant differences in treatment outcomes (BCVA, CRT, number of injections) between ranibizumab and bevacizumab after 6 months of follow up in patients treated for mCNV (Gharbiya et al., 2010). A follow-up study confirmed the lack of significant differences between the two groups (Ruiz-Moreno et al. 2015; Ruiz-Moreno et al. 2013a,b).

Yoon et al. identified several prognostic factors for visual outcome (BCVA and vision improvement) after treatment with bevacizumab or ranibizumab injections in patients with mCNV. They found that the following factors were predictors of good treatment outcomes were: baseline BCVA, peripapillary choroidal atrophy size, and presence of lacquer crack extending to the fovea (Yoon et al., 2012).

**Table 1**
Published papers in patients treated with ranibizumab injections in myopic CNV and a minimum follow-up of 12 months.

| Author | Design | Year | Follow-up (months) | N | Mean age | Mean BCVA change(ETDRS letters) | Mean number of injections |
|---|---|---|---|---|---|---|---|
| Monés | Prospective | 2009 | 12 | 23 | 51.1 | +9.5 | 1.5 |
| Silva | Prospective | 2010 | 12 | 34 | 54 | +8 | 3.6 |
| Lalloum | Prospective | 2010 | 17 | 32 | 57 | +9.5 | 3 |
| Lorenzo | Retrospective | 2011 | 12 | 29 | 56.8 | +8.9 | 1.4 |
| Clavo-González | Prospective | 2011 | 15.9 | 67 | 59 | +12 | 4.2 |
| Franqueira | Retrospective | 2012 | 36 | 40 | 55 | +8 | 7.6 |
| Cohen | Retrospective | 2015 | 39.3 | 51 | 64 | +7.6 | 3.5 |

*5.6.3.3. Aflibercept*

*5.6.3.3.1. Clinical trials.* The MYRROR study was an international, phase III, multicenter, randomized, double-masked, sham-controlled study conducted in five different countries (Japan, Hong Kong, Republic of Korea, Singapore, and Taiwan) to evaluate the efficacy, safety and tolerability of aflibercept in patients with mCNV. Patients were randomized (3:1 ratio) to receive aflibercept or sham treatment. Follow up was performed every 4 weeks for 48 weeks, with retreatment in cases with active CNV. The primary and secondary endpoints were, respectively, mean change in BCVA at 24 weeks and the proportion of patients with an increase of ≥15 ETDRS letters at weeks 24 and 48. The mean BCVA gain in the treatment group was 12.1 letters versus a loss of 2 letters in the sham group ($p < 0.0001$). The treatment group received a mean of 2.9 intravitreal injections. Compare to the sham group, a higher percentage of patients in the aflibercept group gained ≥15 letters at both week 24 (38.9% vs. 9.7%; $p = 0.0001$) and week 48 (50.0% vs. 29.0%; $p = 0.0308$). Moreover, these significant differences were achieved even though patients in the sham group received an aflibercept injection after week 24. No differences were observed when patients were stratified by age or ocular axial length. Intravitreal aflibercept was generally well tolerated, with a good safety profile. The authors concluded that aflibercept is a safe and efficacious treatment option for mCNV, requiring only a limited number of injections to obtain good anatomic and functional results (Ikuno et al., 2015).

*5.6.3.3.2. Clinical studies.* Several studies have evaluated aflibercept in mCNV. Two studies reported good safety and functional outcomes at 12 months of follow-up after a mean of 2 aflibercept injections using a PRN regimen for retreatment (Korol et al., 2016; Pecce and Milani, 2016). Those studies found that younger patients (< age 50) needed fewer injections and tended to have a greater improvement in BCVA (Bruè et al., 2016; Pecce and Milani, 2016). The reason attributed to these better outcomes in younger patients is that they tend to have a better functioning RPE, which may more effectively inhibit CNV growth compared to older patients, whose RPE may not function as well.

Brue et al. evaluated 38 naïve mCNV patients treated with intravitreal aflibercept and followed for ≥18 months. Overall, BCVA improved from 0.69 to 0.15 logMAR at 18 months ($p < 0.01$) and the mCNV fully resolved in 55% of patients after a single aflibercept injection (Bruè et al., 2016).

Myopic CNV is a leading cause of visual impairment in high myopic patients. Given the potentially devastating consequences of this disease, a prompt diagnosis is crucial. FA and OCT are essential complementary tests when high myopic patients complain of metamorphopsia or decreased BCVA. However, clinicians should pay close attention to symptoms in highly myopic patients given that these patients often present with complaints well before any clinical signs can be detected on any test. It seems evident that OCTA will play a fundamental role in the diagnosis of mCNV in the future due to its noninvasive nature and its rapid image capture. The current treatment of choice for mCNV is anti-VEGF treatment, starting with a single dose and PRN follow-up.

## 6. Myopic traction maculopathy

### 6.1. Vitreous characteristics in myopic patients

The vitreous cortex and the inner limiting membrane (ILM) form the vitreomacular interface (VMI). The ILM is composed of collagen types IV, VI and VIII, associated with glycoproteins. This membrane acts as a basal membrane for retinal Müller cells. The vitreous cortex consists primarily of a dense matrix of collagen that follows a lamellar pattern. VMI attachments are tighter at the vitreous base, optic disc, vascular arcades and fovea; this strong attachment helps to explain numerous vitreoretinal diseases, especially in highly myopic patients, where outpouching of the posterior pole in cases with staphyloma can induce posterior vitreous detachment. Advancements in imaging technology—especially deep penetration OCT—provide many details about the posterior precortical vitreous pocket (PPVP), a physiological lacuna located in the posterior pole of healthy eyes. The PPVP is confined between the cortex in contact with the ILM and the vitreous gel, and it can simulate a fake posterior vitreous detachment (PVD), which is often discovered during vitreoretinal surgery in these patients (Itakura et al., 2014; Itakura et al., 2013).

Vitreous liquefaction, PVD, and PPVP are more prevalent in myopic eyes. PVD is typically diagnosed at a younger age in these patients compared to the general population. Indeed, the prevalence of PVD in myopic eyes is 38%, with greater axial length associated with early development of PVD (Akiba, 1993). Kishi et al., using SD-OCT and SS-OCT, found a prevalence rate of 43.2% for PVD in highly myopic eyes, which is five times higher than in emmetropic eyes (Kishi, 2014). OCT can be useful to correctly characterize the VMI in myopic patients given that biomicroscopy overestimates the prevalence of complete PVD because the posterior cortex may still be attached to the retina despite clear visualization of a Weiss ring (Lorenzo Carrero, 2012).

Using scanning electron microscopy, Kishi et al. were the first to describe the presence of vitreous cortex remnants in cadaver eyes with visible PVD (Kishi et al., 1986). In a more recent study, those authors used SS-OCT imaging to identify the presence of remnants in 6.7% of non-myopic and 37.7% of myopic eyes (Itakura et al., 2014). SS-OCT plays an important role because it provides a basis for the interpretation and diagnosis of several VMI disorders in highly myopic patients.

### 6.2. Epiretinal membrane

*6.2.1. Definition / etiopathology*

Epiretinal membranes (ERM) are described ophthalmoscopically as a reflective, relatively opaque layer on the surface of the retina. These membranes may mimic the appearance of cellophane and can cause traction by inducing folding of the retinal surface. On OCT images, ERM is easily identified as a hyperreflective band located over the ILM. ERMs are found in 11.3%–45.7% of highly myopic patients (Ripandelli et al., 2012; You et al., 2014). They tend to be multilayered, with a predominant glial component (Kampik, 2012). Two ERM patterns (type 1 and 2) can be observed on electron microscopy. Depending on the pattern, the surgical approach may vary. In type I ERM, a sheath of type II collagen is present between the ILM and the proliferating cells that

form the ERM. In type II ERM, cells proliferate directly over the ILM with little to no collagen, acting as a cleavage plane (unlike type I) (Kampik, 2012). Cell lineages in this pathology do not seem to differ between VTM and idiopathic ERM, although some studies report a marked presence of glial components (Kampik, 2012).

Previously, it was hypothesized that mini-retinal breaks develop after PVD, inducing proliferation of fibroblasts, astrocytes, and glial cells (Vinores et al., 2016). However, more recent hypotheses suggest that ERM proliferate from residual vitreous remnants that remain on the surface of the retina after a complete or incomplete PVD and grow over the ILM (Gupta et al., 2011; Gandorfer et al., 2009). Longer eyes in highly myopic patients, especially those with posterior staphyloma, tend to develop PVD earlier, which is often incomplete due to schisis of the posterior vitreous, thus leaving cortex remnants tightly attached to the ILM. These remnants, together with Müller cell activation, induce the development of ERM (Foos 1977; Snead et al., 2008; Lorenzo Carrero, 2012; Kampik, 2012).

#### 6.2.2. Treatment

Surgery is required to remove an ERM, but this may prove challenging in highly myopic patients due to their usual anatomical characteristics (i.e., longer axial length), especially in cases with posterior staphyloma or posterior pole atrophy that may impede visualization. The type I ERM pattern theoretically requires a double ERM-ILM peeling, given that a simple ERM peeling may leave collagen residue on the surface of the ILM, which could induce recurrence. By contrast, type II ERM can be managed with a simple ERM peeling, as there is no collagen between the ERM and the ILM (Blanco Teijeiro et al., 2015). Nevertheless, ILM removal remains controversial despite the proven reduction in recurrence rates after double peeling (Shimada et al., 2009).

### 6.3. Myopic traction maculopathy / myopic foveoschisis

#### 6.3.1. Definition / etiopathology / classification

Myopic traction maculopathy (MTM) is an umbrella term that encompasses a wide spectrum of related disorders, including vitreomacular traction (VMT) in highly myopic patients, myopic foveoschisis, and myopic MH. Retinoschisis affects from 8% to 34% of patients with posterior staphyloma (Baba et al., 2003; Benhamou et al., 2002). The presence of posterior staphyloma in highly myopic patients plays a key role in the subsequent development of MTM, as the retina in these cases cannot match the scleral outpouching of the posterior pole due to its greater rigidity. This rigidity may be caused by numerous factors, including vascular rigidity, the presence of ERM or VMT syndrome, cortical vitreous remnants, or simply the fact that the retina, its vessels, and the ILM seem to be less elastic than the surrounding tissues (Vanderbeek and Johnson, 2012; Ikuno et al., 2005; Shimada et al. 2013).

Myopic foveoschisis can be diagnosed ophthalmoscopically in certain cases, but OCT examination is essential to establish the correct diagnosis and for follow-up purposes. Myopic foveoschisis involves a progressive separation of retinal layers, which remain connected by Müller cells—a process known as myopic foveoschisis, which was first described by Phillips in 1958 (Phillips, 1958). Ohno Matsui's group classified this disease into five different categories based on location and the size of the affected area, ranging from no apparent foveoschisis (S0) to complete macular involvement (S4) (Shimada et al., 2013) (Table 2).

Others have classified myopic foveoschisis according to the location of the splitting within the retina into inner (affecting inner plexiform layer, ganglion cell layer, and retinal nerve fibre layer), outer (affecting outer plexiform and outer nuclear layers) or inner + outer (Fujimoto et al., 2010; Ceklic et al., 2017). The growth of a posterior staphyloma generates an evident external traction, which in combination with the factors that cause retinal rigidity and with the potential presence of tractions caused by vitreous adherences, lead to the development and progression of the disease.

**Table 2**
Myopic foveoschisis classification (Shimada et al. Am J Ophthalmol 2013).

| | |
|---|---|
| S0 | Absent |
| S1 | Extrafoveal |
| S2 | Foveal only |
| S3 | Foveal but not entire macula |
| S4 | Entire macula |

Shimada et al. Am J Ophthalmol 2013

#### 6.3.2. Course of disease

Although myopic foveoschisis may remain stable (including stable BCVA) during long periods, it is considered to be a slowly-progressive condition (Gaucher et al., 2007). However, a few cases of spontaneous improvement have been reported (Hoang et al., 2016). Several studies—all of which reached similar conclusions—have described the natural course of this disease. Gaucher et al. studied 29 eyes from 23 highly myopic patients with foveoschisis, both with and without previous surgery, finding that 20 of those eyes suffered a BCVA loss during the nearly three-year (31.2 months) follow-up period (Gaucher et al., 2007). In a more recent study, Shimada et al. (Shimada et al., 2013) analyzed 207 highly myopic eyes from 168 consecutive patients (> 3 years of follow up), finding that BCVA improved in only 3.9% of the eyes, with the improvement attributable either to complete PVD or to spontaneous traction release. By contrast, 24 of the 207 eyes (11.6%) progressed, with a decrease in BCVA during follow-up. These results led the authors to conclude that eyes with more severe macular involvement had higher progression rates, based on the finding that eyes with less extensive foveoschisis progressed in only 6.7% of cases versus 42.9% of the eyes with more extensive foveoschisis (Shimada et al., 2013).

The progressive nature of this disease may lead to foveal detachment and full-thickness MH in more severe cases (Shimada et al., 2013; Forte et al., 2007), leading to a substantial decrease in BCVA. The most severe potential complication is development of a MH, which may lead to retinal detachment in patients with persistent traction over the margins of the MH.

#### 6.3.3. Treatment

*6.3.3.1. Approach.* In some cases of MTM, both the macular anatomy and BCVA remain stable. In eyes with stable disease, the most widely accepted approach is conservative treatment. However, due to the progressive nature of MTM, routine follow-up is mandatory, with surgery being the only option in patients whose condition worsens. The optimal time to perform surgery in these patients has long been a topic of intense debate, and even today this question remains controversial.

Traction in the vitreomacular interface in the context of deep staphylomas causes retinal cleavage. While there seems to be no evidence linking the presence of VMT syndrome or ERM to final visual outcomes, damage to the ellipsoid layer or the emergence of full-thickness MH can both lead to worse functional and anatomical results.

Several reports suggest that preoperative BCVA is one of the key predictors of final BCVA in these patients. Lehman et al. found that preoperative BCVA was the only predictor of postoperative BCVA, concluding that the lower the preoperative BCVA, the greater the postoperative improvement in BCVA (Lehmann et al., 2017). While some authors have not found any correlation between foveal status and final BCVA, others report that the presence of foveal detachment (versus no foveal detachment) leads to a statistically greater improvement in BCVA, which may be explained by regeneration of the photoreceptors after foveal re-attachment (Kumagai et al., 2010). In this same

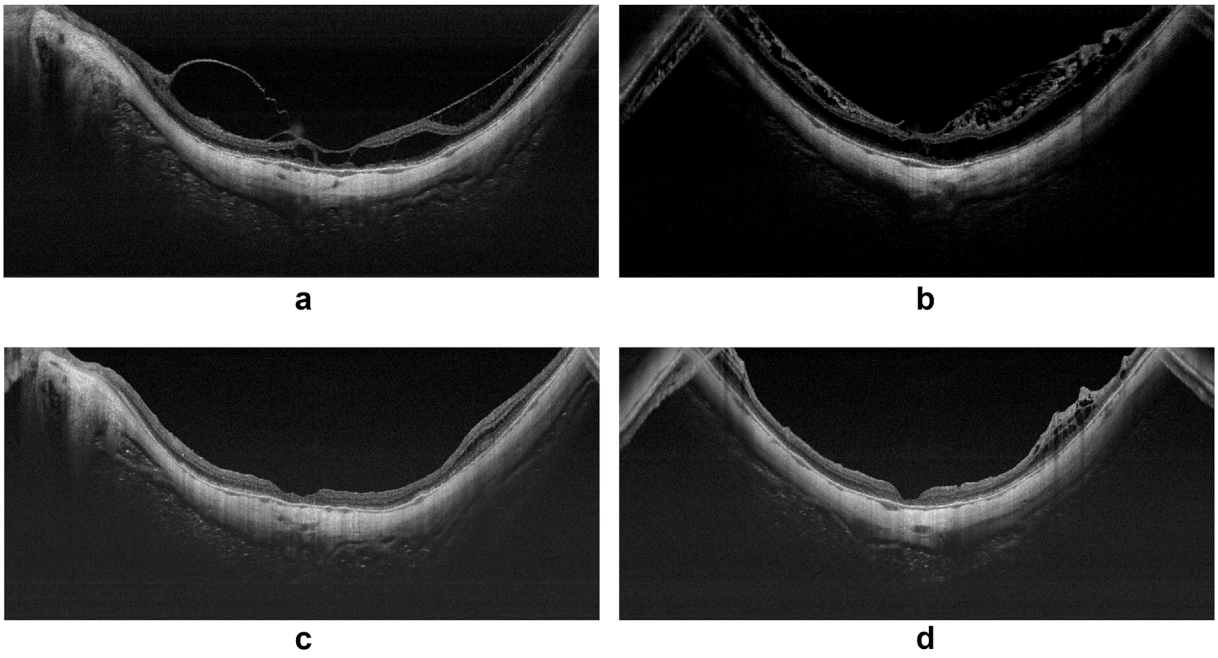


**Fig. 16.** Horizontal (a, b) and vertical (c, d) optical coherence tomography b-scans of a highly myopic patient before and after pars plana vitrectomy treatment with posterior hyaloid and epiretinal membrane dissection and inner limiting membrane peeling for myopic traction maculopathy.

line of investigation, Figueroa et al. performed vitrectomy surgery on 30 eyes with MTM (mean follow-up, 33.8 months), finding that gains in BCVA were more likely in patients with preoperative BCVA of 20/63 or more (Figueroa et al., 2015).

Highly myopic patients with MTM who experience a progressive loss of BCVA in the context of an anatomical worsening on OCT seem to be the most suitable candidates for an interventional approach. A range of surgical techniques are available, as we describe in the next section.

*6.3.3.2. Surgical techniques*. Retinal surgery in highly myopic patients is among the most difficult and challenging types of ophthalmological surgery, even in expert hands. Not surprisingly, this type of surgery carries a risk of iatrogenic complications. The main aim of surgery in MTM is to reduce traction forces at the macula while avoiding inflicting further damage to the retina in the process. To achieve this relaxation of the macula, surgery can be performed *ab interno* using vitrectomy, with or without the aid of an external modification of the scleral curvature at the fovea, thus bringing the two structures closer together.

Pars plana vitrectomy (23-gauge) is a proven approach to improving macular anatomy (Fig 16). However, the role of ILM peeling is not clear. While ILM peeling reportedly reduces postoperative cellular proliferation and ERM formation, it presents a higher risk of iatrogenic lesions such as full-thickness MH while achieving a similar rate of anatomic resolution (Qi et al., 2016). Supporters of ILM peeling believe it is the most efficient way to completely remove all cortical vitreous remnants from the retinal surface and that an ILM-free retina is more elastic and thus more amenable to reattachment (Gaucher et al., 2007; Bando et al., 2005). However, findings from a recent meta-analysis of 239 eyes treated with vitrectomy with or without ILM peeling showed that although ILM peeling appears to yield better anatomic results (a statistically significant odds ratio of 2.15), no statistically-significant differences were achieved with regard to gains in BCVA or fewer complications (Meng et al., 2017). For this reason, some groups have proposed foveal-sparing modified peeling techniques, which leave part of the ILM (between 300 and 2000 μm) in the centre of the macula, thus protecting Müller cells and theoretically reducing the risk of MH development, while also obtaining better visual and anatomic outcomes (Fig 17); however, these findings are based on studies with relatively small sample sizes (Shimada et al., 2012; Ho et al., 2014; Ho et al., 2012).

Published reports indicate that the use of gas tamponade after vitrectomy results in more rapid anatomic improvements but with the trade-off of higher complication rates and without any significant differences (Meng et al., 2017; Uchida et al., 2014; Figueroa et al., 2015).

Scleral indentation, also known as macular buckling, was first described by Schepens in 1957 (Schepens et al., 1957). This technique can be used separately or in combination with pars plana vitrectomy to further reduce tractional forces in MTM. However, it is a difficult procedure with a long learning curve. The procedure consists of placing an external device (which can be made of a range of different materials, including donor sclera, silicone with and without stainless steel wires, gore-tex, or long-lasting hyaluronic acid) to flatten the posterior staphyloma to facilitate foveal attachment. This technique yields anatomic success rates ranging from 25% to 100%, and, in most cases, no further procedures are required (Alkabes and Mateo, 2018). The most commonly reported complications are RPE alterations, choroidal effusion, buckle removal or malpositioning, and scleral perforations (Alkabes and Mateo, 2018).

## 7. Myopic macular hole

### 7.1. Macular hole: overview

The development of a MH—a relatively common complication in high myopia—is associated with significant visual impairment (Ikuno, 2017). Anteroposterior and tangential traction exerted by the vitreous over the macula is closely related to the development of MH in myopic eyes, similar to what occurs in emmetropic eyes. However, in the presence of a posterior staphyloma, which promotes retinal layer splitting, myopic MH is commonly associated with foveoschisis, an important difference compared to emmetropic MH. Overall, the presence of concomitant foveoschisis indicates a worse anatomic and functional prognosis, which may even lead to retinal detachment (Ikuno and Tano, 2006). Increased axial length in conjunction with posterior staphyloma are key factors for the development of myopic MH, which differentiates it from non-myopic MH.

Lamellar or non-full-thickness MH is a common finding on OCT in asymptomatic myopic patients. However, these cases can usually be

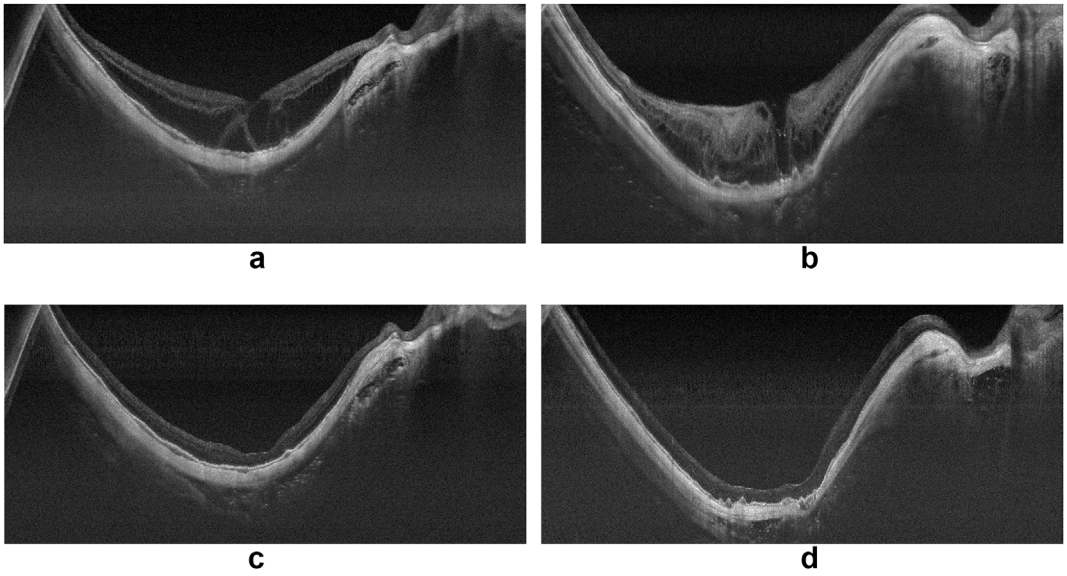


**Fig. 17.** Progressive myopic traction maculopathy causing a foveal detachment (a) and a full-thickness macular hole (b). Macular anatomy was restored after pars plana vitrectomy with epiretinal membrane and inner limiting membrane peeling (c, d).

managed by observation alone. Surgical intervention is necessary only in the presence of a clear vitreous traction or visual decrease attributable to the lamellar MH. Recently it has been reported that epiretinal proliferation associated with lamellar myopic MH tend to be more widespread and adherent to the posterior hyaloid than in non-myopic eyes (Lai and Yang, 2017).

#### 7.1.1. Macular hole: treatment

The goal of surgical repair is total closure of the MH to preserve or improve BCVA. The gold standard treatment is posterior vitrectomy, posterior hyaloid dissection, and ILM peeling (Fig. 18 and 19). Posterior vitrectomy can be performed with 23-gauge or smaller instruments. Importantly, the entire vitreous should be removed from the macular surface. Vitreoschisis is common in myopic eyes and failure to identify and remove this poses a risk to successful MH closure. Triamcinolone can be used as an adjuvant to detect vitreoschisis and to induce a complete posterior vitreous detachment. Likewise, trypan blue and brilliant blue are helpful for ILM and ERM peeling. Current recommendations favour the use of blue dyes rather than indocyanine green to stain the ILM due to potential retinal toxicity. ILM peeling in a highly myopic eye is a challenging surgical manoeuvre due to several factors: 1) greater length of the eye, 2) retinal thinning, 3) poor staining, 4) difficult identification of the exact location of the MH.

Most surgeons perform a complete ILM peeling over the entire macula in an attempt to reach the main vascular arcades. Nevertheless, several alternative techniques have been proposed, particularly in MH with foveoschisis, to achieve a successful closure (Ikuno, 2014). Some authors perform an incomplete peeling, leaving an ILM shield over the macula to protect the fovea (Shimada et al., 2012). This approach is especially recommended in myopic MH with concomitant foveoschisis, where retinal layer splitting weakens the fovea, making it more susceptible to damage.

The overall percentage of MH closure is lower in myopic eyes than in emmetropic eyes. For this reason, an inverted ILM flap technique has been proposed to enhance the probability of successful closure in myopic MH (Kuriyama et al., 2013). This technique involves peeling the ILM without breaking its attachment to the edge of the MH. Next, a sheet of ILM is placed inside or over the MH bed to create a scaffold to facilitate anatomical closure of the MH (Yamashiro et al., 2018). Importantly, fluid-air exchange should be performed carefully to avoid displacing the ILM flap.

Recently published studies report a clear advantage for the inverted ILM flap technique versus standard ILM peeling—regardless of the diameter—to achieve complete MH closure without any detrimental visual results (Mete et al., 2017; Rizzo et al., 2017).

In most cases, gas tamponade with either sulphur hexafluoride (SF6) or perfluoropropane (C3F8) is used. Facedown positioning is recommended for 3–7 days after surgery. However, silicone oil tamponade can be used in selected patients in whom facedown positioning cannot be guaranteed.

In cases of primary surgical failure or recurrence, two techniques have been proposed: 1) placement of an ILM graft, obtained from a peripheral area of the primary ILM peeling, over the MH, or 2) macular buckling (Fig 20). Visual recovery after surgery depends on closure of the MH and the status of the underlying photoreceptors and RPE. However, the combination of increased axial length with a posterior staphyloma is a risk factor for surgical failure (Ohsugi et al., 2018).

### 7.2. Macular hole retinal detachment: overview

Macular hole retinal detachment (MHRD) occurs mainly in patients with high myopia who present a posterior staphyloma (Fig 21). However, it is not clear why some myopic patients with MH develop a retinal detachment while others do not. A recently published retrospective study reviewed consecutive cases with axial length > 28 mm treated with vitrectomy for MH or MHRD. That study showed that, compared to eyes with MHRD, eyes with MH had significantly greater choroidal and scleral thickness, a higher frequency of DSM, and a lower staphyloma height (Ohsugi et al., 2018). Nevertheless, the cut-off point for extreme myopia is generally considered to be 30 mm in axial length based on published results indicating that surgical outcomes are worse in those eyes (Arias et al., 2015; Nadal et al., 2012). Therefore, MHRD is mainly determined by the presence of an increased axial length with concomitant staphyloma, similar to myopic MH.

#### 7.2.1. Macular hole retinal detachment: treatment

MHRD is among the most difficult types of retinal detachment to treat. Moreover, visual outcomes in these patients are often poor (Ortisi et al., 2012). Before the advent of vitrectomy, MHRD patients were treated with macular buckling and diathermy, or by cryo- or laser retinopexy of the MH. However, anatomic outcomes were usually suboptimal due to excessive atrophy and fibrosis in the macular area.

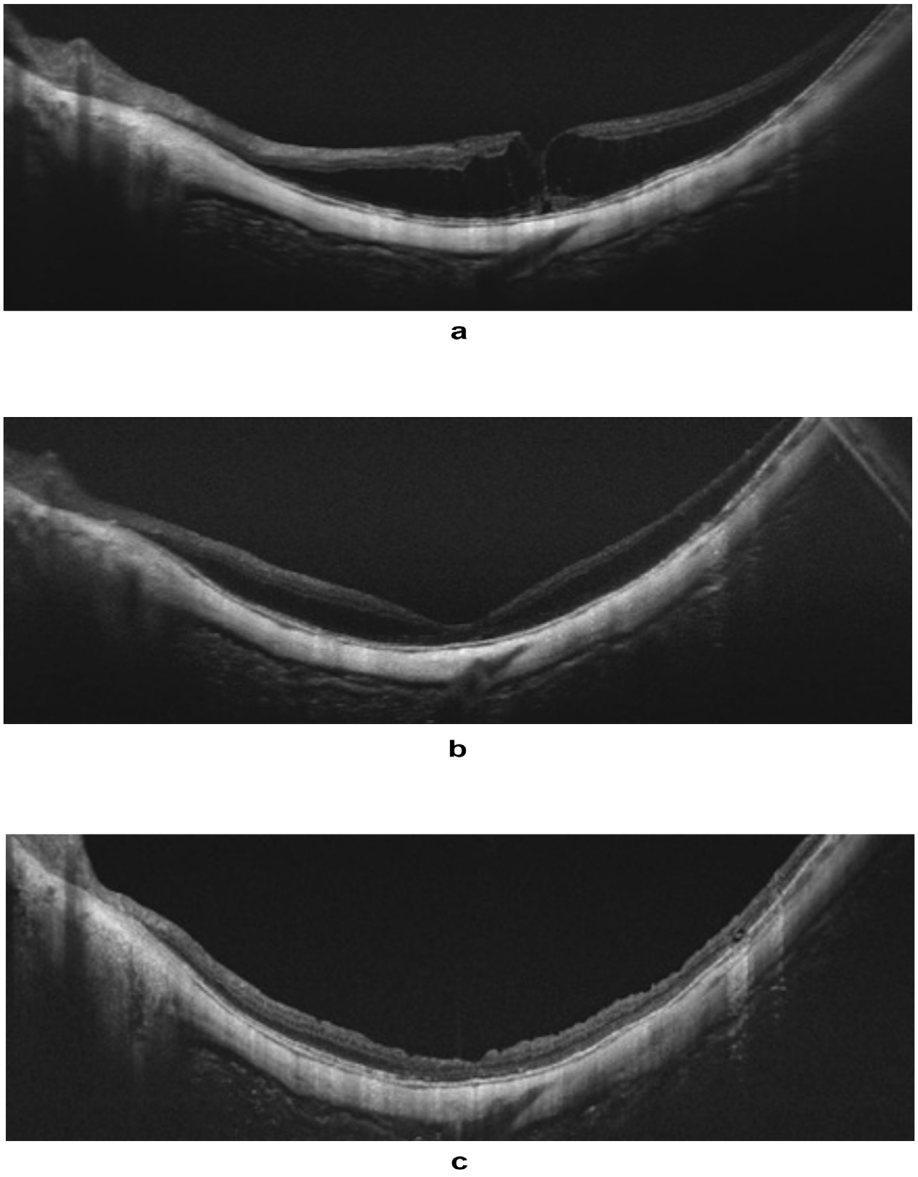


**Fig. 18.** 81-year-old female who presented with 20/200 visual acuity (VA). Swept-source optical coherence tomography (SS-OCT) showed an outer foveoschisis with a full-thickness macular hole (a). The patient underwent pars plana vitrectomy surgery + inner limiting membrane peeling + SF6 tamponade. Two months after surgery her VA was 20/32, with resolution of the macular hole and improvement of the foveoschisis (b). Two years after surgery, SS-OCT imaging showed no signs of foveoschisis and VA was 20/50 (c).

Vitrectomy consists of vitreous dissection and peeling of the ILM and ERMs to reduce tangential and anteroposterior traction. It is these tractions, in conjunction with posterior staphyloma, which lead to the development of MHRD. Peeling is easier and safer when blue dyes are used to stain the ILM and ERMs. Perfluorocarbon liquid can be used to stabilize and flatten the macular surface before ILM peeling. Any subretinal fluid displaced from the macula by the perfluorocarbon can be removed through peripheral retinotomy. To avoid damaging the underlying RPE, subretinal fluid aspiration through the MH should be avoided. A recent study reported excellent results using the inverted ILM flap technique to treat MHRD (Chen and Yang, 2016).

The choice of tamponade is controversial. While some authors prefer gas, others recommend silicone oil to overcome reduced natural adhesion due to staphyloma and chorioretinal atrophy (Chen et al., 2006; Mancino et al., 2013; Nadal et al., 2012). Heavy silicone oil has also been used, with favourable anatomical results (Avitabile et al., 2011).

Various patterns of retinoschisis and MHRD evidence on FAF have been described in high myopia (Sayanagi et al., 2007). On FAF, an axial length > 30 mm and macular atrophy appear to be prognostic factors for worse anatomic and visual outcomes (Arias et al., 2015).

Macular buckling is an alternative approach to treating recurrent or difficult cases of MHRD because it facilitates MH closure by inserting a ridge that pushes the whole macula forward. This could explain why myopic eyes with MH and DSM are less susceptible to retinal detachment; as occurs in eyes with implanted macular buckles, DSM reduces the curvature of the staphyloma and may prevent retinal detachment (Ohsugi et al., 2018). In this regard, some studies have reported better results with macular buckling than with vitrectomy, even in primary MHRD (Ando et al., 2007; Siam et al., 2012). Recent reports suggest that combining macular buckling and vitrectomy with ILM peeling may be a promising alternative in refractory cases (Ma et al., 2017).

Finally, posterior scleral contraction has been used to treat recurrent or persistent MHRD in highly myopic eyes (Zheng et al., 2018). Scleral expansion may contribute to the development of MHRD, which is why contracting the posterior sclera could be an effective treatment to

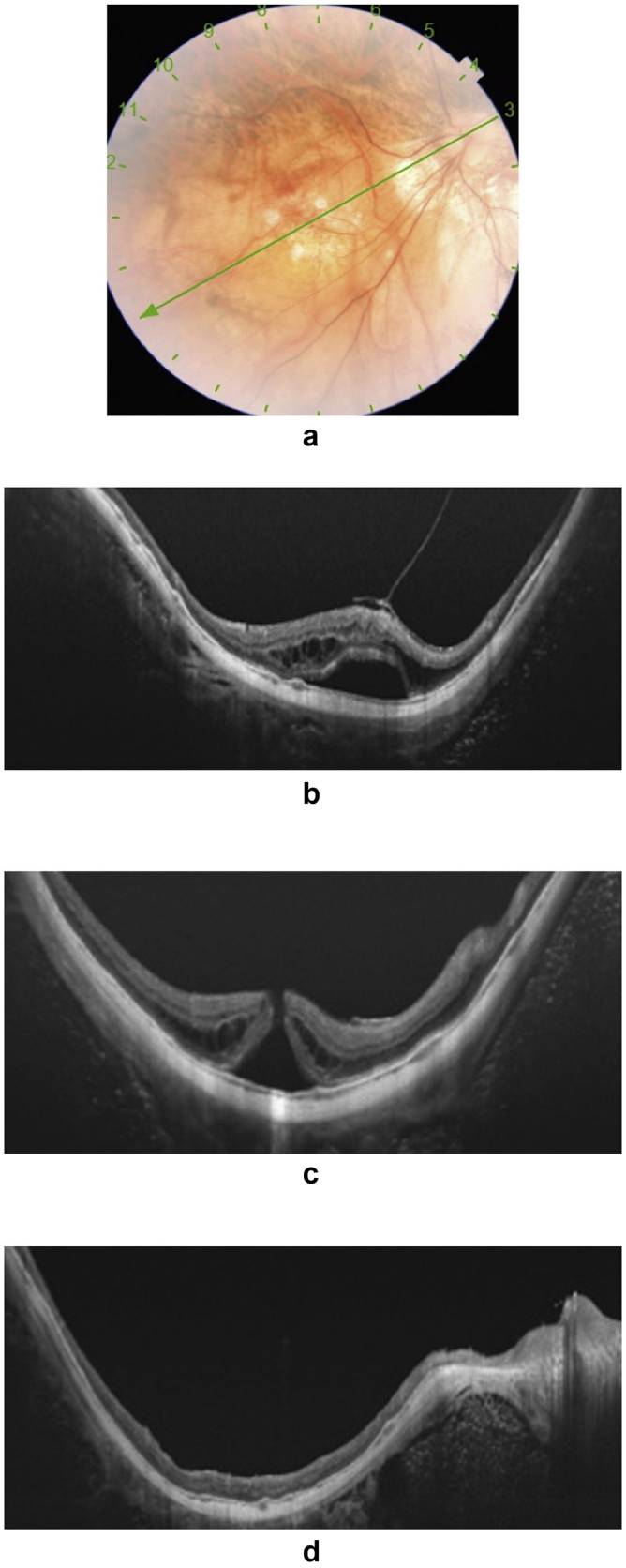


**Fig. 19.** 68-year-old female patient showing a macular foveoschisis with foveal detachment and a visual acuity (VA) of 20/100 (a,b). Two weeks later, the patient's condition worsened, with the development of a full-thickness macular hole (MH) and a decrease in VA to 20/400 (c). Three months after pars plana vitrectomy + inner limiting membrane peeling + silicone oil tamponade, optical coherence tomography demonstrated complete resolution of the MH and an improvement in VA to 20/40 (d).

reattach the retina and sclera and to relieve the outer traction exerted on the retina.

## 8. Dome-shaped macula

DSM was first described by Gaucher et al. in highly myopic eyes with visual impairment, metamorphopsia, and atrophic changes in the RPE combined with focal points of limited leakage. On ultrasound and OCT scans, there is a bulge in the macular retina, choroid, and RPE within the posterior staphyloma; in a high percentage of cases, these features are combined with a localized shallow retinal detachment at the top of the macula (Gaucher et al., 2008) (Fig 22).

DSM was defined as a new type of staphyloma by Gaucher (Gaucher et al., 2008). However, DSM was not included in Curtin's initial classification (Curtin, 1977), and Imamura et al. stated that DSM was "the result of a relative localized thickness variation of the sclera under the macula in highly myopic patients", which could not be classified into any known type of staphyloma (Imamura et al., 2011). Previously, it was suggested that all types of staphyloma might present single or multiple septa, terraces and steps and therefore DSM might be considered one of these septa or steps, round shaped and located in the macula (Fernandez-Vega Sanz et al., 2015).

Based on OCT findings, three different DSM morphologies have been described according to the primary orientation. The most common morphology is an oval-shaped, horizontally-oriented macula, which accounts for approximately 60% of cases; the other two types are rounded (20% of cases) and oval-shaped, vertically-oriented DSMs (20%) (Caillaux et al., 2013).

Ohno-Matsui found that 18.5% of highly myopic eyes presented DSM on MRI, even though most of the eyes had no posterior staphyloma (Ohno-Matsui, 2014). Gaucher and colleagues described DSM as a convex protrusion of the macula within a posterior staphyloma, generally in highly myopic eyes but also in eyes with low refractive error (Gaucher et al., 2008).

Although the pathogenesis of DSM remains unclear, several authors believe that it is related to a relative thickening of the sclera compared to the surrounding areas (Fernandez-Vega Sanz et al., 2015; Ohsugi et al., 2013). It has also been suggested that the RPE might be mechanically damaged by the protrusion of the dome within the staphyloma, thus leading to the accumulation of subretinal fluid, which might also occur at the border of the staphyloma. Chronic subfoveal fluid—whose presence is associated with decreased vision—is more common when the macular bulge is highly elevated. Curtin had previously suggested that the septa and steps were less ectatic than the rest of the staphyloma (Curtin, 1977). Focal resistance to scleral deformation may also play a role in DSM development. Focal defects in the macular Bruch's membrane may be associated with areas of focal relaxation of the posterior sclera, which permits the sclera in these areas to bulge inward, thus leading to the formation of DSM (Fajardo Sánchez et al., 2017). These focal defects of Bruch's membrane have also been associated with DSM (Fang et al., 2017). Fang et al. suggest that a weakened Bruch's membrane cannot push the sclera outwards, and so the sclera bulges inwards, inducing the DSM (Fang et al., 2017). Several authors have suggested that other factors may be involved in DSM, including localized thickening of the choroid (Gaucher et al., 2008), ocular hypotony, scleral folds secondary to the collapse of the posterior ocular wall, tangential vitreoretinal traction (Mehdizadeh and Nowroozzadeh, 2008), and areas of increased and decreased scleral thickness under the macula (Imamura et al., 2011). Other reports indicate that DSM can occur independently of staphyloma and might even develop prior to staphyloma (Ellabban et al., 2014), a hypothesis that is potentially supported by the early emergence of asymptomatic DSM in children.

The pathogenesis of neurosensory retinal detachment in DSM and at the edge of the staphyloma has been attributed to a mild thickening of the submacular choroid, which may be associated with subretinal fluid (Errera et al., 2014; Gaucher et al., 2008). However, other authors have

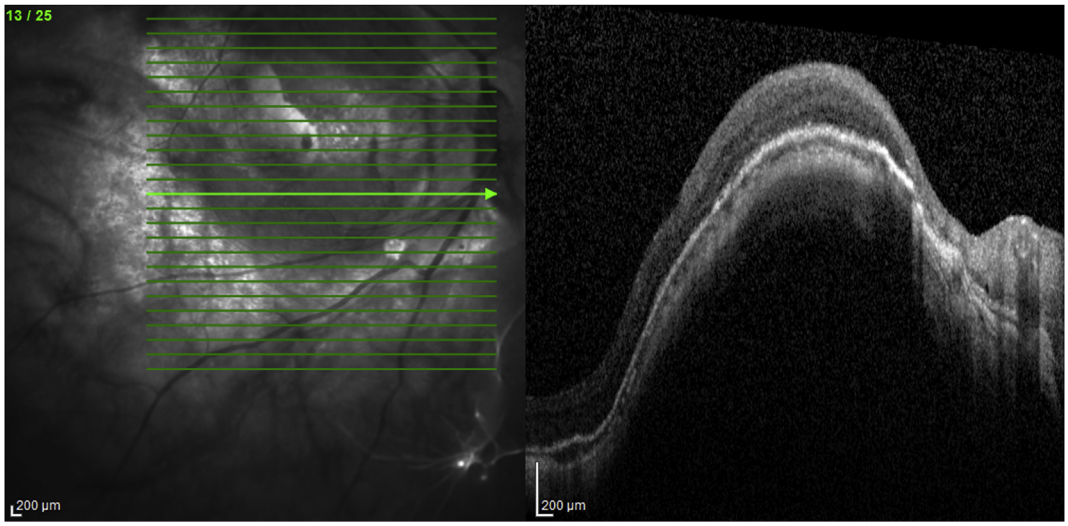


**Fig. 20.** Macular buckling can be used separately or in combination with pars plana vitrectomy to further reduce tractional forces in myopic traction maculopathy. It is seen on optical coherence tomography images as a hyporeflective mass that indents the posterior pole of the eye under the fovea.

**Fig. 21.** The progressive nature myopic traction maculopathy may induce the development of a full-thickness macular hole (MH) in severe cases, which can lead to retinal detachment in patients with persistent traction over the margins of the MH.

not found any differences between highly myopic eyes with and without DSM (Imamura et al., 2011). A mechanism similar to what occurs in nanophthalmia may be responsible for the formation of subfoveal fluid and for the increased scleral thickness that affects choroidal flow, thus inducing serous detachment. However, other authors (Ohsugi et al., 2013) have found no differences in choroidal thickness in eyes with or without DSM-associated subfoveal fluid. Other reports suggest the possible involvement of compressive changes in the choriocapillaris as well as secondary RPE changes (Byeon and Chu, 2011). DSM may represent an adaptive mechanism to scleral expansion in highly myopic eyes (Viola et al., 2015).

Retinal serous detachment, typically associated with localized RPE atrophy, may spontaneously appear and disappear in eyes with DSM. In this regard, Soudier et al. evaluated a small series of patients, finding that eyes without RPE atrophy did not present serous detachment during follow-up (Soudier et al., 2016).

Several studies have described a marked thinning of the choroid at the border of the staphyloma associated with retinal detachment and mCNV (Ellabban et al., 2014; Maruko et al., 2011; Yamagishi et al., 2012). Nevertheless, other authors have reported areas of choroidal thinning and thickening, respectively, in the lower and upper borders of the staphyloma, which might be related to the presence of subretinal fluid (Fernandez-Vega Sanz et al., 2015).

On FA and ICGA, multiple pinpoint focal areas of hyperfluorescence are often observed in the macular area due to RPE atrophy, without vascular hyperpermeability, a finding that is occasionally associated with minimal leakage.

A bulge height > 400 µm has been associated with decreased BCVA, subfoveal serous detachment, and greater RPE atrophy (Fajardo Sánchez et al., 2017). In eyes with DSM, BCVA usually remains stable over time, even though the bulge height tends to increase. Subretinal fluid may increase or disappear spontaneously, and RPE atrophy seems to correlate with bulge height and fluid duration (Soudier et al., 2016). It is likely that the DSM and subretinal fluid develop at early ages but the RPE only becomes atrophic several years later, a hypothesis that is supported by recent reports of DSM in children (Ellabban et al., 2014) (Fig 23). This finding of DSM in children suggests that the presence of DSM and subretinal fluid only become apparent when the RPE has become atrophic and BCVA has started to decrease—thus prompting a visit to the optometrist or ophthalmologist—and thus late in the development of the condition.

DSM-associated subretinal fluid usually remains stable over time while the RPE atrophies over time, leading to decreased visual function. Complications include mCNV, ERM, lamellar and full-thickness MH, and foveal and extrafoveal retinoschisis (Liang et al., 2015). However, these complications can be successfully managed by intravitreal anti-VEGF or surgery (Soudier et al., 2016).

### 8.1. Management

Presently, there is a lack of effective treatments to manage DSM-associated subretinal fluid and fluid at the border of the staphyloma. However, spontaneous resolution of subfoveal fluid in DSM has been reported (Tamura et al., 2014). This possible spontaneous resolution may mask the results of the treatments used in other series (laser photocoagulation, verteporfin PDT, and intravitreal injection of anti-angiogenic drugs, and steroids). Fernandez-Vega et al. retrospectively evaluated patients treated with intravitreal bevacizumab and/or PDT, finding that neither treatment (whether administered alone or in combination) significantly improved BCVA or the quantity of subretinal fluid; however, there were no treatment-related adverse effects

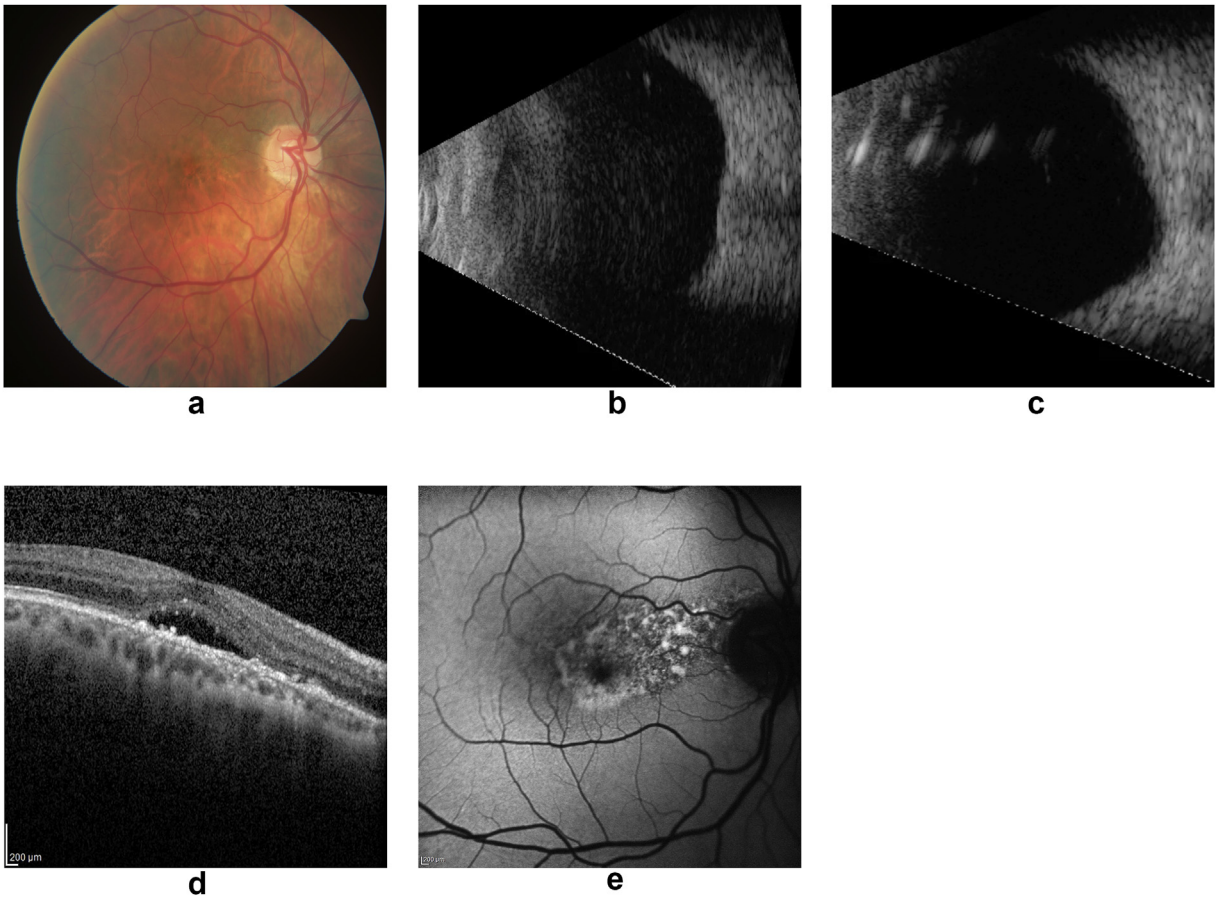


**Fig. 22.** Horizontally-oriented dome-shaped maculopathy with subfoveal fluid. (a) Colour fundus photography shows a juxtapapillary area of choroidal pallor. (b–c) Vertical and horizontal B-scan imaging show posterior pole staphyloma. (d) Spectral-Domain optical coherence tomography shows the presence of subfoveal fluid with oblique orientation of the posterior pole sclera, which is associated with (e) defective subfoveal autofluorescence corresponding to the area affected by subfoveal fluid.

(Fernandez-Vega Sanz et al., 2015). Several small studies involving patients treated by bevacizumab and PDT have reported similar findings—that is, no changes in BCVA, OCT findings, or symptoms after treatment (Chinskey and Johnson, 2013; Donati et al., 2013; Milani et al., 2010). More recent studies in patients with DSM-associated subretinal fluid treated by spironolactone have reported partial or complete resolution of the subretinal fluid with no changes in BCVA (Dirani et al., 2014; Fernández-Vega Sanz et al., 2016; Rocha Cabrera et al., 2017).

In our experience, the DSM-associated decline in BCVA occurs very slowly, usually appearing only several years after disease onset, an observation that is consistent with previous reports (Alakeely and Alrashaed, 2016; Soudier et al., 2016). Current therapies, such as threshold laser photocoagulation and PDT to the hyperfluorescent spots, may further damage the RPE, thus contributing to accelerated BCVA loss.

A recent study in 2 eyes of patients with DSM-related serous retinal detachment reported promising results at 12 months of follow-up after subthreshold laser treatment(Battaglia Parodi et al., 2017). Patients in that study underwent a single session of subthreshold laser treatment to cover the hyperfluorescent area evidenced on ICGA. Importantly, outcomes included a significant gain in BCVA, a decrease in central foveal thickness and subretinal fluid, and complete resolution in one case. After treatment, the hyperfluorescence was no longer evident on FA and ICGA.

## 9. Current challenges and future directions

Many unanswered questions remain about both high and pathologic myopia. For example, the mechanism driving the development of posterior staphyloma remains unclear. Axial length cannot be the only cause given the existence of reports of patients with staphyloma without high myopia (Wang et al., 2016) in which changes in collagen fibres surrounding the optic nerve have been implicated (McBrien and Gentle, 2003). The emergence of newer imaging modalities, such as polarization-sensitive OCT (Yamanari et al., 2008) and deep-penetrance SS-OCT will allow us to better evaluate the sclera and broaden our understanding of the sclera in the posterior pole of highly myopic eyes.

There are many open questions. Are high and pathologic myopia the same disease at different stages? Is it a matter of gene penetrance? Are they two independent diseases? Is the presence of posterior staphyloma sufficient to define high myopia? Given that pathologic myopia is a progressive disease, what is the first sign? What is the best surgical technique to assess MTM, given the difficulty and potential complications of surgery?

Posterior staphyloma plays a key role in myopic maculopathy by inducing anatomic alterations that stretch the tissues of the posterior pole, leading to traction, atrophy, and CNV. Multimodal imaging is the best approach to achieving an accurate diagnosis in those patients. The value of multimodal imaging can be seen in early stage MTM, which can only be detected by OCT. In addition, the “low” activity of mCNV makes a multimodal approach essential. FA is more sensitive than SD-OCT in detecting mCNV (82% vs. 48.6%) (Leveziel et al., 2013), but combing these two modalities increases the sensitivity to 97% (García-

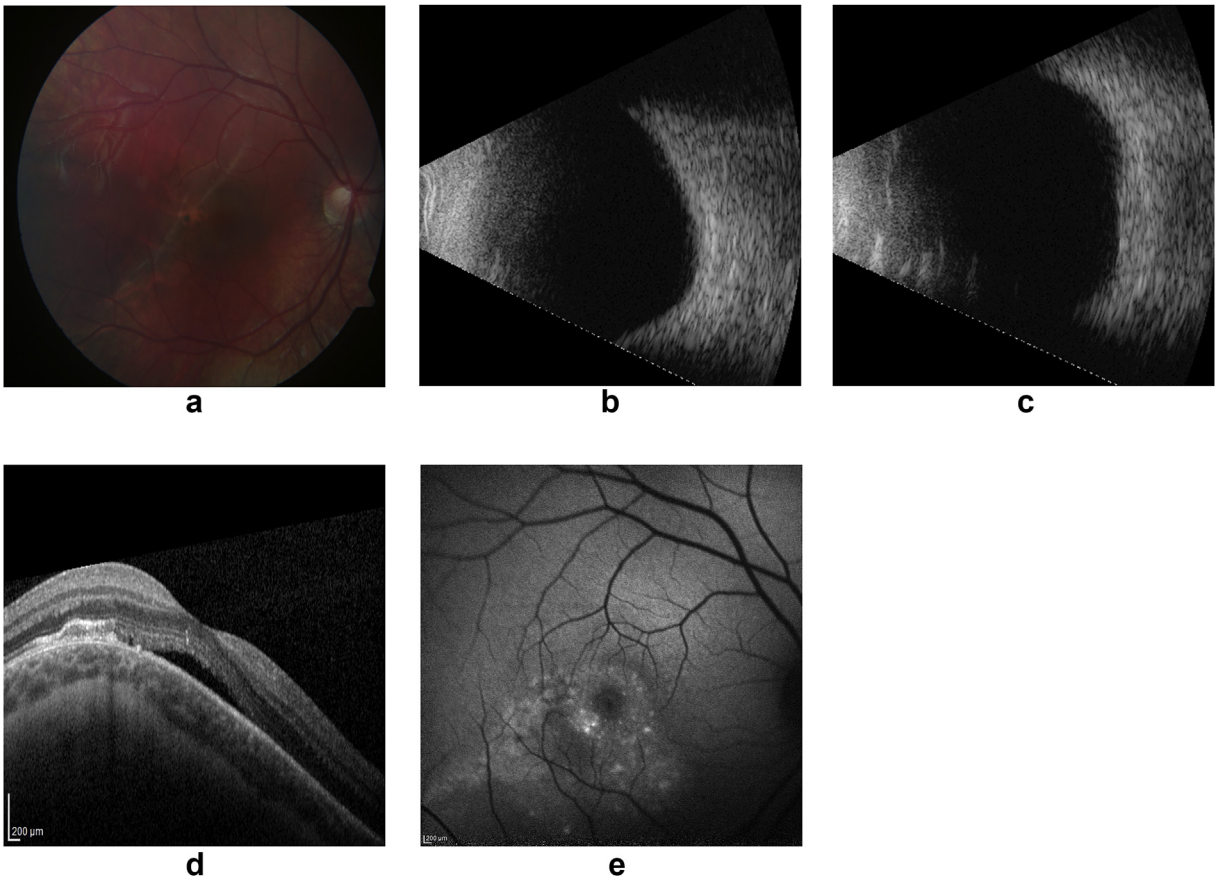


**Fig. 23.** Obliquely-oriented dome-shaped maculopathy with subfoveal fluid in an asymptomatic 6-year-old boy with visual acuity of 20/25. (a) Colour fundus photography shows an oblique staphyloma between the fovea and the optic disk. (b–c) Vertical and horizontal B-scan imaging show posterior pole staphyloma. (d) Spectral-Domain optical coherence tomography reveals an extremely obliquely-oriented posterior pole without subretinal fluid. (e) Defective subfoveal autofluorescence corresponding to the area affected by subfoveal fluid.

Layana et al., 2006). OCTA is another promising imaging technique in retinal vascular diseases, including mCNV. However, this technology requires further refinement to improve image quality, to minimize artefacts, and to improve field-of-view and segmentation in high myopic eyes with thin choroids, thin sclera, and posterior staphyloma. Aside from imaging studies, the symptoms of myopic patients must also be considered when signs of activity are not evident on imaging scans.

Myopic CNV often turns into scar tissue (stage 2 disease on OCT studies). Atrophic changes tend to develop around this scar tissue, thus leading to stage 3 disease on OCT. Similarly, chorioretinal atrophy will develop around this lesion, leading to atrophic myopic maculopathy over time. Chorioretinal atrophy around the regressed neovascular lesion, probably secondary to RPE damage, is a key factor in the progressive decrease in BCVA over time (Neelam et al., 2012). There are reports that state that this atrophy is, in fact, caused by enlarged defects of the Bruch's membrane rather than simply chorioretinal atrophy. For this reason, if fibrosis can be prevented, then BCVA loss due to CNV-related atrophy could be reduced in the medium to long-term. Currently, new treatments to reduce fibrosis induction in neovascular AMD are being evaluated in clinical studies. Future therapies should focus on preventing subretinal fibrosis, a characteristic feature of the scarring stage in mCNV, where atrophic areas eventually develop over time, resulting in vision loss. One possible treatment target is the inhibition of platelet-derived growth factor (PDGF), which is involved in pericyte loss. This target is interesting because pericytes are a major source of myofibroblasts, which are critical in the formation of tissue fibrosis. A clinical trial evaluated Fovista, an anti-PDGF aptamer (Ophthotech, New York, NY), administered by intravitreal injection in combination with anti-VEGF drugs for the treatment of neovascular AMD (Jaffe et al., 2016). Fovista (or similar molecules) could be applied to mCNV to reduce or prevent scarring, thus avoiding the chorioretinal atrophy that develops around the scar tissue.

The use of modified ILM peeling techniques will improve outcomes in MTM. A recent meta-analysis of patients treated with vitrectomy with or without ILM peeling concluded that although ILM peeling may lead to better anatomic outcomes, the use of ILM peeling did not result in a statistically-significant improvement in BCVA, nor did it lead to fewer complications (Meng et al., 2017). Modified peeling techniques that involve foveal sparing of the ILM in the centre of the macula have been proposed to protect Müller cells, thus reducing the risk of MH while also obtaining better outcomes (Ho et al., 2014, 2012; Shimada et al., 2012). Compared to ILM peeling, the inverted ILM flap technique can be used to treat myopic MH regardless of the diameter (Mete et al., 2017; Rizzo et al., 2017). When axial elongation and posterior staphyloma are both present, there is an increased risk of surgical failure in MH closure (Ohsugi et al., 2018); the definition of extreme myopia was established as axial length > 30 mm, as studies have shown that surgical results are worse in these eyes (Arias et al., 2015; Nadal et al., 2012).

Macular buckling (Schepens et al., 1957), performed alone or in combination with pars plana vitrectomy, facilitates foveal attachment (success rates range from 25% to 100%) but may induce some complications (Alkabes and Mateo, 2018). Combining macular buckling, vitrectomy, and ILM peeling has shown promising results in refractory cases (Ma et al., 2017).

Two mechanisms contribute to scleral deformation: elasticity and creep (Lewis et al., 2014). Elasticity refers to a reversible, instantaneous deformation associated with a change in an applied stress. By contrast,

**Table 3**
TCL Pterygium classification.

| | T (body) | C (central invasion) | L (limal invasion) |
|---|---|---|---|
| **1** | Atrophic | 0–2 mm | 0–4 mm |
| **2** | Moderate | 2–4 mm | 4–6 mm |
| **3** | Hypertrophic | > 4 mm | > 6 mm |

creep refers to a time-dependent deformation associated with a constant applied stress. Intraocular pressure can provide a constant applied stress to scleral collagen fibres. Scleral collagen exhibits a relatively annular organization around the optic nerve and macular area, which are the areas most susceptible to expansion under the constant force associated with normal intraocular pressure (McBrien and Gentle, 2003). Myopic eyes exhibit reduced scleral rigidity compared to emmetropic and hyperopic eyes (Sergienko and Shargorogska, 2012). In preclinical models, inhibition of collagen crosslinking augments the degree of induced myopia (Mcbrien and Norton, 1994). A number of different approaches have been used to induce scleral collagen crosslinking with the goal of increasing scleral rigidity to reduce expansion of the vitreous cavity (Babar et al., 2015; Liu and Wang, 2013; Stewart et al., 2009; Trier et al., 1999; Wollensak et al., 2003; Wollensak and Iomdina, 2009; Wong et al., 2012). Depending on the treatment parameters, some of these methods have been associated with retinal toxicity (Zhang et al., 2013) or discoloration of the sclera (Liu and Wang, 2013). Non-selective crosslinking may damage collagen components of blood vessels supplying the choroid and outer retina (Elsheikh and Phillips, 2013). Given that scleral thinning in high myopia is most pronounced in the posterior pole and peripapillary retina (Curtin et al., 1979), treatment should probably be directed at the sclera overlying the area centralis; however, one preclinical study suggested that equatorial treatment might be effective (Dotan et al., 2014) Scleral myofibroblasts, which may also influence scleral mechanical properties (Phillips and McBrien, 2004), might also be damaged with this approach. Transscleral solute diffusion and hydraulic conductivity are altered by crosslinking (Stewart et al., 2009), and it is not clear what effect this change might have on ocular health.

Cell-based therapies might be useful to stabilize scleral tissue biomechanics (Janowski et al., 2015). Scleral fibroblasts seem to play a critical role in modulating scleral biomechanical properties (McBrien, 2013; McBrien and Gentle, 2003). Scleral fibroblast transplants might provide a means to stabilize scleral biomechanics without the attendant risks of altered scleral diffusion properties, retinal or blood vessel damage; moreover, such a procedure would be quite simple, similar to retrobulbar fibroblast injection. Shinohara et al. used this technique experimentally, successfully reinforcing the sclera of rats using newly synthesized collagen fibrils, thereby reducing axial elongation and the risk of myopia (Shinohara et al., 2018).

At present it is not known whether there are genetic differences between high and pathologic myopia. Some authors suggest the existence of a pathological difference between the high myopia induction phase and the development of myopic maculopathy that may be mediated, at least in part, by genetics. Treatments targeting *CCDC*102B may thus prevent the development of myopic maculopathy and blindness, even after the patient has developed high myopia (Hosoda et al., 2018).

Determination of the genetic basis of myopic maculopathy could lead to the development of new strategies to prevent myopia-induced low vision and blindness. It is important to clarify whether myopic maculopathy is an inevitable consequence of high myopia or if these are independent processes with their own genetic and environmental influences. New studies, with larger sample sizes from a range of different populations and ethnicities, would help us to better understand myopic maculopathy and to better estimate possible responses to novel therapies. New experimental models of posterior staphyloma and chorioretinal atrophy may also be a promising approach to broadening our understanding (Cases et al., 2015).

**Table 5**
Myopic maculopathy atrophy-based classification (Ohno-Matsui et al., 2015).

| | Atrophy degree | "Plus" signs |
|---|---|---|
| 0 | no myopic retinal lesions | Lacquer cracks |
| 1 | tessellated fundus only | Fuch's spot |
| 2 | diffuse chorioretinal atrophy | Myopic CNV |
| 3 | patchy chorioretinal atrophy | |
| 4 | macular atrophy | |

CNV: Choroidal neovascularization.

In the introduction to the present document, we noted the clear need for a simple, universally-accepted classification system for myopic maculopathy that could be used in future studies to ensure comparability. Although the current classification system for atrophic myopic maculopathy (Ohno-Matsui et al., 2015) is well-suited to identify the various stages of atrophy, it is insufficient, in our opinion, because it fails to account for the tractional component and also considers mCNV as a "plus sign" only.

Several simple, practical classification systems are currently used to classify many eye diseases. For example, the pterygium classification system shown below (Table 3) is quite simple, and the most important characteristics of the disease can be easily coded using only three letters (Pastor-Vivas et al., 2011). In this system, a hypertrophic pterygium invading 3.5 mm of the cornea and covering 6.1 mm of limbus would be a T3C2L3. Other fields, most notably oncology, also use relatively simple classification systems, with the TNM cancer staging system being one of the best examples (Gospodarowicz et al., 2004).

We believe that a similar classification system would be useful in myopic maculopathy. Such a system would integrate some of the currently existing classification systems (Ohno-Matsui et al., 2015), but would include tractional and neovascular components, which play a highly relevant clinical role.

The main classification systems currently available the following:

- Foveoschisis: extension. (Shimada et al., 2013) (Table 2).
- Foveoschisis: layers involved (Fujimoto et al., 2010; Ceklic et al., 2017) (Table 4)
- Atrophy (Ohno-Matsui et al., 2015) (Table 5)

We propose a new system based on three key factors: atrophy (A), traction (T), and neovascularization (N), which we call the ATN classification system. This system would include the three most important myopic alterations, thus allowing classification in a simple, systematic manner that is both easy to apply and understand. This proposed classification system does not make any changes to the current atrophy classification, but it does include new proposals for the classification of the tractional and neovascular components, as follows (Table 6).

For example: a patient with patchy atrophy, foveal tractional

**Table 4**
Myopic foveoschisis classification according to layer involvement (Fujimoto et al., 2010; Ceklic et al., 2017).

| | Inner | Outer | Inner + Outer |
|---|---|---|---|
| Involved layers | IPL + GCL + RNFL | OPL + ONL | IPL + GCL + RNFL + OPL + ONL |

IPL: Inner plexiform layer; GCL: Ganglion cell layer; RNFL: Retinal fiber layer; OPL: Outer plexiform layer; IPL: Inner plexiform layer.

**Table 6**
New proposed classification system for myopic maculopathy, which considers atrophic (A), tractional (T) and neovascular (N) components.

| Atrophic component (A) | Tractional component (T) | Neovascular component (N) |
|---|---|---|
| A0: no myopic retinal lesions | T0: No macular schisis | N0: No Myopic CNV |
| A1: tessellated fundus only | T1: Inner or outer foveoschisis | N1: Macular lacquer cracks |
| A2: diffuse chorioretinal atrophy | T2: Inner + outer foveoschisis | N2a: Active CNV |
| A3: patchy chorioretinal atrophy | T3: Foveal detachment | N2s: Scar / Fuch's spot |
| A4: complete macular atrophy | T4: Full-thickness MH | |
| | T5: MH + Retinal detachment | |

CNV: Choroidal neovascularization; MH: Macular hole.

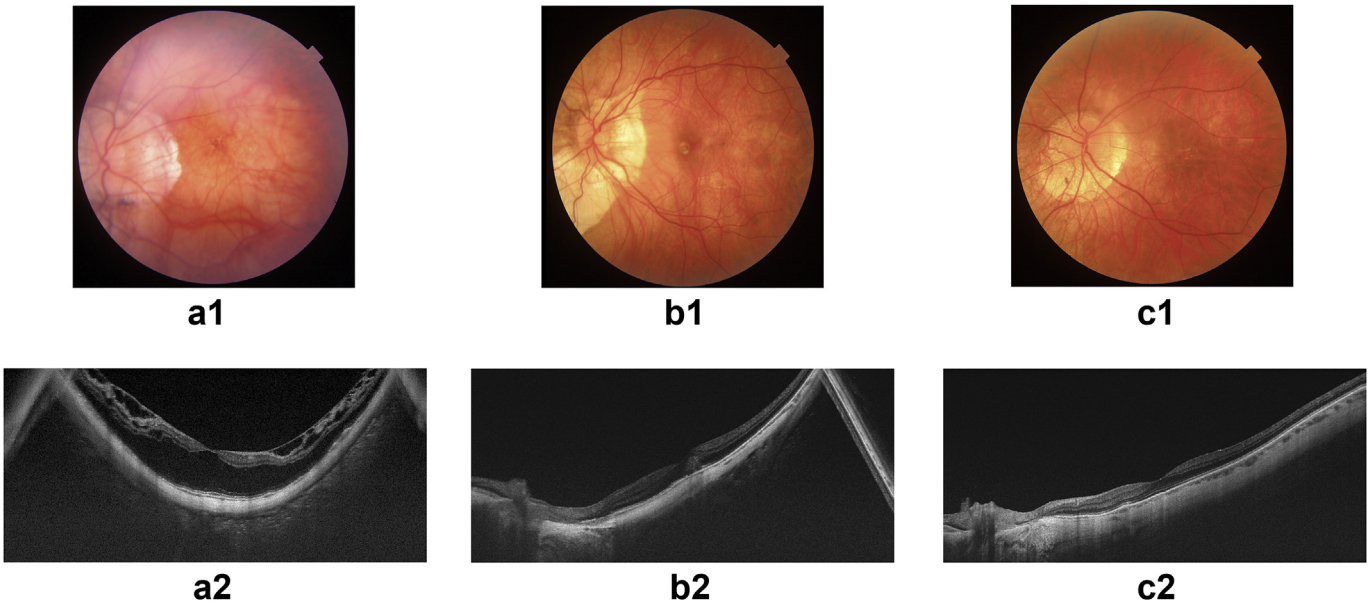


**Fig. 24.** Examples of the proposed new ATN classification system for myopic maculopathy. a) A highly myopic patient with a lacquer crack on fundus photography and inner and outer retinoschisis on optical coherence tomography (OCT); ATN classification: A1T2N1. b) Patient with diffuse atrophy and a subtle foveal haemorrhage on fundus photography accompanied by an active choroidal neovascularization (CNV) lesion on OCT would be classified as A2T0N2a. c) Highly myopic patient with a tessellated fundus and no lesions or tractions identified on OCT would be ATN stage A1T0N0.

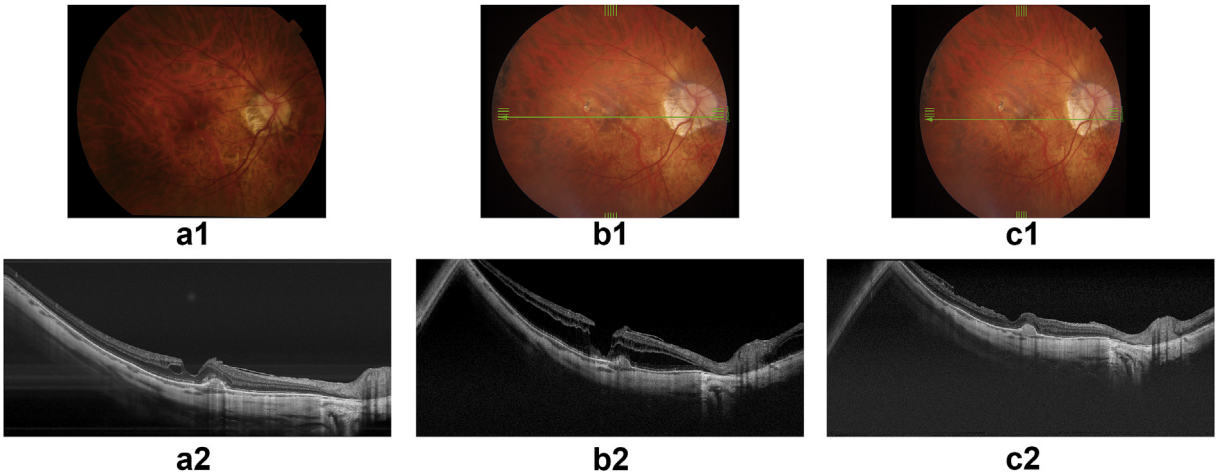


**Fig. 25.** Example of the follow-up and evolution of a highly myopic patient using the ATN classification system a) Tessellated fundus, active CNV lesion with subretinal and intreretinal fluid with no foveoschisis (A1T0N2a). b) Eight years later the patient complaint of visual acuity loss and showed patchy chorioretinal atrophy with a Fuch's spot and an inner foveoschisis (A3T1N2s). c) The patient underwent pars plana vitrectomy with inner limiting membrane peeling with a complete resolution of his foveoschisis, turning into stage (A3T0N2s).

detachment without MH, and a CNV scar would be classified as A3T3N2s. Precisely defining the stage of myopic maculopathy would allow for a better follow-up and would help to unify clinical findings for research purposes (Fig. 24 and 25). Changes of a patient's ATN classification with time would give us information about the course and evolution of the disease and its natural history. Currently, our group is carrying out a study to verify the value of this proposed classification system and to determine the inter-observer correlation and potential applications.

## Declarations of interest

None.

## Acknowledgements

This study was supported in part by a grant from the Spanish Ministry of Health, Instituto de Salud Carlos III, Red Temática de Investigación Cooperativa en Salud: ""“Prevención, detección precoz, y tratamiento de la patología ocular prevalente, degenerativa y crónica” (RD16/0008/0021).

## Appendix A. Supplementary data

Supplementary data to this article can be found online at https://doi.org/10.1016/j.preteyeres.2018.10.005.

## References

Ahmad, R., Al-Aqaba, M.A., Fares, U., Otri, A.M., Miri, A., Said, D.G., Dua, H.S., 2010. Correlation between the pattern of myopic fundal changes and the axis of astigmatism of the eye. Br. J. Ophthalmol. 94, 307–310.
Akiba, J., 1993. Prevalence of posterior vitreous detachment in high myopia. Ophthalmology 100, 1384–1388.
Alakeely, A., Alrashaed, S., 2016. Serous retinal detachment in dome-shaped macula with 7 years follow-up. Middle East Afr. J. Ophthalmol. 23, 323.
Alkabes, M., Mateo, C., 2018. Macular buckle technique in myopic traction maculopathy: a 16-year review of the literature and a comparison with vitreous surgery. Graefe's Arch. Clin. Exp. Ophthalmol. 256, 863–877.
Ando, F., Ohba, N., Touura, K., Hirose, H., 2007. Anatomical and visual outcomes after episcleral macular buckling compared with those after pars plana vitrectomy for retinal detachment caused by macular hole in highly myopic eyes. Retina 27, 37–44.
Arias, L., Caminal, J.M., Rubio, M.J., Cobos, E., Garcia-Bru, P., Filloy, A., Padron, N., Mejia, K., 2015. Autofluorescence and axial length as prognostic factors for outcomes of macular hole retinal detachment surgery in high myopia. Retina 35, 423–428.
Arias, L., Planas, N., Prades, S., Caminal, J., Rubio, M., Pujol, O., Roca, G., 2008. Intravitreal bevacizumab (Avastin) for choroidal neovascularisation secondary to pathological myopia: 6-month results. Br. J. Ophthalmol. 92, 1035–1039.
Asakuma, T., Yasuda, M., Ninomiya, T., Noda, Y., Arakawa, S., Hashimoto, S., Ohno-Matsui, K., Kiyohara, Y., Ishibashi, T., 2012. Prevalence and risk factors for myopic retinopathy in a Japanese population: the hisayama study. Ophthalmology 119, 1760–1765.
Astroz, P., Miere, A., Mrejen, S., Sekfali, R., Souied, E.H., Jung, C., Nghiem-Buffet, S., Cohen, S.Y., 2018. Optical coherence tomography angiography to distinguish choroidal neovascularization from macular inflammatory lesions in multifocal choroiditis. Retina 38, 299–309.
Avila, M.P., Weiter, J.J., Jalkh, A.E., Trempe, C.L., Pruett, R.C., Schepens, C.L., 1984. Natural history of choroidal neovascularization in degenerative myopia. Ophthalmology 91, 1573–1581.
Avisar, R., Friling, R., Snir, M., Avisar, I., Weinberger, D., 2006. Estimation of prevalence and incidence rates and causes of blindness in Israel, 1998-2003. Isr. Med. Assoc. J. 8, 880–881.
Avitabile, T., Bonfiglio, V., Buccoliero, D., Castiglione, F., Reibaldi, M., Castaing, M., Mistretta, A., 2011. Heavy versus standard silicone oil in the management of retinal detachment with macular hole in myopic eyes. Retina 31, 540–546.
Baba, T., Ohno-Matsui, K., Futagami, S., Yoshida, T., Yasuzumi, K., Kojima, A., Tokoro, T., Mochizuki, M., 2003. Prevalence and characteristics of foveal retinal detachment without macular hole in high myopia. Am. J. Ophthalmol. 135, 338–342.
Baba, T., Ohno-Matsui, K., Yoshida, T., Yasuzumi, K., Futagami, S., Tokoro, T., Mochizuki, M., 2002. Optical coherence tomography of choroidal neovascularization in high myopia. Acta Ophthalmol. Scand. 80, 82–87.
Babar, N., Kim, M., Cao, K., Shimizu, Y., Kim, S.Y., Takaoka, A., Trokel, S.L., Paik, D.C., 2015. Cosmetic preservatives as therapeutic corneal and scleral tissue cross-linking agents. Investig. Ophthalmol. Vis. Sci. 56, 1274–1282.
Bandello, F., Lanzetta, P., Battaglia Parodi, M., Roman-Pognuz, D., Saviano, S., Ravalico, G., 2003. Photodynamic therapy of subfoveal recurrences after laser photocoagulation of extrafoveal choroidal neovascularization in pathologic myopia. Graefe's Arch. Clin. Exp. Ophthalmol. 241, 567–570.
Bando, H., Ikuno, Y., Choi, J.S., Tano, Y., Yamanaka, I., Ishibashi, T., 2005. Ultrastructure of internal limiting membrane in myopic foveoschisis. Am. J. Ophthalmol. 139, 197–199.
Barteselli, G., Lee, S.N., El-Emam, S., Hou, H., Ma, F., Chhablani, J., Conner, L., Cheng, L., Bartsch, D.U., Freeman, W.R., 2014. Macular choroidal volume variations in highly myopic eyes with myopic traction maculopathy and choroidal neovascularization. Retina 34, 880–889.
Battaglia Parodi, M., Iacono, P., Bandello, F., 2017. Subthreshold laser treatment for serous retinal detachment in dome-shaped macula associated with pathologic myopia. Retina.
Battaglia Parodi, M., Iacono, P., Bandello, F., 2016. Correspondence of leakage on fluorescein angiography and optical coherence tomography parameters in diagnosis and monitoring of myopic choroidal neovascularization treated with bevacizumab. Retina 36, 104–109.
Benhamou, N., Massin, P., Haouchine, B., Erginay, A., Gaudric, A., 2002. Macular retinoschisis in highly myopic eyes. Am. J. Ophthalmol. 133, 794–800.
Blach, R., Jay, B., Macfaul, P., 1965. The concept of degenerative myopia. Proc R Soc Med 58, 109–112.
Blach, R.K., Jay, B., Kolb, H., 1966. Electrical activity of the eye in high myopia. Br. J. Ophthalmol. 50, 629–641.
Blanco Teijeiro, M., Gomez-Ulla, F., Piñeiro Ces, A., 2015. Síndrome de tracción vitreomacular y membrana epirretiniana. In: JM, R.-M., Gomez-Ulla, F., L, A.-B. (Eds.), Patología Retiniana En Alta Miopía. Sociedad Española de Oftalmología, Madrid, pp. 150–157.
Blinder, K.J., Blumenkranz, M.S., Bressler, N.M., Bressler, S.B., Donati, G., Lewis, H., Lim, J.I., Menchini, U., Miller, J.W., Mones, J.M., Potter, M.J., Pournaras, C., Reaves, A., Rosenfeld, P., Schachat, A.P., Schmidt-Erfurth, U., Sickenberg, M., Singerman, L.J., Slakter, J.S., Strong, H.A., Virgili, G., Williams, G.A., 2003. Verteporfin therapy of subfoveal choroidal neovascularization in pathologic myopia: 2-Year results of a randomized clinical trial - VIP report no. 3. Ophthalmology 110, 667–673.
Bray, N., Brand, A., Taylor, J., Hoare, Z., Dickinson, C., Edwards, R.T., 2017. Portable electronic vision enhancement systems in comparison with optical magnifiers for near vision activities: an economic evaluation alongside a randomized crossover trial. Acta Ophthalmol 95, e415–e423.
Brown, D., Kaiser, P., Michels, M., Soubrane, G., Heier, J., Kim, R., Sy, J., Schneider, S., 2006. Ranibizumab versus verteporfin for neovascular age-related macular degeneration. N Engl J Med 355, 1432–1444.
Bruè, C., Pazzaglia, A., Mariotti, C., Reibaldi, M., Giovannini, A., 2016. Aflibercept as primary treatment for myopic choroidal neovascularisation: a retrospective study. Eye 30, 139–145.
Bruyere, E., Miere, A., Cohen, S.Y., Martiano, D., Sikorav, A., Popeanga, A., Semoun, O., Querques, G., Souied, E.H., 2017. Neovascularization secondary to high myopia imaged by optical coherence tomography angiography. Retina 37, 2095–2101.
Buch, H., Vinding, T., La Cour, M., Appleyard, M., Jensen, G.B., Nielsen, N.V., 2004. Prevalence and causes of visual impairment and blindness among 9980 scandinavian adults: the copenhagen city eye study. Ophthalmology 111, 53–61.
Byeon, S., Chu, Y., 2011. Dome-shaped macula. Am. J. Ophthalmol. 151, 1101.
Caillaux, V., Gaucher, D., Gualino, V., Massin, P., Tadayoni, R., Gaudric, A., 2013. Morphologic characterization of dome-shaped macula in myopic eyes with serous macular detachment. Am. J. Ophthalmol. 156.
Calvo-Gonzalez, C., Reche-Frutos, J., Donate, J., Fernandez-Perez, C., Garcia-Feijoo, J., 2011. Intravitreal ranibizumab for myopic choroidal neovascularization: factors predictive of visual outcome and need for retreatment. Am. J. Ophthalmol. 151, 529–534.
Cases, O., Joseph, A., Obry, A., Santin, M.D., Ben-Yacoub, S., Pâques, M., Amsellem-Levera, S., Bribian, A., Simonutti, M., Augustin, S., Debeir, T., Sahel, J.A., Christ, A., De Castro, F., Lehéricy, S., Cosette, P., Kozyraki, R., 2015. Foxg1-Cre mediated Lrp2 inactivation in the developing mouse neural retina, ciliary and retinal pigment epithelia models congenital high myopia. PLoS One 10, e0129518.
Cedrone, C., Culasso, F., Cesareo, M., Nucci, C., Palma, S., Mancino, R., Cerulli, L., 2003. Incidence of blindness and low vision in a sample population the Priverno eye study. Italy. Ophthalmology 110, 584–588.
Cedrone, C., Nucci, C., Scuderi, G., Ricci, F., Cerulli, A., Culasso, F., 2006. Prevalence of blindness and low vision in an Italian population: a comparison with other European studies. Eye 20, 661–667.
Ceklic, L., Munk, M.R., Wolf-Schnurrbusch, U., Gekkieva, M., Wolf, S., 2017. Visual acuity outcomes of ranibizumab treatment in pathologic myopic eyes with macular retinoschisis and choroidal neovascularization. Retina 37, 687–693.
Ceklic, L., Wolf-schnurrbusch, U., Gekkieva, M., Wolf, S., 2014. Visual acuity outcome in RADIANCE study patients with dome-shaped macular features. Ophthalmology 121, 2288–2289.
Chan, N.S.-W., Teo, K., Cheung, C.M.G., 2016. Epidemiology and diagnosis of myopic choroidal neovascularization in Asia. Eye Contact Lens Sci. Clin. Pract. 42, 48–55.
Chan, W.-M., Lai, T.Y.Y., Chan, K.-P., Li, H., Liu, D.T.L., Lam, D.S.C., Pang, C.-P., 2008. Changes in aqueous vascular endothelial growth factor and pigment epithelial-derived factor levels following intravitreal bevacizumab injections for choroidal neovascularization secondary to age-related macular degeneration or pathologic myopia. Retina 28, 1308–1313.
Chan, W., Lai, T., Liu, D., Lam, D., 2009. Intravitreal bevacizumab (Avastin) for myopic choroidal neovascularisation: 1-year results of a prospective pilot study. Br. J. Ophthalmol. 93, 150–154.
Chan, W.M., Lai, T.Y.Y., Wong, A.L., Liu, D.T.L., Lam, D.S.C., 2007. Combined photodynamic therapy and intravitreal triamcinolone injection for the treatment of choroidal neovascularisation secondary to pathological myopia: a pilot study. Br. J. Ophthalmol. 91, 174–179.
Chang, L., Pan, C.W., Ohno-Matsui, K., Lin, X., Cheung, G.C.M., Gazzard, G., Koh, V., Hamzah, H., Tai, E.S., Lim, S.C., Mitchell, P., Young, T.L., Aung, T., Wong, T.Y., Saw, S.M., 2013. Myopia-related fundus changes in Singapore adults with high myopia. Am. J. Ophthalmol. 155, 991–999.
Chen, S.-J.J., Cheng, C.-Y.Y., Li, A.-F.F., Peng, K.-L.L., Chou, P., Chiou, S.-H.H., Hsu, W.-M.M., 2012. Prevalence and associated risk factors of myopic maculopathy in elderly Chinese: the Shihpai eye study. Investig. Ophthalmol. Vis. Sci. 53, 4868–4873.
Chen, S.N., Yang, C.M., 2016. Inverted internal limiting membrane insertion for macular hole-associated retinal detachment in high myopia. Am. J. Ophthalmol. 162, 99–106.
Chen, Y.P., Chen, T.L., Yang, K.R., Lee, W.H., Kuo, Y.H., Chao, A.N., Wu, W.C., Chen, K.J., Lai, C.C., 2006. Treatment of retinal detachment resulting from posterior staphyloma-associated macular hole in highly myopic eyes. Retina 26, 25–31.
Cheng, J.-W., Cheng, S.-W., Cai, J.-P., Li, Y., Wei, R.-L., 2013. The prevalence of visual

impairment in older adults in mainland China: a systematic review and meta-analysis. Ophthalmic Res 49, 1–10.
Cheng, Y., Li, Y., Huang, X., Qu, Y., 2017. Application of optical coherence tomography angiography to assess anti-vascular endothelial growth factor therapy in myopic choroidal neovascularization. Retina.
Cheung, C.M.G., Arnold, J.J., Holz, F.G., Park, K.H., Lai, T.Y.Y., Larsen, M., Mitchell, P., Ohno-Matsui, K., Chen, S.J., Wolf, S., Wong, T.Y., 2017. Myopic choroidal neovascularization: review, guidance, and consensus statement on management. Ophthalmology 124, 1690–1711.
Chinskey, N.D., Johnson, M.W., 2013. Treatment of subretinal fluid associated with dome-shaped macula. Ophthalmic Surgery, Lasers Imaging Retin 44, 593–595.
Coco, R.M., Sanabria, M.R., Alegría, J., 2012. Pathology associated with optical coherence tomography macular bending due to either dome-shaped macula or inferior staphyloma in myopic patients. Ophthalmologica 228, 7–12.
Cohen, S.Y., Laroche, A., Leguen, Y., Soubrane, G., Coscas, G.J., 1996. Etiology of choroidal neovascularization in young patients. Ophthalmology 103, 1241–1244.
Cohen, S.Y., Nghiem-Buffet, S., Grenet, T., Dubois, L., Ayrault, S., Fajnkuchen, F., Delahaye-Mazza, C., Quentel, G., Tadayoni, R., 2015. Long-term variable outcome of myopic choroidal neovascularization treated with ranibizumab. Jpn. J. Ophthalmol. 59, 36–42.
Cotter, S.A., Varma, R., Ying-Lai, M., Azen, S.P., Klein, R., 2006. Causes of low vision and blindness in adult latinos. The los angeles latino eye study. Ophthalmology 113, 1574–1582.
Coutinho, A.M., Silva, R.M., Nunes, S.G., Cachulo, M.L., Figueira, J.P., Murta, J.N., 2011. Photodynamic therapy in highly myopic eyes with choroidal neovascularization. Retina 31, 1089–1094.
Curcio, C., Saunders, P., Younger, P., Malek, G., 2000. Peripapillary chorioretinal atrophy: Bruch's membrane changes and photoreceptor loss. Ophthalmology 107, 334–343.
Curtin, B.J., 1988. Pathologic myopia. Acta Ophthalmol Suppl 185, 105–106.
Curtin, B.J., 1979. Physiologic vs pathologic myopia: genetics vs environment. Ophthalmology 86, 681–691.
Curtin, B.J., 1977. The posterior staphyloma of pathologic myopia. Trans. Am. Ophthalmol. Soc. 75, 67–86.
Curtin, B.J., Iwamoto, T., Renaldo, D.P., 1979. Normal and staphylomatous sclera of high myopia: an electron microscopic study. Arch. Ophthalmol. 97, 912–915.
Curtin, B.J., Karlin, D.B., 1971. Axial length measurements and fundus changes of the myopic eye. Am. J. Ophthalmol. 71, 42–53.
Curtin, B.J., Teng, C.C., 1985. Scleral changes in pathological myopia. Trans. Am. Acad. Ophthalmol. Otolaryngol. 62, 777–788 discussion 788-90.
Delori, F.C., Goger, D.G., Dorey, C.K., 2001. Age-related accumulation and spatial distribution of lipofuscin in RPE of normal subjects. Investig. Ophthalmol. Vis. Sci. 42, 1855–1866.
Dirani, A., Matet, A., Beydoun, T., Mantel, I., Behar-Cohen, F., 2014. Resolution of foveal detachment in dome-shaped macula after treatment by spironolactone: report of two cases and mini-review of the literature. Clin. Ophthalmol. 8, 999–1002.
Donati, M.C., Miele, A., Abbruzzese, G., Giuntoli, M., Giansanti, F., Menchini, U., 2013. Treatment of macular serous neuroretinal detachment in tilted disk syndrome: report of 3 cases. Eur. J. Ophthalmol. 23, 267–270.
Dotan, A., Kremer, I., Livnat, T., Zigler, A., Weinberger, D., Bourla, D., 2014. Scleral cross-linking using riboflavin and ultraviolet-A radiation for prevention of progressive myopia in a rabbit model. Exp. Eye Res. 127, 190–195.
Ellabban, A.A., Tsujikawa, A., Muraoka, Y., Yamashiro, K., Oishi, A., Ooto, S., Nakanishi, H., Kuroda, Y., Hata, M., Takahashi, A., Yoshimura, N., 2014. Dome-shaped macular configuration: longitudinal changes in the sclera and choroid by swept-source optical coherence tomography over two years. Am. J. Ophthalmol. 158, 1062–1070.
Elsheikh, A., Phillips, J.R., 2013. Is scleral cross-linking a feasible treatment for myopia control? Ophthalmic Physiol. Opt. 33, 385–389.
Ergun, E., Heinzl, H., Stur, M., 2004. Prognostic factors influencing visual outcome of photodynamic therapy for subfoveal choroidal neovascularization in pathologic myopia. Am. J. Ophthalmol. 138, 434–438.
Errera, M.H., Michaelides, M., Keane, P.A., Restori, M., Paques, M., Moore, A.T., Yeoh, J., Chan, D., Egan, C.A., Patel, P.J., Tufail, A., 2014. The extended clinical phenotype of dome-shaped macula. Graefe's Arch. Clin. Exp. Ophthalmol. 252, 499–508.
Fajardo Sánchez, J., Chau Ramos, C.E., Roca Fernández, J.A., Urcelay Segura, J.L., 2017. Clinical, fundoscopic, tomographic and angiographic characteristics of dome shaped macula classified by bulge height. Arch. la Soc. Española Oftalmol. (English Ed. 92, 458–463.
Fang, Y., Jonas, J.B., Yokoi, T., Cao, K., Shinohara, K., Ohno-Matsui, K., 2017. Macular Bruch's membrane defect and dome-shaped macula in high myopia. PLoS One 12.
Fang, Y., Yokoi, T., Nagaoka, N., Shinohara, K., Onishi, Y., Ishida, T., Yoshida, T., Xu, X., Jonas, J.B., Ohno-Matsui, K., 2018. Progression of myopic maculopathy during 18-year follow-up. Ophthalmology 125, 863–877.
Fernandez-Vega Sanz, A., Rangel, C., Villota Deleu, E., 2015. Estafiloma miópico, mácula en cúpula y patología relacionada con el borde de los estafilomas. In: Ruiz-Moreno, J.M., Arias, L., Gomez-Ulla, F. (Eds.), Patología Retiniana En Alta Miopía. Sociedad Española de Retina y Vitreo, Madrid, pp. 255–274.
Fernández-Vega Sanz, Á., Rangel, C.M., Villota Deleu, E., Fernández-Vega Sanz, B., Sánchez-Ávila, R.M., 2016. Serous retinal detachment associated with dome-shaped macula and staphyloma edge in myopic patients before and after treatment with spironolactone. J. Ophthalmol. 2016, 8491320.
Figueroa, M.S., Ruiz-Moreno, J.M., Gonzalez Del Valle, F., Govetto, A., De La Vega, C., Plascencia, R.N., Contreras, I., Medina, J.L., 2015. Long-term outcomes of 23-gauge pars plana vitrectomy with internal limiting membrane peeling and gas tamponade for myopic traction maculopathy. Retina 35, 1836–1843.
Flores-Moreno, I., Lugo, F., Duker, J.S., Ruiz-Moreno, J.M., 2013. The relationship between axial length and choroidal thickness in eyes with high myopia. Am. J. Ophthalmol. 155, 314–319.
Foos, R.Y., 1977. Vitreoretinal juncture; epiretinal membranes and vitreous. Invest. Ophthalmol. Vis. Sci. 16, 416–422.
Forte, R., Pascotto, F., Napolitano, F., Cennamo, G., de Crecchio, G., 2007. En face optical coherence tomography of macular holes in high myopia. Eye 21, 436–437.
Foster, P.J., Jiang, Y., 2014. Epidemiology of myopia. Eye 28, 202–208.
Franqueira, N., Cachulo, M.L., Pires, I., Fonseca, P., Marques, I., Figueira, J., Silva, R., 2011. Long-term follow-up of myopic choroidal neovascularization treated with ranibizumab. Ophthalmologica 227, 39–44.
Freund, K.B., Zweifel, S. a, Engelbert, M., 2010. Do we need a new classification for choroidal neovascularization in age-related macular degeneration? Retina 30, 1333–1349.
Fujimoto, M., Hangai, M., Suda, K., Yoshimura, N., 2010. Features associated with foveal retinal detachment in myopic macular retinoschisis. Am. J. Ophthalmol. 150, 863–870.e1.
Fujiwara, T., Imamura, Y., Margolis, R., Slakter, J.S., Spaide, R.F., 2009. Enhanced depth imaging optical coherence tomography of the choroid in highly myopic eyes. Am. J. Ophthalmol. 148, 445–450.
Gandorfer, A., Scheler, R., Schumann, R., Haritoglou, C., Kampik, A., 2009. Interference microscopy delineates cellular proliferations on flat mounted internal limiting membrane specimens. Br. J. Ophthalmol. 93, 120–122.
Gao, L.Q., Liu, W., Liang, Y.B., Zhang, F., Wang, J.J., Peng, Y., Wong, T.Y., Wang, N.L., Mitchell, P., Friedman, D.S., 2011. Prevalence and characteristics of myopic retinopathy in a rural Chinese adult population: the Handan Eye Study. Arch. Ophthalmol. 129, 1199–1204.
García-Layana, A., Salinas-Alamán, A., Maldonado, M.J., Sainz-Gómez, C., Fernández-Hortelano, A., 2006. Optical coherence tomography to monitor photodynamic therapy in pathological myopia. Br. J. Ophthalmol. 90, 555–558.
Gaucher, D., Erginay, A., Lecleire-Collet, A., Haouchine, B., Puech, M., Cohen, S., Massin, P., Gaudric, A., 2008. Dome-shaped macula in eyes with myopic posterior staphyloma. Am. J. Ophthalmol. 145, 909–914.
Gaucher, D., Haouchine, B., Tadayoni, R., Massin, P., Erginay, A., Benhamou, N., Gaudric, A., 2007. Long-term follow-up of high myopic foveoschisis: natural course and surgical outcome. Am. J. Ophthalmol. 143, 455–462.
Gharbiya, M., Allievi, F., Mazzeo, L., Gabrieli, C., 2009. Intravitreal bevacizumab treatment for choroidal neovascularization in pathologic myopia: 12-month results. Am. J. Ophthalmol. 147, 84–93.
Gharbiya, M., Giustolisi, R., Allievi, F., Fantozzi, N., Mazzeo, L., Scavella, V., Gabrieli, C.B., 2010. Choroidal neovascularization in pathologic myopia: intravitreal ranibizumab versus bevacizumab-A randomized controlled trial. Am. J. Ophthalmol. 149, 148–164.
Gomez-Ulla, F., Gil-Martinez, M., 2015. Epidemiología de la miopía patológica en España. In: Ruiz-Moreno, J.M., Arias, L., Gomez-Ulla, F. (Eds.), Patología Retiniana En Alta Miopía. Sociedad Española de Retina y Vitreo, Madrid, pp. 37–47.
Gomez-Ulla, F., Ondategui-Parra, S., 2012. Informe sobre la ceguera en España. [WWW Document]. http://www.fundacionretinaplus.es.
Gospodarowicz, M.K., Miller, D., Groome, P.A., Greene, F.L., Logan, P.A., Sobin, L.H., 2004. The process for continuous improvement of the TNM classification. Cancer 100, 1–5.
Gözüm, N., Çakir, M., Gücukoglu, A., Sezen, F., 1997. Relationship between retinal lesions and axial length, age and sex in high myopia. Eur. J. Ophthalmol. 7, 277–282.
Grossniklaus, H.E., Green, W.R., 1992. Pathologic findings in pathologic myopia. Retina 12, 127–133.
Gupta, P., Cheung, C.Y., Saw, S.M., Koh, V., Tan, M., Yang, A., Zhao, P., Cheung, C.M.G., Wong, T.Y., Cheng, C.Y., 2016. Choroidal thickness does not predict visual acuity in young high myopes. Acta Ophthalmol 94, e709–e715.
Gupta, P., Yee, K.M.P., Garcia, P., Rosen, R.B., Parikh, J., Hageman, G.S., Sadun, A.A., Sebag, J., 2011. Vitreoschisis in macular diseases. Br. J. Ophthalmol. 95, 376–380.
Hayashi, K., Ohno-Matsui, K., Shimada, N., Moriyama, M., Hayashi, W., Wang, J., Yoshida, T., Tokoro, T., Mochizuki, M., 2011. Long-term results of photodynamic therapy for choroidal neovascularization in Japanese patients with pathologic myopia. Am. J. Ophthalmol. 151, 137–147.
Hayashi, K., Ohno-Matsui, K., Shimada, N., Moriyama, M., Kojima, A., Hayashi, W., Yasuzumi, K., Nagaoka, N., Saka, N., Yoshida, T., Tokoro, T., Mochizuki, M., 2010. Long-term pattern of progression of myopic maculopathy: a natural history study. Ophthalmology 117, 1595–1611 e4.
Hayashi, K., Ohno-Matsui, K., Teramukai, S., Shimada, N., Moriyama, M., Hayashi, W., Yoshida, T., Tokoro, T., Mochizuki, M., 2009. Comparison of visual outcome and regression pattern of myopic choroidal neovascularization after intravitreal bevacizumab or after photodynamic therapy. Am J Ophthalmol 148, 396–408.
Hayashi, M., Ito, Y., Takahashi, A., Kawano, K., Terasaki, H., 2013. Scleral thickness in highly myopic eyes measured by enhanced depth imaging optical coherence tomography. Eye 27, 410–417.
Henaine-Berra, A., Zand-Hadas, I.M., Fromow-Guerra, J., García-Aguirre, G., 2013. Prevalence of macular anatomic abnormalities in high myopia. Ophthalmic Surgery, Lasers Imaging Retin 44, 140–144.
Hidajat, R., Mclay, J., Burley, C., Elder, M., Morton, J., Goode, D., 2003. Influence of axial length of normal eyes on PERG. Doc. Ophthalmol. 107, 195–200.
Hirakata, A., Hida, T., 2006. Vitrectomy for myopic posterior retinoschisis or foveal detachment. Jpn. J. Ophthalmol.
Ho, T.C., Chen, M.S., Huang, J.S., Shih, Y.F., Ho, H., Huang, Y.H., 2012. Foveola non-peeling technique in internal limiting membrane peeling of myopic foveoschisis surgery. Retina 32, 631–634.
Ho, T.C., Yang, C.M., Huang, J.S., Yang, C.H., Yeh, P.T., Chen, T.C., Ho, A., Chen, M.S., 2014. Long-term outcome of foveolar internal limiting membrane nonpeeling for

myopic traction maculopathy. Retina 34, 1833–1840.
Hoang, Q.V., Chen, C.L., Garcia-Arumi, J., Sherwood, P.R., Chang, S., 2016. Radius of curvature changes in spontaneous improvement of foveoschisis in highly myopic eyes. Br. J. Ophthalmol. 100, 222–226.
Holden, B.A., Fricke, T.R., Wilson, D.A., Jong, M., Naidoo, K.S., Sankaridurg, P., Wong, T.Y., Naduvilath, T.J., Resnikoff, S., 2016. Global prevalence of myopia and high myopia and temporal trends from 2000 through 2050. Ophthalmology 123, 1036–1042.
Hosoda, Y., Yoshikawa, M., Miyake, M., Tabara, Y., Shimada, N., Zhao, W., Oishi, A., Nakanishi, H., Hata, M., Akagi, T., Ooto, S., Nagaoka, N., Fang, Y., Kawaguchi, T., Setoh, K., Takahashi, Y., Kosugi, S., Nakayama, T., Ohno-Matsui, K., Cheng, C.Y., Saw, S.M., Yamada, R., Matsuda, F., Tsujikawa, A., Yamashiro, K., 2018. CCDC102B confers risk of low vision and blindness in high myopia. Nat. Commun. 9, 1782.
Hsiang, H.W., Ohno-Matsui, K., Shimada, N., Hayashi, K., Moriyama, M., Yoshida, T., Tokoro, T., Mochizuki, M., 2008. Clinical characteristics of posterior staphyloma in eyes with pathologic myopia. Am. J. Ophthalmol. 146.
Ikuno, Y., 2017. Overview of the complications of high myopia. Retina.
Ikuno, Y., 2014. Current concepts and cutting-edge techniques in myopic macular surgeries. Taiwan J. Ophthalmol. 4, 147–151.
Ikuno, Y., Fujimoto, S., Jo, Y., Asai, T., Nishida, K., 2013. Choroidal thinning in high myopia measured by optical coherence tomography. Clin. Ophthalmol. 7, 889–893.
Ikuno, Y., Gomi, F., Tano, Y., 2005. Potent retinal arteriolar traction as a possible cause of myopic foveoschisis. Am. J. Ophthalmol. 139, 462–467.
Ikuno, Y., Ohno-Matsui, K., Wong, T.Y., Korobelnik, J.F., Vitti, R., Li, T., Stemper, B., Asmus, F., Zeitz, O., Ishibashi, T., 2015. Intravitreal aflibercept injection in patients with myopic choroidal neovascularization: the MYRROR study. Ophthalmology 122, 1220–1227.
Ikuno, Y., Sayanagi, K., Soga, K., Sawa, M., Tsujikawa, M., Gomi, F., Tano, Y., 2009. Intravitreal bevacizumab for choroidal neovascularization attributable to pathological myopia: one-year results. Am. J. Ophthalmol. 147, 94–100.
Ikuno, Y., Tano, Y., 2006. Vitrectomy for macular holes associated with myopic foveoschisis. Am. J. Ophthalmol. 141, 774–776.
Imamura, Y., Iida, T., Maruko, I., Zweifel, S.A., Spaide, R.F., 2011. Enhanced depth imaging optical coherence tomography of the sclera in dome-shaped macula. Am. J. Ophthalmol. 151, 297–302.
Ishida, T., Watanabe, T., Yokoi, T., Shinohara, K., Ohno-Matsui, K., 2018. Possible connection of short posterior ciliary arteries to choroidal neovascularisations in eyes with pathologic myopia. Br. J. Ophthalmol.
Ishikawa, M., Miyake, Y., Shiroyama, N., 1990. [Focal macular electroretinogram in high myopia]. Nihon. Ganka Gakkai Zasshi 94, 1040–1047.
Itakura, H., Kishi, S., Li, D., Akiyama, H., 2013. Observation of posterior precortical vitreous pocket using swept-source optical coherence tomography. Investig. Ophthalmol. Vis. Sci. 54, 3102–3107.
Itakura, H., Kishi, S., Li, D., Nitta, K., Akiyama, H., 2014. Vitreous changes in high myopia observed by swept-source optical coherence tomography. Investig. Ophthalmol. Vis. Sci. 55, 1447–1452.
Iwase, A., Araie, M., Tomidokoro, A., Yamamoto, T., Shimizu, H., Kitazawa, Y., 2006. Prevalence and causes of low vision and blindness in a Japanese adult population. The Tajimi study. Ophthalmology 113, 1354–1362.e1.
Jaffe, G.J., Eliott, D., Wells, J.A., Prenner, J.L., Papp, A., Patel, S., 2016. A phase 1 study of intravitreous E10030 in combination with ranibizumab in neovascular age-related macular degeneration. Ophthalmology 123, 78–85.
Janowski, M., Bulte, J.W.M., Handa, J.T., Rini, D., Walczak, P., 2015. Concise review: using stem cells to prevent the progression of myopia-A concept. Stem Cells 33, 2104–2113.
Kampik, A., 2012. Pathology of epiretinal membrane, idiopathic macular hole, and vitreomacular traction syndrome. Retina 32, 194–199.
Kashani, A.H., Chen, C.L., Gahm, J.K., Zheng, F., Richter, G.M., Rosenfeld, P.J., Shi, Y., Wang, R.K., 2017. Optical coherence tomography angiography: a comprehensive review of current methods and clinical applications. Prog. Retin. Eye Res. 60, 66–100.
Kishi, S., 2014. Vitreous changes in myopia. In: Spaide, R.F., Ohno-Matsui, K., Yannuzzi, L.A. (Eds.), Pathologic Myopia. Springer-Verlag New York, New York, pp. 143–166.
Kishi, S., Demaria, C., Shimizu, K., 1986. Vitreous cortex remnants at the fovea after spontaneous vitreous detachment. Int. Ophthalmol. 9, 253–260.
Klaver, C.C., Wolfs, R.C., Vingerling, J.R., Hofman, A., de Jong, P., 1998. Age-specific prevalence and causes of blindness and visual impairment in an older population: the rotterdam study. Arch. Ophthalmol.
Klein, R., Deng, Y., Klein, B.E.K., Hyman, L., Seddon, J., Frank, R.N., Wallace, R.B., Hendrix, S.L., Kuppermann, B.D., Langer, R.D., Kuller, L., Brunner, R., Johnson, K.C., Thomas, A.M., Haan, M., 2007. Cardiovascular disease, its risk factors and treatment, and age-related macular degeneration: women's health initiative sight exam ancillary study. Am. J. Ophthalmol. 143, 473–483.
Kobayashi, K., Ohno-Matsui, K., Kojima, A., Shimada, N., Yasuzumi, K., Yoshida, T., Futagami, S., Tokoro, T., Mochizuki, M., 2005. Fundus characteristics of high myopia in children. Jpn. J. Ophthalmol. 49, 306–311.
Koh, V., Tan, C., Tan, P.T., Tan, M., Balla, V., Nah, G., Cheng, C.Y., Ohno-Matsui, K., Tan, M.M.H., Yang, A., Zhao, P., Wong, T.Y., Saw, S.M., 2016a. Myopic maculopathy and optic disc changes in highly myopic young asian eyes and impact on visual acuity. Am. J. Ophthalmol. 164, 69–79.
Koh, V., Tan, C., Tan, P.T., Tan, M.M.H.M., Balla, V., Nah, G., Cheng, C.Y., Ohno-Matsui, K., Tan, M.M.H.M., Yang, A., Zhao, P., Wong, T.Y., Saw, S.M., 2016b. Myopic maculopathy and optic disc changes in highly myopic young asian eyes and impact on visual acuity. Am. J. Ophthalmol. 164, 69–79.
Koh, V., Yang, A., Saw, S.M., Chan, Y.H., Lin, S.T., Tan, M.M.H., Tey, F., Nah, G., Ikram, M.K., 2014. Differences in prevalence of refractive errors in young asian males in Singapore between 1996-1997 and 2009-2010. Ophthalmic Epidemiol.
Kollbaum, P.S., Jansen, M.E., Tan, J., Meyer, D.M., Rickert, M.E., 2013. Vision performance with a contact lens designed to slow myopia progression. Optom. Vis. Sci. 90, 205–214.
Korol, A., Zadorozhnyy, O., Naumenko, V., Kustryn, T., Pasyechnikova, N., 2016. Intravitreal aflibercept for the treatment of choroidal neovascularization associated with pathologic myopia : a pilot study. Clin. Ophthalmol. 10, 2223–2229.
Kumagai, K., Furukawa, M., Ogino, N., Larson, E., 2010. Factors correlated with postoperative visual acuity after vitrectomy and internal limiting membrane peeling for myopic foveoschisis. Retina 30, 874–880.
Kung, Y.-H., Wu, T.-T., Huang, Y.-H., 2014. One-year outcome of two different initial dosing regimens of intravitreal ranibizumab for myopic choroidal neovascularization. Acta Ophthalmol 92, 615–620.
Kuriyama, S., Hayashi, H., Jingami, Y., Kuramoto, N., Akita, J., Matsumoto, M., 2013. Efficacy of inverted internal limiting membrane flap technique for the treatment of macular hole in high myopia. Am. J. Ophthalmol. 156, 125–131.e1.
Kwak, N., Okamoto, N., Wood, J.M., Campochiaro, P.A., 2000. VEGF is major stimulator in model of choroidal neovascularization. Investig. Ophthalmol. Vis. Sci. 41, 3158–3164.
Lai, T., Yang, C., 2017. Lamellar hole-associated epiretinal proliferation in lamellar macular hole and full-thickness macular hole in high myopia. Retina 1–8.
Lalloum, F., Souied, E.H., Bastuji-Garin, S., Puche, N., Querques, G., Glacet-Bernard, A., Coscas, G., Soubrane, G., Leveziel, N., 2010. INTRAVITREAL RANIBIZUMAB FOR CHOROIDAL NEOVASCULARIZATION COMPLICATING PATHOLOGIC MYOPIA. Retina 30, 399–406.
Lam, D.S.C., King, S.L., Mohamed, S., Chan, W.M., Palanivelu, M.S., Cheung, C.Y.L., Li, E.Y.M., Lai, R.Y.K., Leung, C.K.S., 2007. Regional variations in the relationship between macular thickness measurements and myopia. Investig. Ophthalmol. Vis. Sci. 48, 376–382.
Lee, J.H., Jee, D., Kwon, J.W., Lee, W.K., 2013. Prevalence and risk factors for myopia in a rural Korean population. Investig. Ophthalmol. Vis. Sci. 54, 5466–5470.
Lee, S.J., Urm, S.H., Yu, B.C., Sohn, H.S., Hong, Y.S., Noh, M.S., Lee, Y.H., 2011. The prevalence of high myopia in 19 year-old men in Busan, Ulsan and Gyeongsangnam-Do. J. Prev. Med. Public Heal. 44, 56–64.
Lehmann, M., Devin, F., Rothschild, P., Massin, P., Couturier, A., Tadayoni, R., 2017. Preoperative factors influencing visual recovery after vitrectomy for myopic foveoschisis. Retina 1–9.
Leveziel, N., Caillaux, V., Bastuji-Garin, S., Zmuda, M., Souied, E.H., 2013. Angiographic and optical coherence tomography characteristics of recent myopic choroidal neovascularization. Am. J. Ophthalmol. 155, 913–919.e1.
Lewis, J.A., Garcia, M.B., Rani, L., Wildsoet, C.F., 2014. Intact globe inflation testing of changes in scleral mechanics in myopia and recovery. Exp. Eye Res. 127, 42–48.
Liang, I.C., Shimada, N., Tanaka, Y., Nagaoka, N., Moriyama, M., Yoshida, T., Ohno-Matsui, K., 2015. Comparison of clinical features in highly myopic eyes with and without a dome-shaped macula. Ophthalmology 1591–1600.
Liu, H.H., Xu, L., Wang, Y.X., Wang, S., You, Q.S., Jonas, J.B., 2010. Prevalence and progression of myopic retinopathy in Chinese adults: the Beijing eye study. Ophthalmology 117, 1763–1768.
Liu, T.X., Wang, Z., 2013. Collagen crosslinking of porcine sclera using genipin. Acta Ophthalmol 91, e253–e257.
Lorenzo Carrero, J., 2012. Incomplete posterior vitreous detachment: prevalence and clinical relevance. Am. J. Ophthalmol. 153, 497–503.
Lorenzo, D., Arias, L., Alcubierre, R., Pujol, O., Caminal, J.M., Rubio, M., Català, J., Garcia-Bru, P., Arruga, J., 2011. Intravitreal ranibizumab for choroidal neovascularization secondary to pathological myopia: 12-month follow-up. Ophthalmologica 226, 103–109.
Ma, J., Li, H., Ding, X., Tanumiharjo, S., Lu, L., 2017. Effectiveness of combined macular buckle under direct vision and vitrectomy with ILM peeling in refractory macular hole retinal detachment with extreme high axial myopia: a 24-month comparative study. Br. J. Ophthalmol. bjophthalmol 2016-310123.
Mancino, R., Ciuffoletti, E., Martucci, A., Aiello, F., Cedrone, C., Cerulli, L., Nucci, C., 2013. Anatomical and functional results of macular hole retinal detachment surgery in patients with high myopia and posterior staphyloma treated with perfluoropropane gas or silicone oil. Retina 33, 586–592.
Marticorena, J., Gomez-Ulla, F., Fernandez, M., Pazos, B., Rodriguez-Cid, M., Sanchez-Salorio, M., 2006. Combined photodynamic therapy and intravitreal triamcinolone acetonide for the treatment of myopic subfoveal choroidal neovascularization. Am. J. Ophthalmol. 142, 335–337.
Maruko, I., Iida, T., Sugano, Y., Oyamada, H., Sekiryu, T., 2011. Morphologic choroidal and scleral changes at the macula in tilted disc syndrome with staphyloma using optical coherence tomography. Investig. Ophthalmol. Vis. Sci. 52, 8763–8768.
Mateo, C., Burés-Jelstrup, A., Navarro, R., Corcóstegui, B., 2012. Macular buckling for eyes with myopic foveoschisis secondary to posterior staphyloma. Retina 32, 1121–1128.
McBrien, N.A., 2013. Regulation of scleral metabolism in myopia and the role of transforming growth factor-beta. Exp. Eye Res. 114, 128–140.
McBrien, N.A., Gentle, A., 2003. Role of the sclera in the development and pathological complications of myopia. Prog. Retin. Eye Res. 22, 307–338.
Mcbrien, N.A., Norton, T.T., 1994. Prevention of collagen crosslinking increases form-deprivation myopia in tree shrew. Exp.Eye Res. 59, 475–486.
Mcmonnies, C.W., 2016. An examination of the relation between intraocular pressure, fundal stretching and myopic pathology. Clin. Exp. Optom.
Mehdizadeh, M., Nowroozzadeh, M.H., 2008. Dome-shaped macula in eyes with myopic posterior staphyloma. Am. J. Ophthalmol. 146, 478.
Meng, B., Zhao, L., Yin, Y., Li, H., Wang, X., Yang, X., You, R., Wang, J., Zhang, Y., Wang, H., Du, R., Wang, N., Zhan, S., Wang, Y., 2017. Internal limiting membrane peeling and gas tamponade for myopic foveoschisis: a systematic review and meta-analysis.

BMC Ophthalmol 17, 1–10.
Mete, M., Alfano, A., Guerriero, M., Prigione, G., Sartore, M., Polito, A., Pertile, G., 2017. Inverted internal limiting membrane flap technique versus complete interal limiting membrane removal in myopic macular hole surgery. Retina 37, 1.
Milani, P., Pece, A., Pierro, L., Seidenari, P., Radice, P., Scialdone, A., 2010. Bevacizumab for macular serous neuroretinal detachment in tilted disk syndrome. J. Ophthalmol. 2010, 970580.
Miyake, M., Yamashiro, K., Akagi-Kurashige, Y., Kumagai, K., Nakata, I., Nakanishi, H., Oishi, A., Tsujikawa, A., Yamada, R., Matsuda, F., Yoshimura, N., 2014a. Vascular endothelial growth factor gene and the response to anti-vascular endothelial growth factor treatment for choroidal neovascularization in high myopia. Ophthalmology 121, 225–233.
Miyake, M., Yamashiro, K., Akagi-Kurashige, Y., Oishi, A., Tsujikawa, A., Hangai, M., Yoshimura, N., 2014b. Analysis of fundus shape in highly myopic eyes by using curvature maps constructed from optical coherence tomography. PLoS One 9.
Miyata, M., Ooto, S., Hata, M., Yamashiro, K., Tamura, H., Akagi-Kurashige, Y., Nakanishi, H., Ueda-Arakawa, N., Takahashi, A., Kuroda, Y., Wakazono, T., Yoshikawa, M., Yoshimura, N., 2016. Detection of myopic choroidal neovascularization using optical coherence tomography angiography. Am. J. Ophthalmol. 165, 108–114.
Monés, J., Amselem, L., Serrano, A., Garcia, M., Hijano, M., 2009. Intravitreal ranibizumab for choroidal neovascularization secondary to pathologic myopia: 12-month results. Eye (Lond). 23, 1275–1280 quiz 1281.
Montero, J. a, Ruiz-Moreno, J.M., 2003. Verteporfin photodynamic therapy in highly myopic subfoveal choroidal neovascularisation. Br. J. Ophthalmol. 87, 173–176.
Morgan, I.G., Ohno-Matsui, K., Saw, S.M., 2012. Myopia. The Lancet 1739–1748.
Moriyama, M., Ohno-Matsui, K., Hayashi, K., Shimada, N., Yoshida, T., Tokoro, T., Morita, I., 2011. Topographic analyses of shape of eyes with pathologic myopia by high-resolution three-dimensional magnetic resonance imaging. Ophthalmology 118, 1626–1637.
Nadal, J., Verdaguer, P., Canut, M.I., 2012. Treatment of retinal detachment secondary to macular hole in high myopia: vitrectomy with dissection of the inner limiting membrane to the edge of the staphyloma and long-term tamponade. Retina 32, 1525–1530.
Neelam, K., Cheung, C.M.G., Ohno-Matsui, K., Lai, T.Y.Y., Wong, T.Y., 2012. Choroidal neovascularization in pathological myopia. Prog. Retin. Eye Res. 31, 495–525.
Nguyen, Q.D., Shah, S., Tatlipinar, S., Do, D.V., Anden, E.V., Campochiaro, P.A., 2005. Bevacizumab suppresses choroidal neovascularisation caused by pathological myopia. Br. J. Ophthalmol. 89, 1368–1370.
Ohno-Matsui, K., 2017. What is the fundamental nature of pathologic myopia? Retina 37, 1043–1048.
Ohno-Matsui, K., 2016. Pathologic myopia. Asia-Pacific J. Ophthalmol.
Ohno-Matsui, K., 2014. Proposed classification of posterior staphylomas based on analyses of eye shape by three-dimensional magnetic resonance imaging and wide-field fundus imaging. Ophthalmology 121, 1798–1809.
Ohno-Matsui, K., Akiba, M., Modegi, T., Tomita, M., Ishibashi, T., Tokoro, T., Moriyama, M., 2012. Association between shape of sclera and myopic retinochoroidal lesions in patients with pathologic myopia. Investig. Ophthalmol. Vis. Sci. 53, 6046–6061.
Ohno-Matsui, K., Ikuno, Y., Lai, T.Y.Y., Gemmy Cheung, C.M., 2018. Diagnosis and treatment guideline for myopic choroidal neovascularization due to pathologic myopia. Prog. Retin. Eye Res. 63, 92–106.
Ohno-Matsui, K., Jonas, J.B., Spaide, R.F., 2016a. Macular Bruch membrane holes in highly myopic patchy chorioretinal atrophy. Am. J. Ophthalmol. 166, 22–28.
Ohno-Matsui, K., Jonas, J.B., Spaide, R.F., 2016b. Macular Bruch membrane holes in choroidal neovascularization-related myopic macular atrophy by swept-source optical coherence tomography. Am. J. Ophthalmol. 162, 133–139.
Ohno-Matsui, K., Kawasaki, R., Jonas, J.B., Cheung, C.M.G., Saw, S.M., Verhoeven, V.J.M., Klaver, C.C.W., Moriyama, M., Shinohara, K., Kawasaki, Y., Yamazaki, M., Meuer, S., Ishibashi, T., Yasuda, M., Yamashita, H., Sugano, A., Wang, J.J., Mitchell, P., Wong, T.Y., 2015. International photographic classification and grading system for myopic maculopathy. Am. J. Ophthalmol. 159, 877–883.
Ohno-Matsui, K., Lai, T.Y.Y., Lai, C.C., Cheung, C.M.G., 2016c. Updates of pathologic myopia. Prog. Retin. Eye Res. 52, 156–187.
Ohno-Matsui, K., Shimada, N., Yasuzumi, K., Hayashi, K., Yoshida, T., Kojima, A., Moriyama, M., Tokoro, T., 2011. Long-term development of significant visual field defects in highly myopic eyes. Am J Ophthalmol 152, 256–265.e1.
Ohno-Matsui, K., Tokoro, T., 1996. The progression of lacquer cracks in pathologic myopia. Retina 16, 29–37.
Ohno-Matsui, K., Yoshida, T., Futagami, S., Yasuzumi, K., Shimada, N., Kojima, A., Tokoro, T., Mochizuki, M., 2003. Patchy atrophy and lacquer cracks predispose to the development of choroidal neovascularisation in pathological myopia. Br. J. Ophthalmol. 87, 570–573.
Ohsugi, H., Ikuno, Y., Matsuba, S., Ohsugi, E., Nagasato, D., Shoujou, T., Tabuchi, H., 2018. Morphologic characteristics of macular hole and macular hole retinal detachment associated with extreme myopia. Retina 1.
Ohsugi, H., Ikuno, Y., Oshima, K., Tabuchi, H., 2013. 3-D choroidal thickness maps from EDI-OCT in highly myopic eyes. Optom. Vis. Sci. 90, 599–606.
Oie, Y., Ikuno, Y., Fujikado, T., Tano, Y., 2005. Relation of posterior staphyloma in highly myopic eyes with macular hole and retinal detachment. Jpn. J. Ophthalmol. 49, 530–532.
Okabe, S., Matsuo, N., Okamoto, S., Kataoka, H., 1982. Electron microscopic studies on retinochoroidal atrophy in the human eye. Acta Med. Okayama 36, 11–21.
Okabe, S., Matsuo, N., Okamoto, S., Kataoka, H., 1979. [Electron microscopic studies on retinochoroidal atrophy in the human eyes (author's transl)]. Nihon. Ganka Gakkai Zasshi 83, 674–682.
Ortisi, E., Avitabile, T., Bonfiglio, V., 2012. Surgical management of retinal detachment because of macular hole in highly myopic eyes. Retina.
Pang, C.E., Sarraf, D., Freund, K.B., 2015. Extreme choroidal thinning in high myopia. Retina 35, 407–415.
Panozzo, G., Mercanti, A., 2004. Optical coherence tomography findings in myopic traction maculopathy. Arch. Ophthalmol. 122, 1455–1460.
Parodi, M.B., Iacono, P., Sacconi, R., Iuliano, L., Bandello, F., 2015. Fundus autofluorescence changes after ranibizumab treatment for subfoveal choroidal neovascularization secondary to pathologic myopia. Am. J. Ophthalmol. 160, 322–327.e2.
Pastor-Vivas, A.I., Alejandre-Alba, N., García-Vega, M.I., Ariño-Gutiérrez, M., García-Sandoval, B., Jiménez-Alfaro, I., 2011. Quantifying and classifying postsurgical pain in pterygium surgery with conjunctival autografts. Arch. la Soc. Española Oftalmol. (English Ed. 86, 176–179.
Pecce, A., Milani, P., 2016. Intravitreal aflibercept for myopic choroidal neovascularization. Graefes Arch Clin Exp Ophthalmol 254, 2327–2332.
Pece, A., Isola, V., Vadala, M., Matranga, D., 2006. Photodynamic therapy with verteporfin for subfoveal choroidal neovascularization secondary to pathologic myopia. Long-term study. Retina 26, 746–751.
Phillips, C.I., 1958. Retinal detachment at the posterior pole. Br. J. Ophthalmol. 42, 749–753.
Phillips, J.R., McBrien, N.A., 2004. Pressure-induced changes in axial eye length of chick and tree shrew: significance of myofibroblasts in the sclera. Investig. Ophthalmol. Vis. Sci. 45, 758–763.
Qi, Y., Duan, A.L., Meng, X., Wang, N., 2016. Vitrectomy without inner limiting membrane peeling for macular retinoschisis in highly myopic eyes. Retina 36, 953–956.
Querques, G., Corvi, F., Querques, L., Souied, E.H., Bandello, F., 2016. Optical coherence tomography angiography of choroidal neovascularization. Secondary to Pathologic Myopia 56, 101–106.
Rahimy, E., Beardsley, R.M., Gomez, J., Hung, C., Sarraf, D., 2013. Grading of posterior staphyloma with spectral-domain optical coherence tomography and correlation with macular disease. Can. J. Ophthalmol. 48, 539–545.
Ripandelli, G., Coppé, A.M., Parisi, V., Stirpe, M., 2008. Fellow eye findings of highly myopic subjects operated for retinal detachment associated with a macular hole. Ophthalmology 115, 1489–1493.
Ripandelli, G., Rossi, T., Scarinci, F., Scassa, C., Parisi, V., Stirpe, M., 2012. Macular vitreoretinal interface abnormalities in highly myopic eyes with posterior staphyloma: 5-year follow-up. Retina 32, 1531–1538.
Rizzo, S., Tartaro, R., Barca, F., Caporossi, T., Bacherini, D., Giansanti, F., 2017. Internal limiting membrane peeling versus inverted flap technique for treatment of full-thickness macular holes. Retina 1.
Rocha Cabrera, P., Cordovés Dorta, L., Ángel Pereira, D., Abreu Reyes, J.A., Losada Castillo, M.J., Lorenzo Morales, J., Serrano García, M., 2017. Mácula en cúpula asociada a la retinocoroidosis miópica. Utilidad de la espironolactona. Arch. Soc. Esp. Oftalmol. 92, 499–506.
Rosenfeld, P.J., Brown, D.M., Heier, J.S., Boyer, D.S., Kaiser, P.K., Chung, C.Y., Kim, R.Y., 2006. Ranibizumab for neovascular age-related macular degeneration. N. Engl. J. Med. 355, 1419–1431.
Ruiz-Moreno, J.M., Amat, P., Montero, J.A., Lugo, F., 2008. Photodynamic therapy to treat choroidal neovascularisation in highly myopic patients: 4 Years' outcome. Br. J. Ophthalmol. 92, 792–794.
Ruiz-Moreno, J.M., Arias, L., Montero, J.A., Carneiro, A., Silva, R., 2013a. Intravitreal anti-VEGF therapy for choroidal neovascularisation secondary to pathological myopia: 4-Year outcome. Br. J. Ophthalmol. 97, 1447–1450.
Ruiz-Moreno, J.M., Gomez-Ulla, F., Montero, J.A., Ares, S., Lopez-Lopez, F., Rodriguez, M., Fernandez, M., 2009a. Intravitreous bevacizumab to treat subfoveal choroidal neovascularization in highly myopic eyes: short-term results. Eye 23, 334–338.
Ruiz-Moreno, J.M., López-Gálvez, M.I., Donate, J., Gomez-Ulla, F., García-Arumí, J., García-Layana, A., Sellés, I., Reche, J., Montero, J.A., Pazos, B., Zapata, M.A., Pastor, J.C., 2011. Myopic choroidal neovascularization. Ophthalmology.
Ruiz-Moreno, J.M., López-Gálvez, M.I., Montero Moreno, J.A., Pastor Jimeno, J.C., 2013b. Intravitreal bevacizumab in myopic neovascular membranes: 24-month results. Ophthalmology.
Ruiz-Moreno, J.M., Montero, J.A., Araiz, J., Arias, L., García-Layana, A., Carneiro, A., Figueroa, M.S., Silva, R., Garcia-Layana, A., Carneiro, A., Figueroa, M.S., Silva, R., 2015. Intravitreal anti-vascular endothelial growth factor therapy for choroidal neovascularization secondary to pathologic myopia: six years outcome. Retina 35, 2450–2456.
Ruiz-Moreno, J.M., Montero, J.A., Arias, L., Araiz, J., Gomez-Ulla, F., Silva, R., Piñero, D.P.D., 2010. Twelve-month outcome after one intravitreal injection of bevacizumab to treat myopic choroidal neovascularization. Retina 30, 1609–1615.
Ruiz-Moreno, J.M., Montero, J.A., Gomez-Ulla, F., Ares, S., 2009b. Intravitreal bevacizumab to treat subfoveal choroidal neovascularisation in highly myopic eyes: 1-year outcome. Br. J. Ophthalmol. 93, 448–451.
Ruiz-Moreno, J.M., Ruiz-Medrano, J., 2015. Tomografía de coherencia óptica en la exploración de fondo de ojo. In: Ruiz-Moreno, J.M., Arias, L., Gomez-Ulla, F. (Eds.), Patología Retiniana En Alta Miopía. Sociedad Española de Retina y Vitreo, Madrid, pp. 109–125.
Sawa, M., Gomi, F., Tsujikawa, M., Ikuno, Y., Sakaguchi, H., Sayanagi, K., Tano, Y., 2008. Abnormal fundus autofluorescence patterns in myopic choroidal neovascularisation. Br. J. Ophthalmol. 92, 1236–1240.
Sayanagi, K., Ikuno, Y., Tano, Y., 2007. Different fundus autofluorescence patterns of retinoschisis and macular hole retinal detachment in high myopia. Am. J. Ophthalmol. 144, 299–301.
Schepens, C.L., Okamura, I.D., Brockhurst, R.J., 1957. The scleral buckling procedures. I. Surgical techniques and management. AMA. Arch. Ophthalmol. 58, 797–811.
Sergienko, N.M., Shargorogska, I., 2012. The scleral rigidity of eyes with different

refractions. Graefe's Arch. Clin. Exp. Ophthalmol. 250, 1009–1012.
Shih, Y.F., Ho, T.C., Hsiao, C.K., Lin, L.L.K., 2006. Visual outcomes for high myopic patients with or without myopic maculopathy: a 10 year follow up study. Br. J. Ophthalmol. 90, 546–550.
Shimada, H., Nakashizuka, H., Hattori, T., Mori, R., Mizutani, Y., Yuzawa, M., 2009. Double staining with brilliant blue G and double peeling for epiretinal membranes. Ophthalmology 116, 1370–1376.
Shimada, N., Sugamoto, Y., Ogawa, M., Takase, H., Ohno-Matsui, K., 2012. Fovea-sparing internal limiting membrane peeling for myopic traction maculopathy. Am. J. Ophthalmol. 154, 693–701.
Shimada, N., Tanaka, Y., Tokoro, T., Ohno-Matsui, K., 2013. Natural course of myopic traction maculopathy and factors associated with progression or resolution. Am. J. Ophthalmol. 156, 948–957.e1.
Shinohara, K., Yoshida, T., Liu, H., Ichinose, S., Ishida, T., Nakahama, K.I., Nagaoka, N., Moriyama, M., Morita, I., Ohno-Matsui, K., 2018. Establishment of novel therapy to reduce progression of myopia in rats with experimental myopia by fibroblast transplantation on sclera. J. Tissue Eng. Regen. Med. 12, e451–461.
Siam, A.L.H., El Maamoun, T.A., Ali, M.H., 2012. Macular buckling for myopic macular hole retinal detachment: a new approach. Retina 32, 748–753.
Silva, R., 2012. Myopic maculopathy: a review. Ophthalmologica 228, 197–213.
Silva, R.M., Ruiz-Moreno, J.M., Nascimento, J., Carneiro, A., Rosa, P., Barbosaa, A., Carvalheira, F., Abreu, J.R.F., Cunha-Vaz, J.G., 2008. Short-term efficacy and safety of intravitreal ranibizumab for myopic choroidal neovascularization. Retina 28, 1117–1123.
Silva, R.M., Ruiz-Moreno, J.M., Rosa, P., Carneiro, A., Nascimento, J., Rito, L.F., Cachulo, M.L., Carvalheira, F., Murta, J.N., 2010. INTRAVITREAL RANIBIZUMAB FOR MYOPIC CHOROIDAL NEOVASCULARIZATION. Retina 30, 407–412.
Snead, D.R.J., James, S., Snead, M.P., 2008. Pathological changes in the vitreoretinal junction 1: epiretinal membrane formation. Eye 22, 1310–1317.
Soubrane, G., 2008. Choroidal neovascularization in pathologic myopia: recent developments in diagnosis and treatment. Surv. Ophthalmol 53, 121–138.
Soudier, G., Gaudric, A., Gualino, V., Massin, P., Nardin, M., Tadayoni, R., Speeg-Schatz, C., Gaucher, D., 2016. Long-term evolution of dome-shaped macula. Retina 36, 944–952.
Spaide, R.F., 2013. Staphyloma: Part 1. Springer, New York.
Stafford, W., 1982. Degeneration and atrophy of the choroid. In: Duane, T. (Ed.), Clinical Ophthalmology. Harper & Row, Hagerstown.
Steidl, S.M., Pruett, R.C., 1997. Macular complications associated with posterior staphyloma. Am J Ophthalmol 123, 181–187.
Stewart, J.M., Schultz, D.S., Lee, O.T., Trinidad, M.L., 2009. Exogenous collagen crosslinking reduces scleral permeability: modeling the effects of age-related cross-link accumulation. Investig. Ophthalmol. Vis. Sci. 50, 352–357.
Takano, M., Kishi, S., 1999. Foveal retinoschisis and retinal detachment in severely myopic eyes with posterior staphyloma. Am. J. Ophthalmol. 128, 472–476.
Tamura, N., Sakai, T., Tsuneoka, H., 2014. Spontaneous resolution of foveal detachment in dome-shaped macula observed by spectral domain optical coherence tomography. Clin. Ophthalmol. 8, 83–86.
Tokoro, T., 1998. Types of fundus changes in the posterior pole BT - atlas of posterior fundus changes in pathologic myopia. In: Tokoro, T. (Ed.), Atlas of Posterior Fundus Changes in Pathologic Myopia. Springer-Verlag, Tokio, pp. 5–22.
Tokoro, T., 1988. On the definition of pathologic myopia in group studies. Acta Ophthalmol 66, 107–108.
Tong, J.P., Chan, W.M., Liu, D.T.L., Lai, T.Y.Y., Choy, K.W., Pang, C.P., Lam, D.S.C., 2006. Aqueous humor levels of vascular endothelial growth factor and pigment epithelium-derived factor in polypoidal choroidal vasculopathy and choroidal neovascularization. Am. J. Ophthalmol. 141, 456–462.
Trier, K., Olsen, E.B., Kobayashi, T., Ribel-Madsen, S.M., 1999. Biochemical and ultrastructural changes in rabbit sclera after treatment with 7-methylxanthine, theobromine, acetazolamide, or L-ornithine. Br. J. Ophthalmol. 83, 1370–1375.
Tufail, A., Narendran, N., Patel, P.J., Sivaprasad, S., Amoaku, W., Browning, A.C., Osoba, O., Gale, R., George, S., Lotery, A.J., Majid, M., McKibbin, M., Menon, G., Andrews, C., Brittain, C., Osborne, A., Yang, Y., 2013. Ranibizumab in myopic choroidal neovascularization: the 12-month results from the REPAIR study. Ophthalmology 120 1944–5.e1.
Uchida, A., Shinoda, H., Koto, T., Mochimaru, H., Nagai, N., Tsubota, K., Ozawa, Y., 2014. Vitrectomy for myopic foveoschisis with internal limiting membrane peeling and no gas tamponade. Retina 34, 455–460.
Uemoto, R., Nakasato-Sonn, H., Kawagoe, T., Akira, M., Okada, E., Mizuki, N., 2012. Factors associated with enlargement of chorioretinal atrophy after intravitreal bevacizumab for myopic choroidal neovascularization. Graefe's Arch. Clin. Exp. Ophthalmol. 250, 989–997.
Usui, S., Ikuno, Y., Akiba, M., Maruko, I., Sekiryu, T., Nishida, K., Iida, T., 2012. Circadian changes in subfoveal choroidal thickness and the relationship with circulatory factors in healthy subjects. Invest. Ophthalmol. Vis. Sci. 53, 2300–2307.
Vanderbeek, B.L., Johnson, M.W., 2012. The diversity of traction mechanisms in myopic traction maculopathy. Am. J. Ophthalmol. 153, 93–102.
Verkicharla, P.K., Ohno-Matsui, K., Saw, S.M., 2015. Current and predicted demographics of high myopia and an update of its associated pathological changes. Ophthalmic Physiol. Opt.
Verteporfin in PhotodynamicTherapy (VIP) Group Study, 2001. Photodynamic therapy of subfoveal choroidal neovascularization in pathologic myopia with verteporfin. Ophthalmology 108, 841–852.
Vincent, S.J., 2017. The use of contact lenses in low vision rehabilitation: optical and therapeutic applications. Clin. Exp. Optom.
Vinores, S.A., Campochiaro, P.A., Conway, B.P., 2016. Ultrastructural and electron-lmmunocytochemical characterization of cells in epiretinal membranes. Investig. Opthalmology Vis. Sci. 31, 14e28.
Viola, F., Dell'Arti, L., Benatti, E., Invernizzi, A., Mapelli, C., Ferrari, F., Ratiglia, R., Staurenghi, G., Barteselli, G., 2015. Choroidal findings in dome-shaped macula in highly myopic eyes: a longitudinal study. Am. J. Ophthalmol. 159, 44–52.
Vongphanit, J., Mitchell, P., Wang, J.J., 2002a. Population prevalence of tilted optic disks and the relationship of this sign to refractive error. Am. J. Ophthalmol 133, 679–685.
Vongphanit, J., Mitchell, P., Wang, J.J., 2002b. Prevalence and progression of myopic retinopathy in an older population. Ophthalmology 109, 704–711.
Wang, N.K., Wu, Y.M., Wang, J.P., Liu, L., Yeung, L., Chen, Y.P., Chen, Y.H., Yeh, L.K., Wu, W.C., Chuang, L.H., Lai, C.C., 2016. Clinical characteristics of posterior staphylomas in myopic eyes with axial length shorter than 26.5 millimeters. Am. J. Ophthalmol. 162, 180–190.
Wolf, S., Balciuniene, V.J., Laganovska, G., Menchini, U., Ohno-Matsui, K., Sharma, T., Wong, T.Y., Silva, R., Pilz, S., Gekkieva, M., 2014. RADIANCE: a randomized controlled study of ranibizumab in patients with choroidal neovascularization secondary to pathologic myopia. Ophthalmology 121, 682–692.
Wollensak, G., Iomdina, E., 2009. Long-term biomechanical properties of rabbit sclera after collagen crosslinking using riboflavin and ultraviolet A (UVA). Acta Ophthalmol 87, 193–198.
Wollensak, G., Spoerl, E., Wilsch, M., Seiler, T., 2003. Endothelial cell damage after riboflavin-ultraviolet-A treatment in the rabbit. J. Cataract Refract. Surg. 29, 1786–1790.
Wong, F.F., Lari, D.R., Schultz, D.S., Stewart, J.M., 2012. Whole globe inflation testing of exogenously crosslinked sclera using genipin and methylglyoxal. Exp. Eye Res. 103, 17–21.
Wong, T.Y., Ferreira, A., Hughes, R., Carter, G., Mitchell, P., 2014. Epidemiology and disease burden of pathologic myopia and myopic choroidal neovascularization: an evidence-based systematic review. Am. J. Ophthalmol. 157, 9–25 e12.
Wong, T.Y., Ohno-Matsui, K., Leveziel, N., Holz, F.G., Lai, T.Y., Yu, H.G., Lanzetta, P., Chen, Y., Tufail, A., 2015. Myopic choroidal neovascularisation: current concepts and update on clinical management. Br. J. Ophthalmol. 99, 289–296.
Wu, P., Chen, Y., 2009. Intravitreal injection of bevacizumab for myopic choroidal neovascularization: 1-year follow-up. Eye 23, 2042–2045.
Wu, P.C., Chen, Y.J., Chen, Y.H., Chen, C.H., Shin, S.J., Tsai, C.L., Kuo, H.K., 2009. Factors associated with foveoschisis and foveal detachment without macular hole in high myopia. Eye 23, 356–361.
Yamada, M., Hiratsuka, Y., Roberts, C.B., Pezzullo, M.L., Yates, K., Takano, S., Miyake, K., Taylor, H.R., 2010. Prevalence of visual impairment in the adult Japanese population by cause and severity and future projections. Ophthalmic Epidemiol 17, 50–57.
Yamagishi, T., Koizumi, H., Yamazaki, T., Kinoshita, S., 2012. Choroidal thickness in inferior staphyloma associated with posterior serous retinal detachment. Retina 32, 1237–1242.
Yamanari, M., Makita, S., Yasuno, Y., 2008. Polarization-sensitive swept-source optical coherence tomography with continuous source polarization modulation. Opt. Express 16, 5892–5906.
Yamashiro, K., Kinoshita-Nakano, E., Ota, T., Jingami, Y., Nakata, I., Hayashi, H., 2018. Floating flap of internal limiting membrane in myopic macular hole surgery. Graefe's Arch. Clin. Exp. Ophthalmol. 256, 693–698.
Yoon, J.U., Kim, Y.M., Lee, S.J., Byun, Y.J., Koh, H.J., 2012. Prognostic factors for visual outcome after intravitreal anti-vegf injection for naive myopic choroidal neovascularization. Retina 32, 949–955.
Yoshihara, N., Yamashita, T., Ohno-Matsui, K., Sakamoto, T., 2014. Objective analyses of tessellated fundi and significant correlation between degree of tessellation and choroidal thickness in healthy eyes. PLoS One 9.
You, Q.S., Peng, X.Y., Xu, L., Chen, C.X., Wang, Y.X., Jonas, J.B., 2014. Myopic maculopathy imaged by optical coherence tomography: the beijing eye study. Ophthalmology 121, 220–224.
Zaben, A., Zapata, M., Garcia-Arumi, J., 2015. Retinal sensitivity and choroidal thickness in high myopia. Retina 35, 398–406.
Zhang, Y., Zou, C., Liu, L., Cao, L., Xia, X., Li, Z., Hu, M., Yu, H., Mu, G., 2013. Effect of irradiation time on riboflavin-ultraviolet-A collagen crosslinking in rabbit sclera. J. Cataract Refract. Surg. 39, 1184–1189.
Zheng, L., Pan, A., Zhu, S., Wu, Y., Dong, L., Xue, A., 2018. Posterior scleral contraction to treat recurrent or persistent macular detachment after previous vitrectomy in highly myopic eyes. Retina May 16 [Epub ahead of print].